SP-1276

ESA's Report to the 35th COSPAR Meeting

Paris, France
July 2004

European Space Agency
Agence spatiale européenne

SP-1276
June 2004

ESA's Report to the 35th COSPAR Meeting

Paris, France
July 2004

European Space Agency
Agence spatiale européenne

Contributors

This report on the scientific missions of the European Space Agency was written by:

A. Chicarro	F. Jansen	R. Marsden	T. Sanderson
J. Clavel	P. Jakobsen	H. Opgenoorth	R. Schulz
C.P. Escoubet	O. Jennrich	A. Parmar	G. Schwehm
F. Favata	M. Kessler	M. Perryman	H. Svedhem
B. Foing	J.-P. Lebreton	G. Pilbratt	J. Tauber
M. Fridlund	D. Lumb	R. Reinhard	C. Winkler
A. Gimenez	D. Macchetto	A. Salama	

The authors acknowledge the use of published and unpublished material supplied by experimenters, observers and colleagues.

The report was completed on 30 April 2004.

Communications should be addressed to the scientific editor:

Prof. A. Gimenez
ESA Research and Scientific Support Department
European Space Research and Technology Centre (ESTEC)
Postbus 299
NL-2200 AG Noordwijk
The Netherlands
Tel: +31 71 565-3552
Email: alvaro.gimenez@esa.int

Cover:
Mars Express is returning stunning views of Mars. The cover shows an overhead view of the complex caldera at the summit of Olympus Mons, the highest volcano in the Solar System. Olympus Mons has an average elevation of 22 km and the caldera has a depth of about 3 km. This is the first high-resolution colour image of the complete caldera. It was recorded by the High Resolution Stereo Camera (HRSC) of Mars Express from a height of 273 km on 21 January 2004. Resolution is 12 m per pixel; the image is centred at 18.3°N / 227°E; south is at the top.

Edited by: A. Wilson
Printed in The Netherlands
Published and distributed by: ESA Publications Division
ESTEC, Noordwijk, The Netherlands

Copyright © 2004 European Space Agency

ISBN 92-9092-989-8
ISSN 0379-6566
Price: €40

Contents

1. Introduction 1

2. Missions in Operation
   - 2.1 Hubble Space Telescope 9
   - 2.2 Ulysses 15
   - 2.3 SOHO 21
   - 2.4 Cassini/Huygens 27
   - 2.5 XMM-Newton 35
   - 2.6 Cluster 41
   - 2.7 Integral 47
   - 2.8 Mars Express 53
   - 2.9 SMART-1 57
   - 2.10 Double Star 61
   - 2.11 Rosetta 63

3. Mission in Post-Operations/Archival Phase
   - 3.1 ISO 71

4. Projects under Development
   - 4.1 Herschel 81
   - 4.2 Planck 87
   - 4.3 Venus Express 91
   - 4.4 Contributions to Nationally-led Missions
     - 4.4.1 COROT 95
     - 4.4.2 Microscope 96
     - 4.4.3 Astro-F 97
     - 4.4.4 Astro-E2 97

5. Missions under Definition
   - 5.1 BepiColombo 101
   - 5.2 Gaia 105
   - 5.3 LISA Pathfinder 109
   - 5.4 LISA 113
   - 5.5 JWST 117
   - 5.6 Eddington 121

6. Missions under Study
   - 6.1 Solar Orbiter 125
   - 6.2 Darwin 127
   - 6.3 XEUS 131
   - 6.4 Hyper 133
   - 6.5 EUSO 135
   - 6.6 Lobster-ISS 137
   - 6.7 ROSITA 139

Acronyms 143

1. Introduction

Table 1.1. ESRO/ESA scientific spacecraft.

	Launch date	*End of operational life*	*Mission*
Launched			
ESRO-II	17 May 1968	9 May 1971	Cosmic rays, solar X-rays
ESRO-IA	3 October 1968	26 June 1970	Auroral and polar-cap phenomena, ionosphere
HEOS-1	5 December 1968	28 October 1975	Interplanetary medium, bow shock
ESRO-IB	1 October 1969	23 November 1969	As ESRO-IA
HEOS-2	31 January 1972	2 August 1974	Polar magnetosphere, interplanetary medium
TD-1	12 March 1972	4 May 1974	Astronomy (UV, X- and gamma-ray)
ESRO-IV	26 November 1972	15 April 1974	Neutral atmosphere, ionosphere, auroral particles
Cos-B	9 August 1975	25 April 1982	Gamma-ray astronomy
Geos-1	20 April 1977	23 June 1978	Dynamics of the magnetosphere
ISEE-2	22 October 1977	26 September 1987	Sun/Earth relations and magnetosphere
IUE	26 January 1978	30 September 1996	Ultraviolet astronomy
Geos-2	24 July 1978	October 1985	Magnetospheric fields, waves and particles
Exosat	26 May 1983	9 April 1986	X-ray astronomy
FSLP	28 November 1983	8 December 1983	Multi-disciplinary; First Spacelab Payload
Giotto	2 July 1985	23 July 1992	Comet Halley and Comet Grigg-Skjellerup encounters
Hipparcos	8 August 1989	15 August 1993	Astrometry
Hubble Space Telescope	24 April 1990		UV/optical/near-IR astronomy
Ulysses	6 October 1990	March 2008	Heliosphere
Eureca	31 July 1992	24 June 1993	Multi-disciplinary
ISO	17 November 1995	8 April 1998	Infrared astronomy
SOHO	2 December 1995	March 2007	Sun (including interior) and heliosphere
Huygens/Cassini	15 October 1997		Titan probe/Saturn orbiter
XMM-Newton	10 December 1999	March 2008	X-ray spectroscopy
Cluster	16 July/9 August 2000	December 2005	3-D space plasma investigation
Integral	17 October 2002	December 2008	Gamma-ray astronomy
Mars Express	2 June 2003	30 November 2005	Mars exploration
SMART-1	27 September 2003	September 2005	Navigation with solar-electric propulsion
Rosetta	2 March 2004	December 2015	Comet rendezvous
Planned launches			
Venus Express	November 2005		Venus exploration
Planck	2007		Cosmic microwave background
Herschel	2007		Far-infrared and submillimetre astronomy
LISA Pathfinder	2007-2008		LISA Technology Package
JWST	2011		Next-generation space telescope
BepiColombo	2011-2012		Mission to Mercury
Gaia	≤ 2012		Galaxy mapper
LISA	2013		Search for gravitational waves
Solar Orbiter	2013-2014		Sun (including polar regions) and inner heliosphere

1. Introduction

The report for the 35th COSPAR Meeting covers, as in previous issues, the missions of the Scientific Programme of ESA in the areas of astronomy, Solar System exploration and fundamental physics. This year's COSPAR Meeting occurs only weeks after the Saturn-orbit insertion of the Cassini spacecraft – carrying Europe's Huygens probe to explore the atmosphere of Titan – and at the same time as the launch of the second satellite of the Double Star project.

A unique characteristic of ESA's science programme in 2004 is the unprecedented number of missions in operation: 14 satellites covering 11 different missions are providing excellent data to the worldwide scientific community. The Research and Scientific Support Department (RSSD) of ESA is responsible for the science operations of these missions and makes every effort to ensure the best possible science return. The Department also supports the realisation of approved projects in all phases of their development.

2003 and early 2004 saw the successful launches of three missions that are significant steps in European exploration of the Solar System. The Mars Express launch from Baikonur in June 2003 was followed by Mars-orbit insertion in December 2003. The subsequent delivery of excellent science data included outstanding stereoscopic high-resolution images. Early results included the confirmation of water ice on the surface of Mars. Unfortunately the Beagle 2 lander, carrying a suite of instruments to analyse possible traces of extinct or extant life, did not communicate with the orbiter.

The first Small Mission for Advanced Research in Technology, SMART-1, was launched in September 2003 from Kourou, French Guiana, by Ariane-5. This is a technology mission to test navigation through the Solar System by solar-electric propulsion. Its trajectory will lead to lunar orbit and permit new observations of the Moon from the end of 2004.

Rosetta was launched in March 2004 from Kourou by Ariane-5 to rendezvous with Comet Churyumov-Gerasimenko in 2014 to search for clues on the origin of the Solar System. After a year's delay, its successful launch provides Europe with the opportunity to analyse a comet nucleus *in situ* using a lander and long-duration monitoring of its behaviour by an orbiter. Rosetta will also fly past two asteroids en route to the comet. This is a major step forward since our last mission to understand the physics of comets: Giotto flew past comet Halley in 1986 and then Grigg-Skjellerup in 1992.

In December 2003, the first of two Double Star satellites, a cooperative effort with the Chinese National Space Administration, was launched from China to explore the Earth's magnetosphere, complementing the science being obtained by the four Cluster satellites. The second is due to be launched in July 2004.

The next challenge, in addition to the continuing scientific exploitation of our in-orbit satellites, is the launch of Venus Express in November 2005. A follow-on development from Mars Express, it will also be launched from Baikonur, to investigate the hostile atmosphere of the Sun's second planet.

Then follow several astronomy missions. Planck is devoted to investigation of the fine spatial variation of the cosmic background radiation, and Herschel is a powerful far-infrared and sub-millimetre observatory. They will be launched together in 2007 and stationed at the L2 Lagrangian point on the Earth-Sun line. In addition, the COROT French-led mission to study stellar oscillations and search for extrasolar planets will be launched in mid-2006 in cooperation with ESA. In the field of fundamental physics, the Microscope cooperative mission, for launch in November 2007, will test the Equivalence Principle.

In the meantime, missions in orbit continue to provide excellent results. XMM-

Newton, launched in 1999, continues to deliver new views of the X-ray Universe thanks to its large photon-collection capability and throughput. It is well into its routine phase of scientific operations as an observatory, and has proved its ability to react rapidly to targets of opportunity identified with short-lived high-energy bursts. The operation of XMM-Newton with the Integral higher-energy observatory has provided a scientific bonus. Integral itself is entering into routine operations after its commissioning and calibration phases. New views of the galactic centre and closely interacting binaries are being made available.

At lower energies, the Hubble Space Telescope (HST) continues to generate exciting results in almost all areas of astronomy, but particularly in our understanding of the extragalactic Universe. The observation of ultra-deep fields and the measurement of very distant supernovae are important examples. While the recent announcement of the cancellation of future servicing missions to HST is a major setback, it is also a challenge to develop innovative ideas to keep HST delivering excellent science for as long as possible.

In solar and heliospheric science, the four Cluster satellites are providing important physical information for understanding the 3-D magnetosphere and its connection with the Sun. To this end, the successful operation of the SOHO observatory, studying the Sun in great detail, has been very useful. SOHO continues its sophisticated and comprehensive study of the Sun's interior and outer atmosphere, as well as the solar wind, even under the difficult new constraints imposed by problems with its high-gain antenna.

For the exploration of the heliosphere outside the plane of the ecliptic, Ulysses continues its journey over the polar regions of the Sun. A second passage over the north polar region was completed during 2001, this time during a solar maximum phase which allowed comparison with the previous passage at a minimum of the activity cycle. The recent approval of another extension to the mission will enable Ulysses to fly over the solar poles for a third time. This time, the Sun's magnetic field will be reversed in polarity, allowing Ulysses to search for differences in behaviour of the interplanetary medium. It will also allow comparison of the measurements during solar minimum concurrent with data from SOHO and Cluster.

Cassini/Huygens continues its journey toward Saturn, already having visited Jupiter. Following arrival at the planet in June 2004, Europe's Huygens probe will be released into the atmosphere of Titan to investigate the physical nature and conditions that are expected to provide important information towards understanding the early evolution of Earth's atmosphere. The descent through Titan's thick atmosphere will take place in January 2005.

Work continues on missions in their post-operational phase, after switch-off of the spacecraft, aimed at obtaining a full homogeneous recalibration of the observations and the delivery of final archives to the scientific community. In the case of the International Ultraviolet Explorer (IUE), the final archive was delivered some time ago and handed over to national organisations. In the case of the Infrared Space Observatory (ISO), the active archive phase continues to improve the quality and accessibility of the data by improving the previous global pipeline analyses that populated the existing archive.

Concerning missions under development, activities now centre on Planck and Herschel. LISA Pathfinder (previously named SMART-2), the technology mission designed to test the technologies for measuring gravitational waves in space, is planned for launch in 2007.

There are also missions in their study or definition phases, some with launch dates planned between 2010 and 2014. These are the European contribution to the James

Webb Space Telescope, the LISA gravitational waves observatory, the BepiColombo mission to planet Mercury, the Gaia mission for unprecedented high-quality 3-D studies of the stellar content of our Galaxy, and Solar Orbiter, a mission to study the Sun. Beyond, missions such as Darwin, to characterise extrasolar planets, and the XEUS new-generation large X-ray observatory, are under study.

2. Missions in Operation

2.1 Hubble Space Telescope

Introduction

The Hubble Space Telescope (HST) continues to return data of unprecedented quality as a result of the instrument upgrades made by the crew of Space Shuttle *Columbia* on its last mission (Servicing Mission 3B, SM3B). Almost 60% of Hubble's observations use the Advanced Camera for Surveys (ACS), installed on HST in April 2002, as one of the third-generation of instruments. It consists of three independent cameras that provide wide-field, high-resolution and UV imaging, respectively, with a broad assortment of filters designed to address a wide range of scientific goals. Additional coronographic, polarimetric and grism capabilities make this a versatile and powerful instrument.

Four major surveys of distant galaxies have been completed or are underway with ACS: the Great Observatories Origins Deep Survey (GOODS), Galaxy Evolution from Morphologies and SEDS (GEMS), COSMOS and the Hubble Ultra Deep Field (HUDF). Observations with HST have had an impact on every area of astronomical research. A few highlights of the results obtained during 2003 are presented here.

Science achievements

Solar System

Astronomers have estimated that there are 100 000 objects larger than 100 km orbiting in the 'Kuiper belt' between about 38 AU and 50 AU from the Sun. They are the remnants of a once more-massive group of planetesimals that formed near the primordial locations of Uranus and Neptune. Twelve years after the discovery of the first Kuiper Belt Object (KBO) after Pluto, 1992 QB1, the orbits of hundreds are now well determined.

Perhaps the most startling and intriguing discovery about KBOs was made in 2001 by C. Veillet and his collaborators (CFHT), during routine follow-up observations of recently discovered KBOs: KBO1998 WW31 turned out to be a pair! Rapid follow-up observations with Hubble quickly confirmed this object is a binary, and eventually led to a determination of the binary orbit. By the end of 2003, it was found that 13 KBOs are gravitationally-bound pairs, including, of course, Pluto itself.

Hubble has discovered more than half of the known KBO binaries, because most ground-based observations do not have the sub-arcsec resolution needed to resolve objects of 23rd to 25th visual magnitude separated by a few tenths of an arcsec or less. These are true binaries with widely separated pairs of similar-mass objects. Nothing like the KBO binaries exists elsewhere in the Solar System. The surveys with Hubble have found that at least 5% of KBOs have binary companions of equal brightness within a magnitude and are separated for at least part of their orbit by more than 0.1 arcsec. As with all binaries, knowledge of the orbit provides the mass of the components, and the measured masses open the way to understanding their composition, structure, formation and collisional history. On the basis of these observations, it was concluded that KBO binaries are primordial. The binaries cannot be produced by any conceivable mechanism in the current Kuiper belt, and they must have formed at a time when the density of objects was hundreds of times greater than it is today.

The intriguing lives of stars

HST continued to provide fascinating details about the lives of the stars, from birth to death, and their effects on the interstellar environment.

The previously unknown variable star V838 Monocerotis erupted in early 2002, brightening suddenly by a factor of almost 10 000 at visual wavelengths. An expanding light echo appeared around the star shortly after, as illumination from the outburst propagated into a surrounding, existing circumstellar dust cloud (Fig. 2.1.1). This is the first light echo seen in the Milky Way since 1936. A series of high-

For further information, see http://ecf.hq.eso.org/

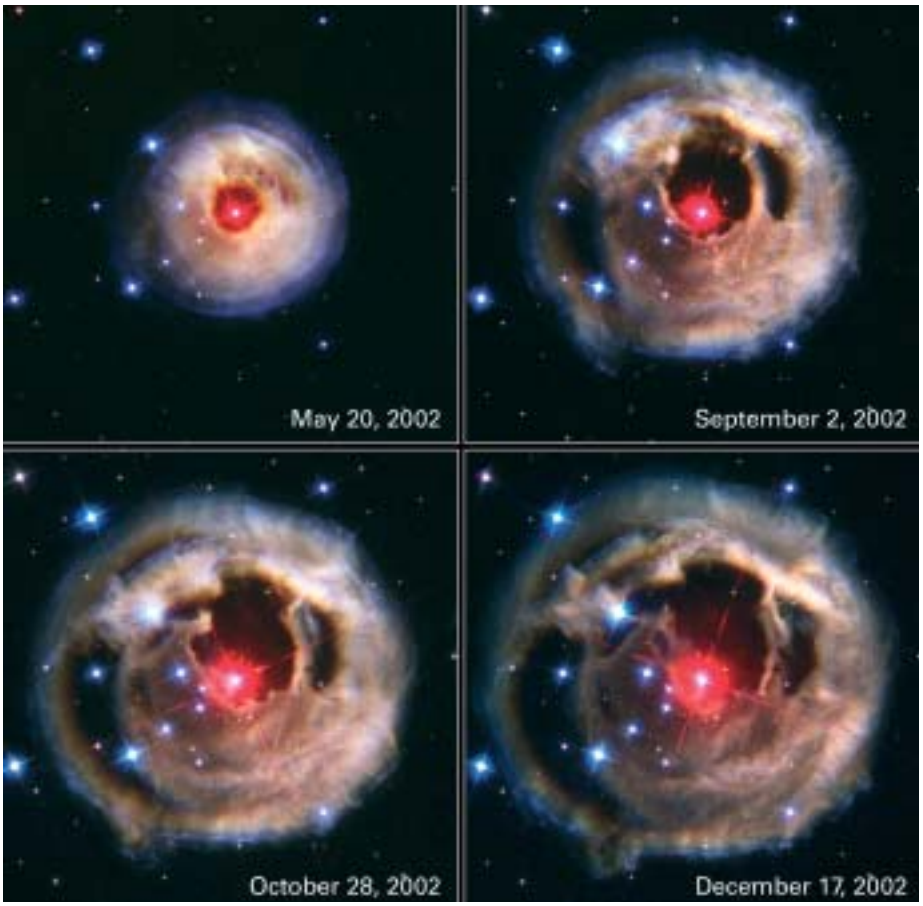

Figure 2.1.1. ACS images of V838 Mon obtained at four epochs, between 20 May 2002 (upper-left) and 17 December 2002 (lower-right). The three-colour (*BVI*) frames have been used to make renditions that are excellent approximations to true-colour images. The nebulosity exhibits a wealth of sub-arcsec cirrus-like structure, but is dominated (especially at early epochs) by a remarkable series of near-circular arcs and rings, centred on the variable star. It should be noted that we are viewing a pre-existing circumstellar dust cloud, temporarily made visible by light from the star's outburst. The exact linear size depends on the distance to the object, but all of the visible material lies within about 1-1.5 pc of the star. (Courtesy NASA; H. Bond, N. Panagia (ESA/STScI)).

resolution images of the star and its surrounding medium, and polarimetry of the light echo, were obtained by ACS.

The echo exhibits a series of circular arcs, whose angular expansion rates show that the distance is > 2 kpc. The polarimetric imaging implies an even greater lower limit to the distance of 6 kpc. Both of these limits mark the first time that these phenomena have been used to constrain an astronomical distance in the Milky Way. At maximum light, the object was extremely luminous, at least as bright as M_V –9.6. The spectrum of the star during the outburst remained that of a cool stellar photosphere, but a composite spectrum appeared as the outburst subsided. V838 Mon thus appears to represent a new class of stellar outbursts, occurring in binary systems containing a relatively hot main-sequence star and a companion that erupts to become a cool supergiant. A remarkably similar event was seen in the Andromeda Galaxy in the late 1980s.

Nearby galaxies

Relying on the deepest visible-light images ever taken in space, astronomers have measured the age of the spherical halo of stars surrounding the neighboring Andromeda Galaxy (M31). They have discovered that approximately a third of the stars in Andromeda's halo were formed only 6-8 billion years ago, a very different value from the 11-13 billion-year age of the stars in our Galaxy's halo.

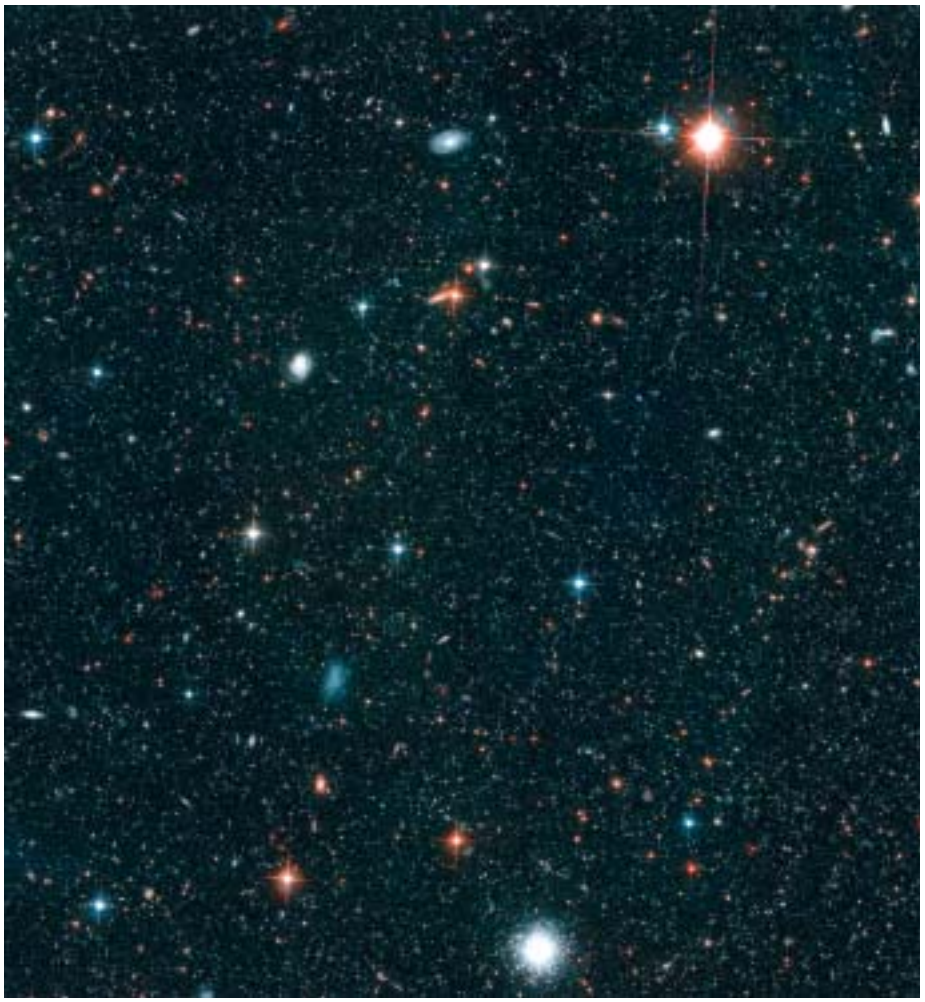

Figure 2.1.2. 300 000 stars belonging to the halo of the nearest neighboring spiral galaxy, Andromeda (M31), are shown in this image, taken by HST/ACS. Note the myriad of stars superimposed on the field of faint far galaxies. Because the image captures both faint dwarf stars and bright giant stars, astronomers can estimate the age of the halo population by analysing its distribution of colour and brightness. (Courtesy NASA; Tom Brown (STScI))

Why the difference in halo ages? Apparently, M31 must have gone through a major merger with another large galaxy, or a series of mergers with smaller galaxies, billions of years ago. It is not clear whether this was one tumultuous event or a more continual acquisition of smaller galaxies. The newly discovered younger stars in Andromeda's halo are richer in heavier elements than the stars in our halo, or in most of the small dwarf galaxies that surround the Milky Way. Indeed, the level of chemical enrichment seen in these younger stars is characteristic of relatively massive galaxies, containing at least a billion stars.

This suggests three possibilities: collisions destroyed the young disc of M31 and dispersed many of its stars into the halo; a single collision destroyed a relatively massive invading galaxy and dispersed its stars and some of Andromeda's disc stars into the halo; and/or many stars formed during the collision itself.

Previously, telescopes could see only the bright giant stars in the halo population, but the population of 'normal' stars like our own Sun was beyond our grasp, because such stars in M31 are so faint. ACS could resolve ~300 000 of these halo stars (Fig. 2.1.2), superimposed on thousands of background galaxies (down to magnitude +31) billions of light-years away.

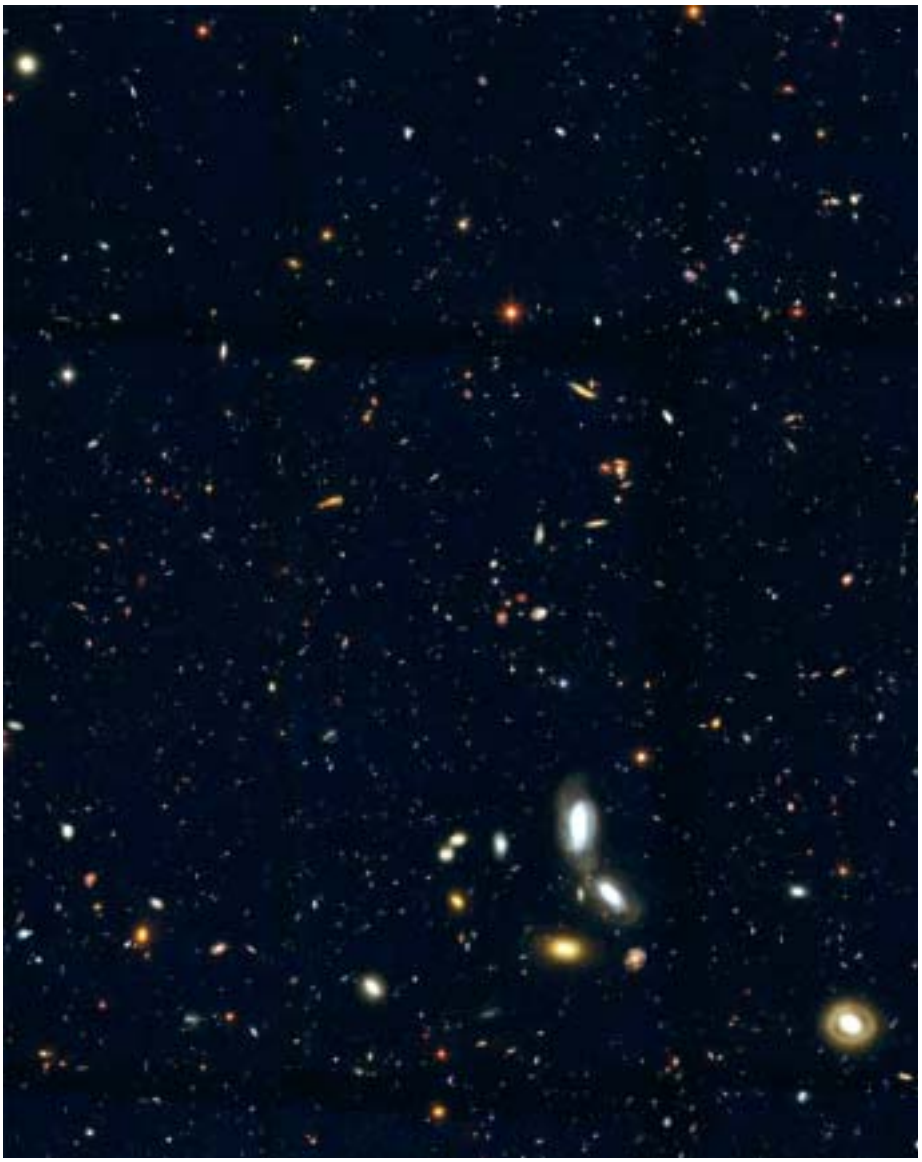

Figure 2.1.3. A colour-composite showing a portion of the GOODS Southern Field extracted from the v1.0 release of the GOODS ACS data. (Courtesy NASA; Mauro Giavalisco (STScI))

Cosmology

The GOODS project is a major survey, which used 398 orbits with ACS, to cover a total area of ~0.1 square degrees in two fields, Hubble Deep Field North (HDF-N) and Chandra Deep Field South (CDF-S), in the four bands B, V, I and z. It is part of a greater collaboration, which includes matched imaging observations with SIRTF, and Chandra, plus systematic follow-up programmes from the ground, including spectroscopic observations from the Keck Telescope.

The primary scientific goals of the survey were: to identify a sample of about 12 Type Ia SNe at $z > 1$ to provide an unambiguous detection of the presence of dark energy in the kinematics of the Hubble expansion; to measure the evolution of stellar mass and star-formation activity in galaxies over the redshift range $0.5 < z < 6$; to

investigate the assembly of the Hubble sequence; to measure the evolution of dark matter structure on galaxy scales at $0.5 < z < 2$ with weak lensing measures; provide a census of obscured and unobscured AGN up to $z < 6$ and investigate the relationship between galaxy and AGN evolution.

On 29 August 2003, the GOODS Team reached a major milestone with the release of the version v1.0 of the reduced ACS multiband imaging data taken. The results have largely exceeded expectations within a few months of the release of the first full-depth science data. The quality of the reduced data and the overall cosmetics of the images is extremely good, with the 10 σ limiting flux (for point sources) being 27.3, 27.5, 27.3 and 27.0 AB magnitude in the *B*, *V*, *I* and *z* band, respectively, only ~0.6 magnitudes shallower than the sensitivity of the original HDF. Fig. 2.1.3 is a colour composite showing a portion of the GOODS Southern Field extracted from the first release of the data.

A truly remarkable result from GOODS has been the identification of a sample of 15 Type Ia supernovae at $z > 1$. This was achieved through the combined efforts of the GOODS Team and the High-*z* SNe Team. The former provided the detections of the optical transients, thanks to the arrangement of the observations into Epochs cadenced by ~45 days, and the identification of the Type Ia candidates based on colour criteria, made possible by the multi-band observations. The latter provided follow-up ACS and NICMOS imaging to measure the light curves of the SNe, and ACS grism spectroscopy to measure their redshifts. This unique sample has been used to provide the strongest constraints to date on the transition from a decelerated cosmic expansion to an accelerated one, plus the most accurate estimate so far of SNe rates and their relation to star formation rate.

The exquisite sensitivity, broad wavelength coverage and the large area covered by GOODS (0.1 square degree or 33 times larger than the two HDFs) have yielded the best samples to date of star-forming galaxies at very high redshfits, namely Lyman-break galaxies at $z \sim 4$, 5, 6. The GOODS Team carefully measured incompleteness and selection bias of the survey through an extensive work of numerical simulations, where artificial galaxies of known properties were inserted into the real data and then retrieved as if they were real. This has allowed the Team to estimate with good confidence level the UV luminosity density, and thus the star formation density, of Lyman-break galaxies from $z \sim 3$ all the way up to $z \sim 6$. There is evidence that intense 'cosmic' star formation, as traced by the star-formation density of Lyman-break galaxies, was occurring very early in the cosmic evolution, at $z \sim 6$ (less than 7% of the cosmic age), and that it continued with approximately the same intensity all the way to $z \sim 1$ (about 43% of the cosmic age). The conclusion is that a large fraction of the current stellar mass density, possibly as much as 50%, formed very early in cosmic history, suggesting that those early galaxies were likely progenitors of present-day spheroids.

The unique angular resolution of HST/ACS has allowed accurate measurement of sizes and light profiles of these galaxies, enabling for the first time a measure of the early evolution of galaxy sizes from $z \sim 6$ to $z \sim 1.5$ and their use to constrain cosmological models. This shows that the evolution is the one predicted by the theory if a major driver is accretion and continuous merging of smaller galaxies.

2.2 Ulysses

Introduction

Ulysses is an exploratory mission being carried out jointly by ESA and NASA. Its primary objective is to characterise the uncharted high-latitude regions of the heliosphere within 5 AU of the Sun, under a wide range of solar activity conditions. Ulysses has, for the first time, permitted *in situ* measurements to be made away from the plane of the ecliptic and over the poles of the Sun. Its unique trajectory (Fig. 2.2.1) has taken the spacecraft into the unexplored third dimension of the heliosphere.

The European contribution to the Ulysses programme consists of the provision and operation of the spacecraft and about half of the experiments. NASA provided the launch aboard Space Shuttle *Discovery* (together with the upper-stage motor) and the spacecraft power generator, and is responsible for the remaining experiments. NASA also supports the mission using its Deep Space Network.

The broad range of phenomena being studied by Ulysses includes the solar wind, heliospheric magnetic field, solar radio bursts and plasma waves, solar and interplanetary energetic particles, galactic cosmic rays, interstellar neutral gas, cosmic dust and gamma-ray bursts. A summary of the nine sets of instruments is presented in Table 2.2.1.

While the focus of the mission is clearly concerned with latitudinal variations, other investigations carried out by Ulysses have included detailed interplanetary-physics studies during the in-ecliptic Earth-Jupiter phase (October 1990 to February 1992), and measurements in the jovian magnetosphere during the Jupiter encounter. The spacecraft and ground telecommunication systems have been used to conduct radio-science investigations into the structure of the corona and a search for gravitational waves. Last, but not least, Ulysses continues to make important contributions to our knowledge of the Local Interstellar Medium, and to topics of a broad astrophysical nature.

In addition to the science teams selected at the start of the project, the group of scientists directly associated with the mission comprises nine European Guest Investigator teams, a similar number of NASA Guest Investigators, and the European Interdisciplinary Investigators who were selected together with the hardware teams.

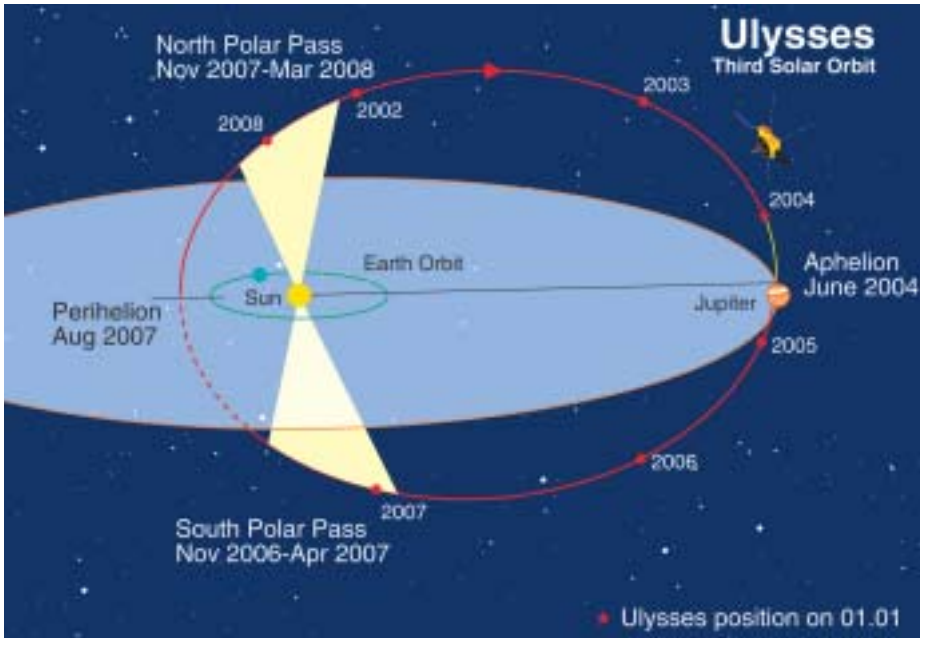

Figure 2.2.1. The Ulysses orbit viewed from 15 deg above the ecliptic plane. Dots mark the start of each year.

For further information, see http://helio2.estec.esa.int/ulysses/

Table 2.2.1. The Ulysses scientific payload.

Expt. Code	*Investigation*	*Scientific Acronym*	*Principal Investigator*	*Collaborating Institutes*
HED	Magnetic field	VHM/FGM	A. Balogh, Imperial College London (UK)	JPL (USA)
BAM	Solar wind plasma	SWOOPS	D.J. McComas, Southwest Research Institute (USA)	Los Alamos National Lab (USA) Ames Research Center (USA); JPL (USA); HAO Boulder (USA) Univ of Boston (USA); MSFC (USA); MPAe Lindau (D)
GLG	Solar wind ion composition	SWICS	J. Geiss, ISSI (CH); G. Gloeckler, Univ of Maryland (USA)	Univ of New Hampshire (USA); GSFC (USA); TU Braunschweig (D); MPAe Lindau (D); Univ of Michigan (USA)
STO	Unified radio and plasma waves	URAP	R.J. MacDowall, GSFC (USA)	Obs de Paris Meudon (F); Univ of Minnesota (USA); CETP Velizy (F)
KEP	Energetic particles and interstellar neutral gas	EPAC/GAS	N. Krupp, MPAe Lindau (D)	Imperial College (UK); Swedish Inst Space Physics Kiruna & Umeå (S); Aerospace Corp (USA); Univ of Bonn (D); MPE Garching (D); Polish Acad Sciences (P)
LAN	Low-energy ions and electrons	HI-SCALE	L.J. Lanzerotti, Bell Laboratories (USA)	APL Laurel (USA); UC Berkeley (USA); Univ of Kansas (USA); Obs de Paris Meudon (F), Univ of Thrace (Gr); Univ of Birmingham (UK)
SIM	Cosmic rays and solar particles	COSPIN	R.B. McKibben, Univ of New Hampshire (USA)	Imperial College (UK); ESA Research & Scientific Support Dept (NL); NRC Ottawa (Can); Univ of Kiel (D); CEN Saclay (F); Danish Space Research Inst (DK); NCR Milan (I); MPK Heidelberg (D); Univ of Maryland (USA); MPAe Lindau (D)
HUS	Solar X-ray and cosmic gamma-ray bursts	GRB	K. Hurley, UC Berkeley (USA) M. Sommer (retired), Samerberg (D)	CESR Toulouse (F); SRON Utrecht (NL); Obs de Paris Meudon (F); GSFC (USA)
GRU	Cosmic dust	DUST	H. Krüger, MPK Heidelberg (D)	Univ of Canterbury (UK); ESA Space Science Dept (NL); MPE Garching (D); JSC (USA); Univ of Florida (USA)

Status

Ulysses was launched by the Space Shuttle on 6 October 1990, using a combined IUS/PAM-S upper-stage to inject the spacecraft into a direct Earth/Jupiter transfer orbit. A gravity-assist manoeuvre at Jupiter in February 1992 placed the spacecraft in its final Sun-centred out-of-ecliptic orbit, which has a perihelion distance of 1.3 AU and an aphelion of 5.4 AU. The orbital period is 6.2 years. Key mission milestones, including details of the polar passes (defined to be the parts of the trajectory when the spacecraft is above 70º heliographic latitude in either hemisphere), are presented in Table 2.2.2.

Table 2.2.2. Key dates in the Ulysses mission.

Events	*Date*
Launch	1990 10 06
Jupiter flyby	1992 02 08
start	1994 06 26
maximum latitude (80.2°, 2.3 AU)	1994 09 13
end	1994 11 05
1st Perihelion (1.34 AU)	1995 03 12
2nd Polar Pass (north)	
start	1995 06 19
maximum latitude (80.2°, 2.0 AU)	1995 07 31
end	1995 09 29
Start of Solar Maximum Mission	1995 10 01
Aphelion (5.40 AU)	1998 04 17
3rd Polar Pass (south)	
start	2000 09 06
maximum latitude (80.2°, 2.3 AU)	2000 11 27
end	2001 01 16
2nd Perihelion (1.34 AU)	2001 05 23
4th Polar Pass (north)	
start	2001 08 31
maximum latitude (80.2°, 2.0 AU)	2001 10 13
end	2001 12 12
Jupiter approach (0.8 AU)	2004 02 04
Aphelion	2004 06 30
5th Polar Pass (south)	
start	2006 11 17
maximum latitude	2007 02 07
end	2007 04 03
3rd Perihelion	2007 08 18
6th Polar Pass (north)	
start	2007 11 30
maximum latitude	2008 01 11
end	2008 03 15
End of Mission	2008 03 15

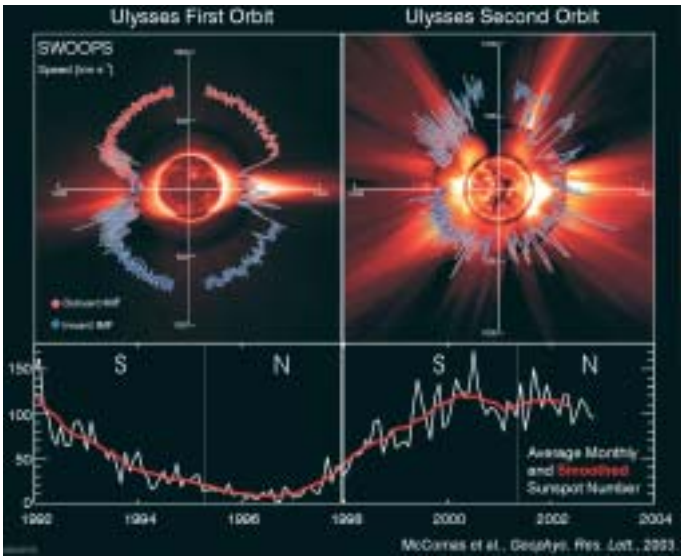

Figure 2.2.2. A comparison of solar wind observations from the solar minimum (left panel) and around solar maximum (right panel) phases of the mission. (Courtesy D.J. McComas)

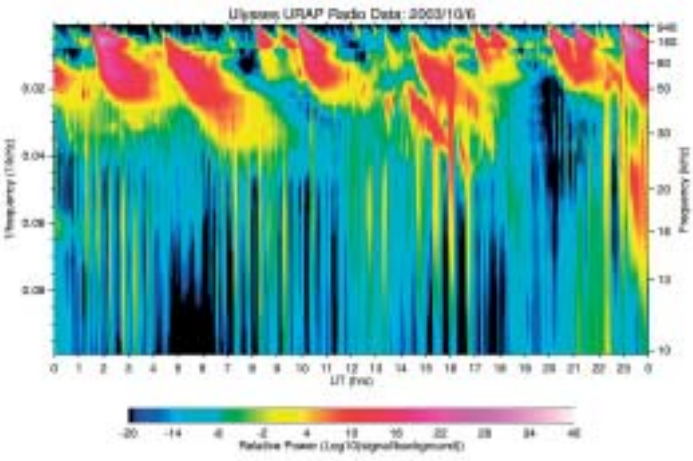

Figure 2.2.3. An example of quasi-periodic (~40-min period) radio bursts from Jupiter, detected by the URAP experiment in October 2003.
(Courtesy R.J. MacDowall)

The mission is well into its 14th year, and all spacecraft systems and the nine sets of scientific instruments continue to function well. Spacecraft operations, conducted by the joint ESA-NASA Mission Operations Team at the Jet Propulsion Laboratory (JPL), have proceeded in a highly efficient and productive way, with very few anomalies. In February 2003, an autonomous switch-over from the prime to the back-up Travelling Wave Tube Amplifier (TWTA) occurred. The planned switch-back to the prime unit was unsuccessful, and a failure of the prime travelling wave tube is considered possible because it has been in continuous operation for 12 years. The back-up TWTA is functioning normally, however, and is expected to support communications for the remainder of the mission. Starting in May 2002, it became necessary to implement a power-sharing strategy for the science payload. This is a result of the decreasing output of the Radioisotope Thermoelectric Generator (RTG) that provides onboard power, and the associated reduction in platform temperature.

Based on both scientific and technical arguments, a sub-set of the instruments (the 'core payload') remains switched on permanently, while the remainder are operated according to a pre-determined switching plan. In this way, the safety of the spacecraft is guaranteed, with the minimum impact on the scientific output of the mission.

A recent highlight from the science operations point of view has been the second 'encounter' with Jupiter that took place in late 2003/early 2004. Although the spacecraft remained relatively far from Jupiter this time (closest approach was 0.8 AU), it was able to observe previously unexplored regions of the jovian magnetosphere. A bonus was the availability of 24 h/day real-time coverage for a 50-day period around the encounter that allowed the onboard tape recorders to be switched off. In this way, sufficient power was available to operate the full payload suite without the need for power sharing. The spacecraft will reach aphelion at the end of June 2004, and then begin its slow climb to high southern latitudes.

At its meeting in Paris on 11-12 February, ESA's Science Programme Committee unanimously approved a proposal to continue operating the highly successful Ulysses spacecraft until March 2008. This latest extension, the third of the mission, will enable Ulysses to fly over the poles of the Sun for a third time, under conditions similar to those in 1994/1995 when it first visited the Sun's poles. However, this time the magnetic field of the Sun will be reversed in polarity, allowing Ulysses to search for differences in behaviour of the interplanetary medium related to the field reversal. Another difference between the solar minimum polar passes in 2007/2008 and those in 1994/1995 will be that Ulysses will have the additional benefit of being part of a fleet of solar and heliospheric spacecraft, including ESA's SOHO and Cluster, and NASA's ACE and Cassini. New missions, like NASA's dual-spacecraft STEREO and the Solar Dynamics Observatory, will add a further dimension over the next few years.

Scientific highlights

From its unique out-of-ecliptic vantage point, Ulysses has continued to monitor the re-structuring of the extended solar corona following the recent solar maximum. The spacecraft spent more than 3 months at the end of 2001 fully immersed in the fast (~750 km/s) solar wind from the newly-formed north polar coronal hole. This was followed by a period of regular excursions back into the slow wind, with Ulysses skimming the boundary of the north polar hole. Observations from the solar wind plasma (SWOOPS) and ion composition (SWICS) instruments have been combined to carry out the first-ever study of solar wind flows from high-latitude coronal holes near solar maximum. This study has shown that, while the wind from coronal holes has unique chromospheric and coronal composition signatures, it can exhibit a range of flow speeds. High-speed wind can be produced in small as well as large coronal holes, although the highest speeds are found to originate in the centres of the largest holes. Ulysses has sampled the edges of coronal holes in detail in recent months as it returned slowly to lower latitudes. Here, the acceleration decreases and the freezing-in temperatures increase relatively smoothly into the surrounding solar wind, indicating a transition layer around the edges of coronal holes. From October 2002 onwards, there were no more excursions into the high-speed solar wind from the northern polar coronal hole, and Ulysses has spent most of the time since in more variable, lower-speed flows.

In line with the decreasing level of solar activity, the Sun's magnetic dipole has started to dominate the global magnetic field configuration again. The angle between the dipole and rotational axes, nearly 90^{o} at solar maximum, has also decreased. As a consequence, the heliospheric current sheet that separates inward (negative) magnetic

fields from outward (positive) magnetic fields has become less inclined with respect to the solar equator. These large-scale changes have had a significant effect on the energetic particles measured at Ulysses. For the majority of the period, only modest increases in particle fluxes have been observed, with very few transient-related events.

Starting at the end of October 2003, however, the Sun underwent a major surge in activity. Strong outbursts in the form of solar flares and coronal mass ejections (CMEs) are often seen during the declining phase of a solar cycle (the sunspot maximum of the current solar cycle (23) occurred in mid-2000); the recent activity, however, was unusual both in its intensity, and its relative lateness. The largest solar flare of the series, rated at X28, occurred on 4 November 2003 while the responsible active region was on the Sun's west limb, rotating off the visible disc. Although quite far from the Sun (5.3 AU), Ulysses was well placed to observe the effects of this violent outburst, being more or less in the 'line of fire'. Analysis of data from the event is still underway, but indications are that the fast CME that was associated with the X28 flare swept over Ulysses, driving a significant interplanetary shock wave. Impressive enhancements in the flux of energetic particles, modulated by the passage of CME-related solar wind transients – and the passage of high-speed solar wind streams originating in a large, persistent, trans-equatorial coronal hole – were seen at Ulysses throughout the period of increased activity. The study of the precise mechanisms whereby solar energetic particles are distributed throughout large volumes of the heliosphere, and under which conditions efficient re-acceleration of these particles occurs, remains an important area of research using data from Ulysses. This unusual solar activity period appears to have been the Sun's final outburst before settling into a more stable configuration leading to the next solar minimum.

Jupiter has figured strongly in the scientific activities of the Ulysses teams in recent months. As noted above, the spacecraft 'encountered' the giant planet for the second time in February 2004. Unlike the 1992 flyby, however, this was a distant encounter. Another difference was that Ulysses this time approached the planet from high northern latitudes. This difference was already apparent in the radio data acquired by the Unified Radio and Plasma Wave (URAP) experiment as far back as February and March 2003. URAP detected intense radio emission from Jupiter, at levels well above those seen in 1993 when Ulysses was at comparable distance from the planet (about 2.8 AU). The unusual approach geometry was particularly well suited to the study of periodic auroral phenomena that produce both radio and X-ray bursts. For example, URAP has detected numerous quasi-periodic (40-min period on average) radio bursts during the encounter. These bursts, which were also seen in 1992/93, are thought to be triggered by solar wind transients impacting Jupiter's magnetosphere. Similar periodicities have been observed in jovian X-rays by the Chandra observatory, primarily from the northern hemisphere. This suggests a common source mechanism. Another interesting result obtained during the encounter concerns jovian dust streams. Thought to originate in the volcanos of Jupiter's moon Io, these dust streams were discovered by Ulysses, and have also been observed by the Galileo and Cassini spacecraft. The recent Ulysses data presented a new aspect, however. The dust streams recurred with a period of approximately 28 days, and showed a fine structure that was not observed previously.

Ulysses is not normally associated with the study of comets. Nonetheless, the probe demonstrated its ability as a 'comet catcher' when it crossed the distant tail of Comet Hyakutake (C/1996 B2) in 1996. The same Ulysses teams who identified that particular comet tail recently presented evidence for one (and possibly two) new tail crossings. This time, however, Ulysses needed a little help from the Sun to make the

right connection. The comets involved were McNaught-Hartley (C/1991 T1) and SOHO (C/2000 S5). Unlike Hyakutake, these comets seemed to be at the wrong location for Ulysses to intercept their tails. By chance, a CME moving from the Sun enveloped both the comet and the spacecraft, carrying the cometary material to Ulysses.

Ulysses data archive

Data from the Ulysses investigations and flight project are being archived and made accessible to the public through two channels: the ESA Ulysses Data Archive at ESTEC, and NASA's National Space Science Data Center (NSSDC). At its meeting in October 2002, the Ulysses Science Working Team agreed unanimously to do away with the formal 1-year proprietary period for Ulysses data. Data are now placed in the public archive immediately following verification by the PI teams. The ESA archive provides an on-line facility to browse and download selected measurements made by the scientific instruments. The user is able to view 26-day and 1-year summary plots of the main parameters measured, and to download ASCII data files and accompanying documentation for further analysis. The ESA archive is accessible via the Ulysses homepage.

2.3 SOHO

Introduction

Since its launch in 1995, the joint ESA/NASA SOHO mission has provided a wealth of information about the Sun, from the interior, through the hot and dynamic atmosphere, to the solar wind and its interaction with the interstellar medium. Research using SOHO observations has revolutionised our understanding of the Sun, and science teams from around the world have made great strides towards a better understanding of 'the big three' areas of research that SOHO set out to tackle: the structure and dynamics of the solar interior, the heating of the solar corona, and the acceleration of the solar wind. However, much remains to be done. The findings have been documented in an impressive body of scientific literature and popular articles, the number of which continues to grow. SOHO enjoys a remarkable 'market share' in the worldwide solar physics community, with more than 1600 papers in refereed journals representing the work of over 1500 scientists. At the same time, SOHO's easily accessible, spectacular data and basic science results have captured the imaginations of the space science community and the general public alike.

In September 2003, the SOHO team was awarded the Laurels for Team Achievement Award of the International Academy of Astronautics. On 2 December 2003, SOHO celebrated its eighth anniversary in space. As part of this celebration, 24 000 participants voted to select the top 10 images from the SOHO mission. The winning picture is featured in Fig. 2.3.1.

A summary of SOHO's 12 instruments, which is the most comprehensive set of solar and heliospheric instruments ever developed and carried on the same platform, is presented in Table 2.3.1.

Mission status

SOHO was launched by an Atlas IIAS from Cape Canaveral on 2 December 1995 and inserted into an halo orbit around the L1 Lagrangian point on 14 February 1996, 6 weeks ahead of schedule. An extension of the SOHO mission for a period of 5 years beyond its nominal lifetime, i.e. until March 2003, was approved in 1997. An extension to March 2007 was approved by ESA's Science Programme Committee in February 2002.

In early May 2003, the east-west pointing mechanism of SOHO's high-gain antenna started missing steps; by late June it appeared to be stuck. Using both primary and redundant motor windings simultaneously, the mechanism was parked in a position that maximises the time it can be used throughout a 6-month halo orbit, with the spacecraft rotated by 180° for half of each orbit and with 'keyhole periods' twice per orbit. During the keyholes, the low-gain antenna can be used with larger Deep Space Network stations to receive science telemetry, but data losses of varying magnitude occur depending on the competition for these resources.

Operations

The SOHO Experiment Operations Facility (EOF), at NASA's Goddard Space Flight Center (GSFC), serves as the focal point for mission science planning and instrument operations. There, the experiment teams receive real-time and playback telemetry, process these data to determine instrument commands, and send commands directly from their workstations through the ground system to their instruments, both in near real-time and on a delayed execution basis.

From the very beginning of the mission, much of the observing time of the SOHO experiments has been devoted to coordinated campaigns. As of mid-February 2004, the SOHO campaign database lists a total of 955 coordinated campaigns. Of these, 315 involved ground-based observatories, 110 involved Yohkoh and 365 involved TRACE.

For further information, see http://soho.estec.esa.nl

Figure 2.3.1. The winner of SOHO's 8th Anniversary Top 10 images vote.

With the successful launch of the RHESSI (Reuven Ramaty High Energy Solar Spectroscopic Imager) mission on 5 February 2002, long-established plans for SOHO-RHESSI collaborations were activated. Daily target selections by a solar flare research group (the 'Max Millennium group') are guiding SOHO and TRACE planners (and numerous ground-based observatories) whenever active-region studies are being contemplated. This ensures the maximum scientific usefulness of the observations for those that want to perform a multi-instrument analysis of data from the SOHO archive.

The Max Millennium group is also responsible for triggering the special Joint Observing Program 'Major Flare Watch – Regions Likely to Produce Major Flares'. It allows for off-hours notification for some instruments (plus TRACE) through the Science Operations Coordinators, pre-empting most other observing plans. The Major Flare Watches have proved very successful in catching powerful flares.

Despite scheduling changes and uncertainties introduced by the developing high-gain antenna situation through part of the year, SOHO's observations are still highly coordinated: more than half the time in 2003, one or more instruments on SOHO was explicitly collaborating with another instrument or observatory. In addition, the regular observing programmes of, for example, EIT and LASCO are designed to maximise the usefulness of both data sets taken together.

An automated system has also been put in place to alert the Science Operations

Table 2.3.1. Instruments in the SOHO payload.

Investigation	*Principal Investigator*	*Collaborating Countries*	*Measurements*	*Technique*
Helioseismology				
Global Oscillations at Low Frequencies (GOLF)	A. Gabriel, IAS, Orsay, F	F, ESA, DK, D, CH, UK, NL, E, USA	Global Sun velocity oscillations (l=0-3)	Na-vapour resonant scattering cell, Doppler shift and circular polarisation
Variability of solar IRradiance and Gravity Oscillations (VIRGO)	C. Fröhlich, PMOD/WRC, Davos, CH	CH, N, F, B, ESA, E	Low-degree (l=0-7) irradiance oscillations and solar constant	Global Sun and low-resolution (12-pixel) imaging and active cavity radiometers
Michelson Doppler Imager (MDI)	P.H. Scherrer, Stanford Univ, California, USA	USA, DK, UK	Velocity oscillations high-degree modes (up to l=4500)	Doppler shift with Fourier tachometer, 4 and 1.3 arcsec resolution
Solar Atmosphere Remote Sensing				
Solar UV Measurements of Emitted Radiation (SUMER)	W. Curdt, MPAe, Lindau, D	D, F, CH, USA	Plasma flow characteristics (temperature, density, velocity); chromosphere through corona	Normal-incidence spectrometer, 50-160 nm, spectral resolution 20000-40000, angular resolution 1.2-1.5 arcsec
Coronal Diagnostic Spectrometer (CDS)	A. Fludra, RAL, Chilton, UK	UK, CH, D, USA, N, I	Temperature and density: transition region and corona	Normal and grazing-incidence spectrometers, 15-80 nm, spectral resolution 1000-10000, angular resolution 3 arcsec
Extreme-ultraviolet Imaging Telescope (EIT)	J-P Delaboudinière, IAS, Orsay, F	F, USA, B	Evolution of chromospheric and coronal structures	Full-disc images (1024×1024 pixels in 42×42 arcmin) at lines of HeII, FeIX, FeXII, FeXV
Ultraviolet Coronagraph Spectrometer (UVCS)	J.L. Kohl, SAO, Cambridge, MA, USA	USA, I, CH, D	Electron and ion temperature densities, velocities in corona (1.3-10 $R_\odot$)	Profiles and/or intensity of selected EUV lines between 1.3 and 10 $R_\odot$
Large Angle and Spectrometric COronagraph (LASCO)	R. Howard NRL, Washington DC, USA	USA, D, F UK	Structures' evolution, mass, momentum and energy transport in corona (1.1-30 $R_\odot$)	One internally and two externally occulted coronagraphs. Spectrometer for 1.1-3 $R_\odot$
Solar Wind ANisotropies (SWAN)	J.L. Bertaux, SA Verrières-le-Buisson, F	F, FIN, USA	Solar wind mass flux anisotropies. Temporal variations	Scanning telescopes with hydrogen absorption cell for Lyman-alpha
Solar Wind 'in situ'				
Charge, ELement and Isotope Analysis System (CELIAS)	P. Bochsler, Univ. Bern, CH	CH, D, USA, Russia	Energy distribution and composition. (mass, charge, charge state) (0.1-1000 keV/e)	Electrostatic deflection, time-of-flight measurements and solid-state detectors
Comprehensive SupraThermal Energetic Particle analyser (COSTEP)	H. Kunow Univ. Kiel, D	D, USA, J, F, E, ESA, IRL	Energy distribution of ions (p, He) 0.04-53 MeV/n and electrons 0.04-5 MeV	Solid-state detector telescopes and electrostatic analysers
Energetic and Relativistic Nuclei and Electron experiment (ERNE)	J. Torsti, Univ. Turku, SF	FIN, UK	Energy distribution and isotopic, composition of ions (p-Ni) 1.4-540 MeV/n and electrons 5-60 MeV	Solid-state and plastic scintillation detectors

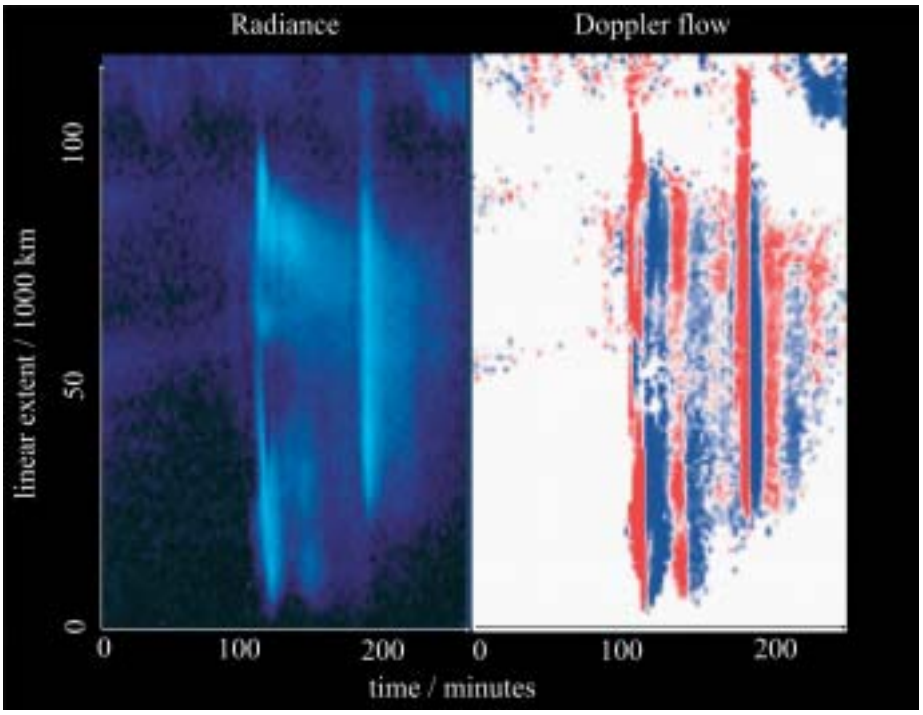

Figure 2.3.2. Hot loop oscillations as observed by SUMER. Intensity (left) and velocity (right) variations of loops observed with a thin slit (time goes from left to right in each half). Red means receding material, blue means approaching.

Centres about ongoing solar energetic particle events. They in turn notify those instrument teams who need to take precautions to minimise detector wear by turning down high voltages.

Scientific highlights

SUMER has discovered strong Doppler-shift oscillations in hot loops above active regions (Fig. 2.3.2). In subsequent studies, these oscillations have been identified as slow magnetoacoustic standing waves. The periods are typically around 10-20 min, with a comparable decay time scale. The oscillations are seen only in hot flare lines (> 6MK, e.g. Fe XVII, Fe XIX, Fe XXI). Lines formed at 'normal' coronal temperatures (1MK, e.g. Fe XII, Ca XIII, Ca X) do not show any signature of these oscillations. These events seem to be rather common. They are seen almost every time the hot lines brighten. These new and previously unexpected results may help to understand the heating of coronal loops, and open a new area of coronal seismology.

The MDI team discovered that supergranulation undergoes oscillations, supporting waves with periods of 6-9 days. This explains the long-standing puzzle of why supergranules appear to rotate faster around the Sun than the plasma. Supergranulation is a pattern of horizontal outflows at a distinct scale of 30 Mm and an apparent lifetime of 1 day, outlined by a network of magnetic features. While it is believed that supergranulation corresponds to a preferred cellular scale of thermal convection, the dynamics of supergranulation is not understood. In particular, there was no explanation for the observation that the pattern appears to rotate faster around the Sun than the magnetic features. The new study based on MDI data shows that supergranules have wave-like properties, with the waves being predominantly prograde, which explains the apparent super-rotation of the supergranulation pattern.

The Mercury transit of 7 May 2003 was a carefully coordinated and well-

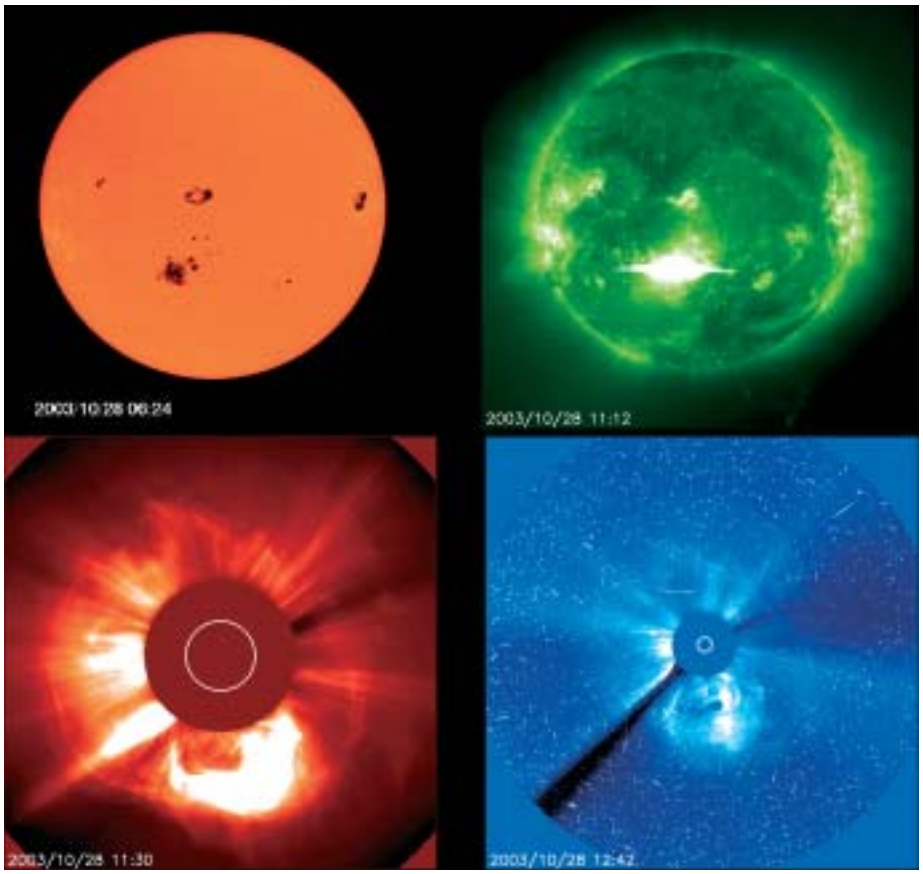

Figure 2.3.3. Region 10486 unleashed a spectacular show on 28 October 2003: an X 17.2 flare, a fast-moving Coronal Mass Ejection and a strong solar energetic particle event. From top left: giant sunspot regions 10484, 10486 and 10488 seen by MDI in white light; flare as seen by EIT in 195 Å emission; the fast-moving CME in the LASCO C2 coronagraph; then in the LASCO C3 coronagraph (with particle shower becoming visible as 'snow' in the image). The fast-moving cloud impacted Earth's magnetosphere a mere 19 h later, almost a record speed.

publicised event worldwide. MDI, EIT and CDS observed the transit mainly for instrument characterisation purposes. The SOHO web server was at times flooded by requests from all over the world.

During 2 weeks in October/November 2003, the Sun featured three unusually large sunspot groups (including the largest one of this solar cycle), 11 X-class flares (including the strongest ever recorded), numerous halo coronal mass ejections (two with near-record speeds) and two significant proton storms (Fig. 2.3.3). Satellites, power grids, radio communications and navigation systems were significantly affected. The events, among the best observed ever, with data from multiple spacecraft and ground observatories, will be analysed for years to come. The events caused unprecedented attention from the media and the public. Images from SOHO and quotes from SOHO scientists appeared in most major news outlets. The attention wiped out all existing SOHO web traffic records (requests/data volume): Monthly (31 million/4.3 TB), weekly (16 million/2.6 TB), daily (4.8 million/0.7 TB), and hourly (0.4 million/33 GB). The daily and hourly volumes were bandwidth-limited.

SOHO is providing new measurements not only of the Sun. As the brightest, most spectacular comet ever observed by SOHO, Comet NEAT (C/2002 V1) provided some enticing data for further study, thanks to a grazing encounter with a coronal mass ejection (Fig. 2.3.4). The LASCO C3 observations during 16-20 February 2003 suggest an interaction between the comet's ion tail and other magnetic fields in the outer corona at the time of the oblique impact with the CME. This would be the first

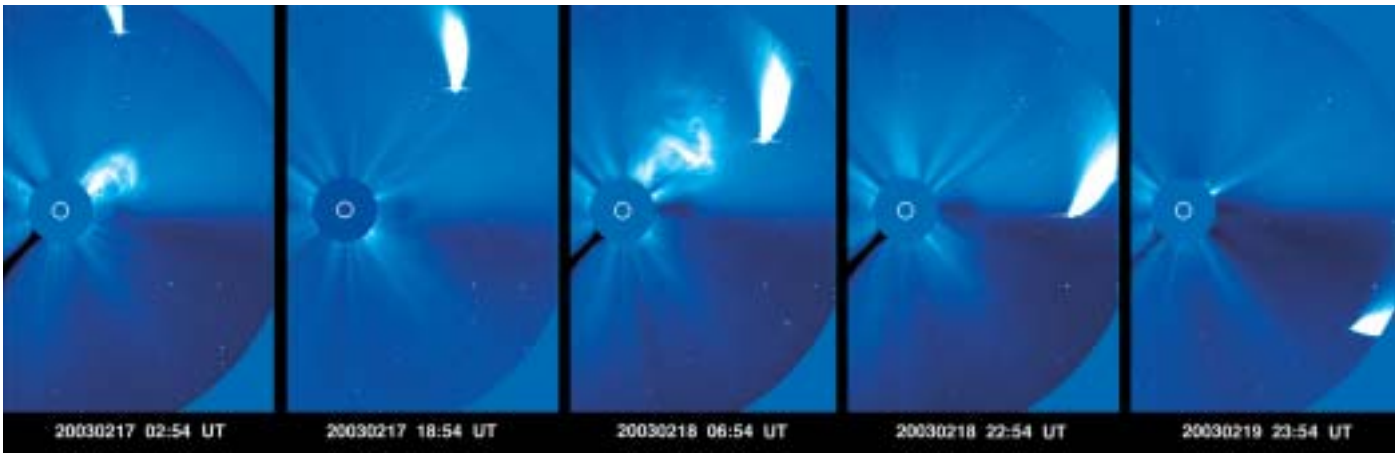

Figure 2.3.4. Perihelion passage of comet NEAT (C/2002 V1) in February 2003, as imaged by the LASCO C3 coronagraph.

time that such an interaction has been imaged, with the observations being especially impressive due to the high-cadence coverage that LASCO offers. It is also the closest to the Sun that a comet has been directly observed, and the first time that a comet's ion tail has been imaged crossing the heliospheric current sheet.

The analysis of high-resolution spectroscopic observations of comet C/2002 X5 (Kudo-Fujikawa) from UVCS reveals a quasi-spherical cloud of neutral hydrogen and a variable tail of ionised carbon (C^{+} and C^{2+}) that disconnected from the comet and subsequently regenerated. The high abundance of C^{2+} and C^{+} relative to water (24%) found is unexplainable by photodissociation of carbon monoxide but instead attributed to the evaporation and subsequent photoionisation of atomic carbon from organic refractory compounds present in the cometary dust grains.

The 11th SOHO Workshop 'From Solar Min to Max: Half a Solar Cycle with SOHO' was held in Davos, Switzerland, on 11-15 March 2002. The Workshop was dedicated to Roger M. Bonnet and attended by over 160 participants. From 27 October to 1 November 2002 the 12th SOHO Workshop was held jointly with the annual meeting of the Global Oscillation Network Group (GONG) on the topic 'Local and Global Helioseismology: The Present and Future'. It focused on the study of the interior of the Sun from a seismic perspective and the prospects for similar study of Sun-like stars. The Workshop provided an excellent opportunity for the scientific community to pause and reflect on the status of this fertile field, with more than half a solar cycle of SOHO and GONG observations. More than 120 participants discussed over 100 papers. The 13th SOHO Workshop 'Waves, Oscillations and Small-scale Transient Events in the Solar Atmosphere: A Joint View of SOHO and TRACE' was held at Palma de Mallorca, Balearic Islands, Spain, on 29 September to 2 October 2003. Nearly 100 participants presented and discussed over 110 papers and posters.

2.4 Cassini/Huygens

Introduction

Huygens is the element contributed by ESA to Cassini/Huygens, the joint NASA/ESA planetary mission to the Saturnian system. Titan, the largest moon of Saturn, is a central target of the mission. The Saturn Orbiter is provided by NASA, while the Italian Space Agency (ASI) has contributed its high-gain antenna and other radio subsystem equipment under a bilateral NASA/ASI agreement. The Jet Propulsion Laboratory (JPL, Pasadena, California) is managing the mission for NASA. The overall mission is named after the French/Italian astronomer Jean-Dominique Cassini, who discovered several Saturnian satellites and ring features, including the Cassini division, during 1671-1685. ESA's probe is named after Dutch astronomer Christiaan Huygens, who discovered Titan in 1655.

The Cassini/Huygens spacecraft was launched on 15 October 1997 by a Titan IVB-Centaur rocket from Cape Canaveral Air Force Station in Florida. The 5.6 t spacecraft was too heavy to be injected into a direct trajectory to Saturn, so the interplanetary voyage of about 6.7 years includes gravity-assist manoeuvres at Venus, Earth and Jupiter (Fig. 2.4.1). Upon arrival at Saturn, the spacecraft will be inserted into orbit around Saturn. At the end of the third revolution around Saturn, the Orbiter will deliver the Huygens Probe to Titan. After completion of the Probe mission, the Orbiter will carry out its exploration of the Saturnian system during 75 orbits around Saturn over 4 years. It will make repeated close flybys of Titan, both for data gathering about the moon and for gravity-assist orbit changes that will permit it to make a tour of Saturn's satellites, reconnoitre the magnetosphere and obtain views of Saturn's higher latitudes. During its 4-year nominal mission, Cassini will make detailed observations of Saturn's atmosphere, magnetosphere, rings, icy satellites and Titan.

The Huygens Probe was selected by ESA's Science Programme Committee in November 1988 as the first medium-size mission of the Horizon 2000 long-term scientific programme. NASA received approval for the start of Cassini in 1990.

Scientific objectives

The Cassini/Huygens mission is designed to explore the Saturnian system and all its elements: the planet and its atmosphere, rings and magnetosphere, and a large number of its moons, particularly Titan and the icy satellites. Titan is the second largest moon in the Solar System after Jupiter's Ganymede. Its atmosphere resembles that of the

Figure 2.4.1. Left: the interplanetary trajectory of the Cassini/Huygens spacecraft. Right: the trajectory upon arrival at Saturn; the Probe is released towards the end of the initial orbit around Saturn.

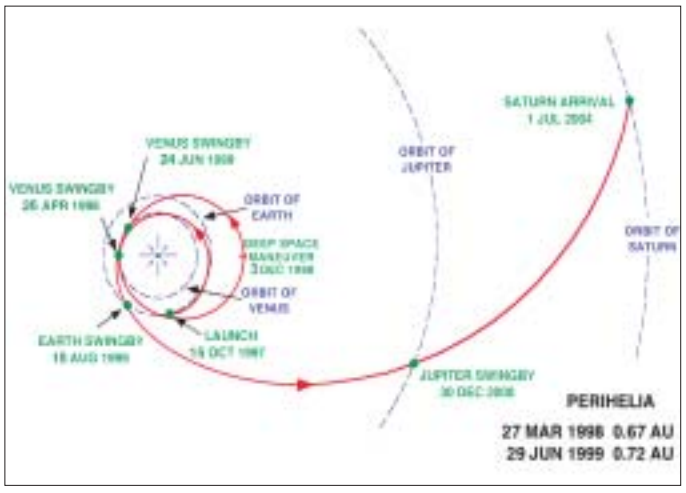

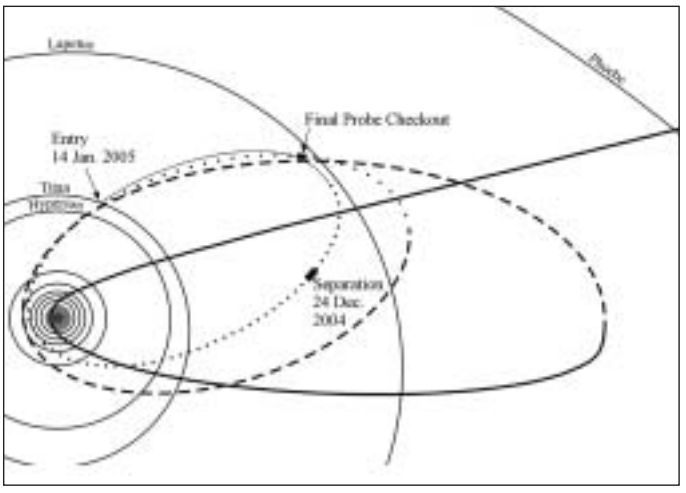

For further information, see http://sci.esa.int/huygens

Table 2.4.1. The principal characteristics of the Huygens payload.

Instrument/PI	*Science objectives*	*Sensors/measurements*	*Mass (kg)*	*Power (typical/ peak, W)*	*Participating countries*
Huygens Atmospheric Structure Instrument (HASI) M. Fulchignoni, University Paris 7/ Obs. Paris-Meudon (France)	Atmospheric temperature and pressure profile, winds and turbulence Atmospheric conductivity. Search for lightning. Surface permittivity and radar reflectivity.	*T*: 50-300K, *P*: 0-2000 mbar γ: 1 μ*g*-20 m*g* AC *E*-field: 0-10 kHz , 80 dB at 2 μV/m Hz DC *E*-field: 50 dB at 40 mV/m Conductivity 10^{-15} Ω/m to ∞ Relative permittivity: 1 to ∞ Acoustic: 0-5 kHz, 90 dB at 5 mPa	6.3	15/85	I, A, D, E, F, N, SF, USA, UK, ESA/RSSD, IS
Gas Chromatograph Mass Spectrometer (GCMS) H.B. Niemann, NASA/GSFC, Greenbelt (USA)	Atmospheric composition profile. Aerosol pyrolysis products analysis.	Mass range: 2-146 dalton Dynamic range: $>10^8$ Sensitivity: 10^{-10} mixing ratio Mass resolution: 10^{-6} at 60 dalton GC: 3 parallel columns, H_2 carrier gas Quadropole mass filter 5 electron impact sources Enrichment cells (×100-×1000)	17.3	28/79	USA, A, F
Aerosol Collector and Pyrolyser (ACP) G.M. Israel, SA/CNRS Verriéres-le-Buisson (France)	Aerosol sampling in two layers – pyrolysis and injection to GCMS	2 samples: 150-40 km; 23-17 km 3-step pyrolysis: 20°C, 250°C, 600°C	6.3	3/85	F, A, USA
Descent Imager/Spectral Radiometer (DISR) M.G. Tomasko, University of Arizona, Tucson (USA)	Atmospheric composition and cloud structure. Aerosol properties. Atmospheric energy budget. Surface imaging.	Upward and downward (480-960 nm) and IR (0.87-1.64 μm) spectrometers, res. 2.4/6.3 nm. Downward and side looking imagers. (0.660-1 μm), res. 0.06-0.20° Solar Aureole measurements: 550±5 nm, 939±6 nm. Surface spectral reflectance with surface lamp.	8.1	13/70	USA, D, F
Doppler Wind Experiment (DWE) M.K. Bird, University of Bonn (Germany)	Probe Doppler tracking from the Orbiter for zonal wind profile measurement.	(Allan Variance) : 10^{-11} (1 s); 5×10^{-12} (10 s); 10^{-12} (100 s) Wind measurements 2-200 m/s Probe spin, signal attenuation	1.9	10/18	D, I, USA
Surface Science Package (SSP) J.C. Zarnecki, University of Kent, Canterbury (UK)	Titan surface state and composition at landing site. Atmospheric measurements.	γ: 0-100 *g*; tilt ±60°; *T*: 65-110K; T_{th}: 0-400 mW m^{-1} K^{-1} Speed of sound: 150-2000 m s^{-1}, Liquid density: 400-700 kg m^{-3} Refractive index: 1.25-1.45 Acoustic sounding, liquid relative permittivity	3.9	10/11	UK, F, USA, ESA/RSSD, PL

Table 2.4.2. The Huygens interdisciplinary scientists.

Scientist/Affiliation	*Field of Investigation*
ESA Selection	
D. Gautier, Obs. de Paris, Meudon, F	Titan aeronomy
J.I. Lunine, Univ. of Arizona, Tucson, USA	Titan atmosphere/surface interactions
F. Raulin, LPCE, Univ. Paris 12, Creteil, F	Titan chemistry and exobiology
NASA Selection	
M. Blanc, Observatoire Midi-Pyrénées, Toulouse, F	Plasma circulation and magnetosphere/ ionosphere coupling
J. Cuzzi, NASA Ames Research Center, Moffett Field, USA	Rings and dust within Saturnian system
T. Gombosi, Univ. of Michigan, Ann Arbor, USA	Plasma environment in Saturn's magnetosphere
T. Owen, Inst. for Astronomy, Honolulu, USA	Atmospheres of Titan and Saturn
J. Pollack (deceased), NASA Ames Research Center, Moffett Field, USA	Origin and evolution of Saturnian system
L. Soderblom, US Geological Survey, Flagstaff, USA	Satellites of Saturn
D. Strobel, Johns Hopkins University, Baltimore, USA	Titan's and Saturn's atmospheric aeronomy

Earth more closely than that of any other Solar System body. Nitrogen is the major constituent, at a surface pressure of 1.5 bar, compared with 1 bar on Earth. Other major constituents are methane (a few percent) and hydrogen (0.2%). It is speculated that argon could also be present (the most recent models suggest an upper limit of 1%), although it has not yet been detected. Another resemblance to Earth is that Titan's surface could be partially covered by lakes or even oceans of methane and ethane mixtures. The photolysis of methane in the atmosphere, owing mainly to the solar UV radiation but also to cosmic rays and precipitating energetic magnetospheric particles, gives rise to a complex organic chemistry. Chemical reactions taking place in the continuously evolving atmosphere provide possible analogues to some of the prebiotic organic chemistry that was at work on the primitive Earth, before the appearance of life some 3.8 Gyr ago.

Huygens will carry out a detailed *in situ* study of Titan's atmosphere and to characterise the surface of the satellite near the Probe's landing site. The objectives are to make detailed *in situ* measurements of the atmosphere's structure, composition and dynamics. Images and spectroscopic measurements of the surface will also be made during the atmospheric descent. Since it is hoped that the Probe will survive after the impact for at least a few minutes, the payload includes the capability for making *in situ* measurements for a direct characterisation of the surface at the landing site.

The payload

On 10 October 1989, NASA and ESA simultaneously released coordinated Announcements of Opportunity (AOs) calling respectively for investigations to be performed with the Saturn Orbiter and the Huygens Probe. The NASA AO called for four types of proposals:

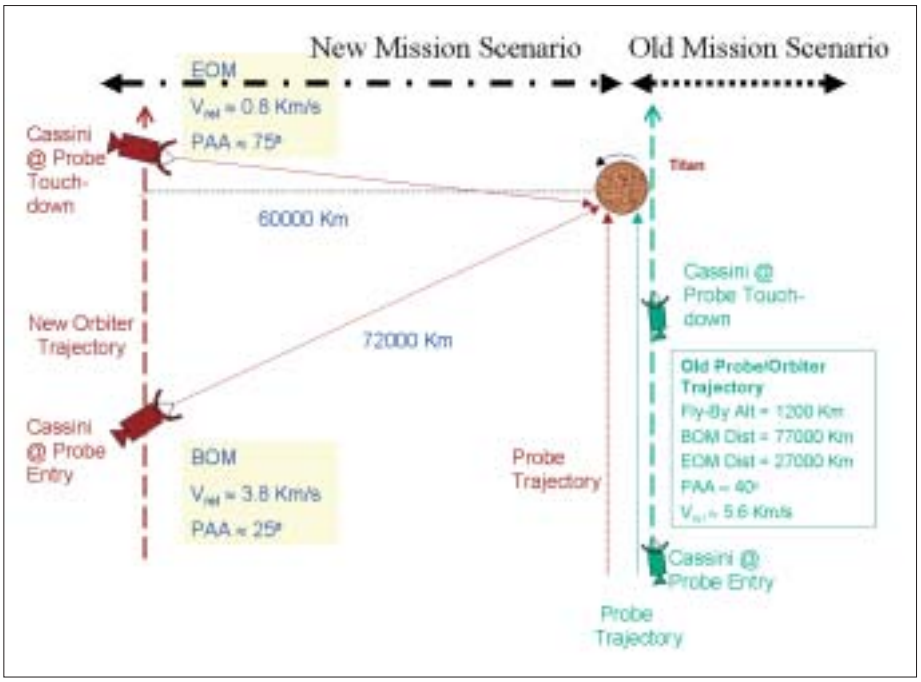

Figure 2.4.2. The revised approach strategy for Huygens at Titan.

— Principal Investigator (PI) Instruments;
— Orbiter facility team leader (TL);
— Orbiter facility team member (TM);
— Interdisciplinary Scientist (IDS) investigation.

The ESA AO called for two types of proposals:
— PI Instrument;
— Interdisciplinary Scientist investigation.

The ESA Huygens selection, which comprises six PI Instruments (Table 2.4.1) and three IDS investigations (Table 2.4.2), was announced in September 1990. The NASA Saturn Orbiter selection, which comprised seven PI Instruments, four Team Leaders, 52 Team Members and seven IDS investigations, was announced in November 1990. During the selection process, NASA included an additional facility instrument on the Orbiter, the Ion and Neutral Mass Spectrometer (INMS), for which a call for Team Leader and Team Member investigation proposals was released in August 1991. The INMS investigation selection was announced in February 1992. The NASA-selected IDS is shown in Table 2.4.2 and the Orbiter Payload in Table 2.4.3.

Cassini/Huygens mission overview

The Cassini/Huygens spacecraft will arrive at Saturn in late June 2004. The Saturn Orbit Insertion (SOI) manoeuvre will be executed while the spacecraft is crossing the ring plane on 1 July 2004. This manoeuvre will place the spacecraft in a 90-day orbit, which includes the first targeted Titan flyby. The second (48-day) orbit, which also includes a targeted Titan flyby, will shape the trajectory so that the Huygens mission can be carried out on the third (32-day) orbit using an Orbiter flyby altitude of 60 000 km. The Huygens mission trajectory was changed in 2001 to accommodate a new geometry requirement during the Probe relay phase that reduces the Doppler shift

Table 2.4.3. Saturn Orbiter payload.

Instrument *PI*	*Measurement*	*Technique*	*Mass (kg)*	*Power (W)*	*Countries*
Optical Remote Sensing					
Composite Infrared Spectrometer (CIRS) V. Kunde, NASA/GSFC, USA	High-resolution spectra, 7-1000 μm	Spectroscopy using 3 interferometric spectrometers	43	43.3	USA, F, D, I, UK
Imaging Science Subsystem (ISS) C. Porco, U. Arizona, USA	Photometric images through filters, 0.2-1.1 μm	Imaging with CCD detectors; 1 wide-angle camera (61.2 mrad FOV); 1 narrow-angle camera (6.1 mrad FOV)	56.5	59.3	USA, F, D, UK
Ultraviolet Imaging Spectrometer (UVIS) L. Esposito, U. Colorado, Boulder, USA	Spectral images, 55-190 nm; occultation photometry, 2 ms; H and D spectroscopy, 0.0002 μm resolution	Imaging spectroscopy, 2 spectrometers; hydrogen-deuterium absorption cell	15.5	14.6	USA, F, D
Visible and Infrared Mapper Spectrometer (VIMS) R. Brown, U. Arizona, Tucson, USA	Spectral images, 0.35-1.05 μm (0.073 μm resolution); 0.85-5.1 μm (0.166 μm resolution); occultation photometry	Imaging spectroscopy; 2 spectrometers	37.1	24.6	USA, F, D, I
Radio Remote Sensing					
Cassini Radar (RADAR) C. Elachi, JPL, USA	Ku-band radar images (13.8 GHz); radiometry, <0.5K resolution	Synthetic aperture radar; radiometry with a microwave receiver	43.3	108.4	USA, F, I, UK
Radio-Science Instrument (RSS) A. Kliore, JPL, USA	Ka/S/X-bands; frequency, phase, timing and amplitude	X/Ka-band uplink; Ka/X/S-band downlink	14.4	82.3	USA, I
Particle Remote Sensing & In-Situ Measurement					
Magnetospheric Imaging Instrument (MIMI) S.T. Krimigis, Johns Hopkins Univ, Baltimore, USA	1. Image energetic neutrals and ions at <10 keV to 8 MeV per nucleon; composition. 2. 10-265 keV/e ions; charge state; composition; directional flux; 3. mass range: 20 keV to 130 MeV ions; 15 keV to >11 MeV electrons; directional flux	1. Particle detection and imaging; ion-neutral camera (time-of-flight, total energy detector); 2. charge energy mass spectrometer; 3. solid-state detectors with magnetic focusing telescope and aperture-controlled ~45° FOV	29	23.4	USA, F, D
In-Situ Measurement					
Cassini Plasma Spectrometer (CAPS) D.T. Young, SWRI, San Antonio, USA	Particle energy/charge: 1. 0.7-30 000 eV/e; 2. 1-50 000 eV/e 3. 1-50 000 eV/e	Particle detection and spectroscopy: 1. electron spectrometer; 2. ion-mass spectrometer; 3. ion-beam spectrometer	23.8	19.2	USA, SF, F, H, N, UK
Cosmic Dust Analyser (CDA) E. Gruen, MPI Heidelberg, D	Directional flux and mass of dust particles in the range 10^{-16}-10^{-6} g; chemical composition	Impact-induced currents	16.8	19.3	D, CZ, F, ESA/RSSD, N, UK, USA
Dual Technique Magnetometer (MAG) D. Southwood, IC, UK	B: DC to 4 Hz up to 256 nT; scalar field DC to 20 Hz up to 44 000 nT	Magnetic field measurement; flux gate magnetometer; vector-scalar magnetometer	8.8	12.4	UK, D, USA
Ion and Neutral Mass Spectrometer (INMS) J.H. Waite, SWRI, San Antonio, USA	Fluxes of +ions and neutrals in mass range 2-66 amu	Mass spectrometery; closed source and open source	10.3	26.6	USA, D
Radio and Plasma Wave Science (RPWS) D. Gurnett, U. Iowa, USA	E: 10 Hz-2 MHz; B: 1 Hz-20 kHz; plasma density and temperature	Radio frequency receivers; 3 electric monopole antennas; 3 magnetic search coils; Langmuir Probe	37.7	17.5	USA, A, F, S, UK, N

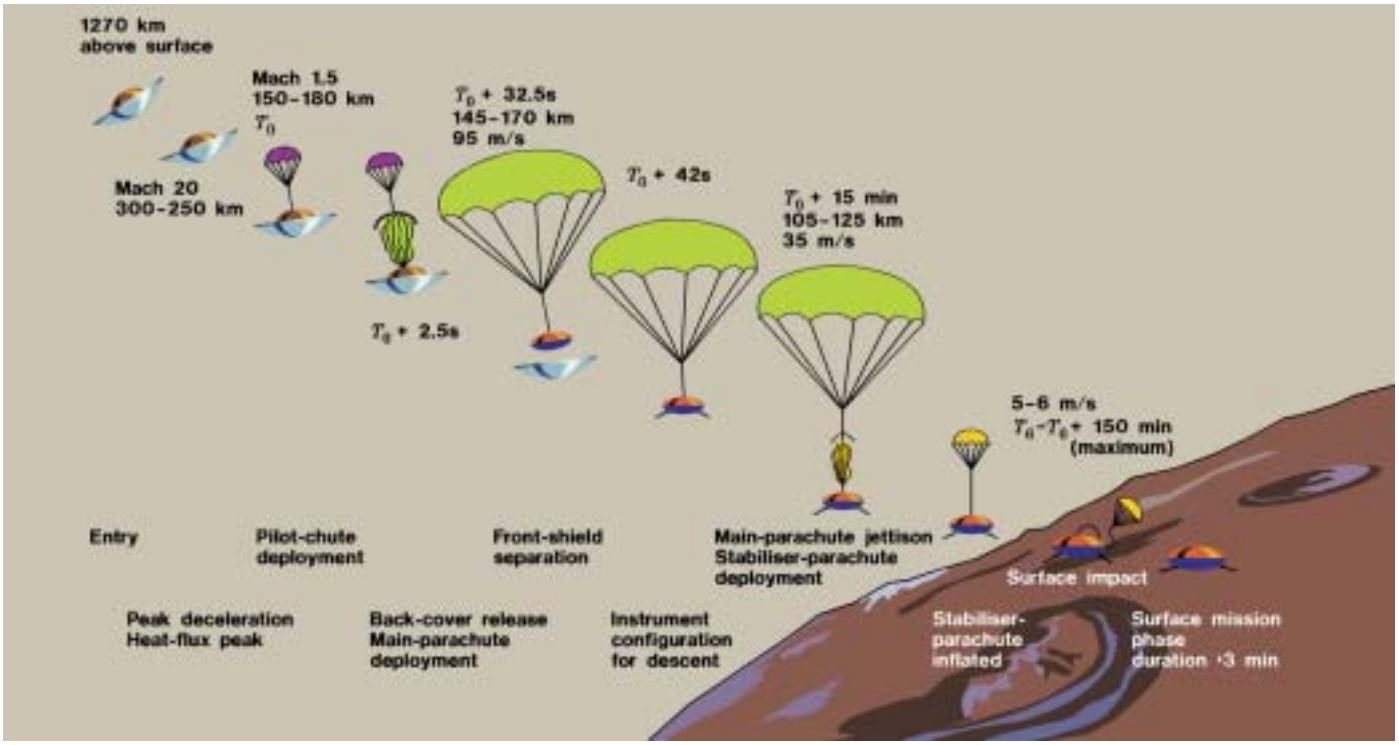

Figure 2.4.3. The entry and descent sequence for the Huygens Probe.

of the radio signal received by the Orbiter (Fig. 2.4.2). This change was necessary to cope with a design flaw of the Huygens radio receiver discovered during inflight testing in 2000. The onboard software of the Probe and several instruments was also modified in December 2003 to optimise the mission recovery. The Probe will be released on 25 December 2004, 22 days before Titan encounter. Five days after release, the Orbiter will perform a deflection manoeuvre in order to avoid impacting Titan. This manoeuvre will also set up the Probe-Orbiter radio communication geometry for the Probe descent phase. Huygens' entry into Titan's atmosphere is planned for 14 January 2005. The Orbiter will act as a relay during the Huygens mission, receiving the data on its High Gain Antenna (HGA). This configuration does not allow the Probe mission to be conducted with a real-time link between the Orbiter and Earth. The Probe data will be stored aboard the Orbiter in the two solid-state recorders for later transmission to Earth after completion of the Probe mission. The main events of the Probe entry and descent are illustrated in Fig. 2.4.3.

After completion of the Probe mission, the Orbiter will begin its 4-year satellite tour of the Saturnian system. This consists of 75 Saturn-centred orbits, connected by Titan gravity-assist flybys or propulsive manoeuvres. The size of these orbits, their orientation to the Sun/Saturn line and their inclination to Saturn's equator are dictated by the various scientific requirements, which include: Probe and landing site ground-track coverage, icy-satellite flybys, Saturn, Titan or ring occultation, magnetosphere coverage, orbit inclinations and ring-plane crossings. Titan is also a principal target for the Orbiter; it will be observed during each of the 44 targeted Titan flybys.

The Orbiter science instruments are mounted on two body-fixed platforms: the remote-sensing pallet and the particle & field pallet; the magnetometer is mounted at the tip of an 11 m-long boom; the magnetic and electric antennas of the RPWS

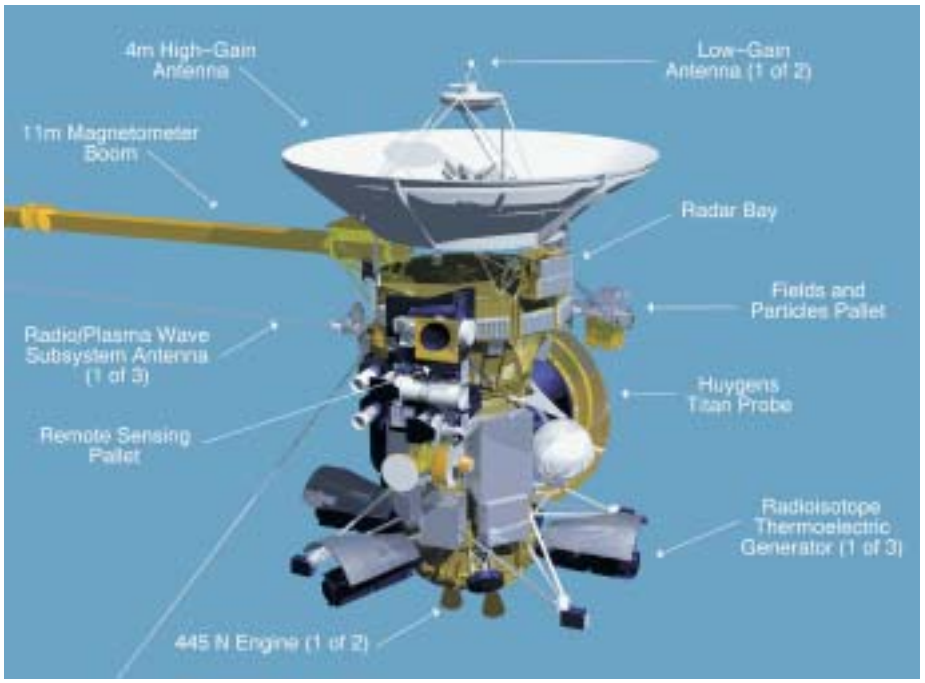

Figure 2.4.4. The Cassini/Huygens spacecraft and its principal features.

Table 2.4.4. Mass breakdown of the Cassini/Huygens spacecraft.

Orbiter (dry, inc. payload)	2068 kg
Probe (inc. 44 kg payload)	318 kg
Probe Support Equipment	30 kg
Launch adaptor	135 kg
Bipropellant	3000 kg
Monopropellant	132 kg
Launch mass	5683 kg

experiment are mounted on the body; both the radar and the radio-science instrument use the HGA. The main elements of the Cassini/Huygens spacecraft are illustrated in Fig. 2.4.4. The mass budget of the spacecraft is shown in Table 2.4.4.

Huygens flight operations

After separation from the Orbiter, the Probe will operate autonomously, the radio relay link to the Orbiter being one-way for telemetry only. Up to that point, telecommands can be sent via an umbilical link from the Orbiter, but this facility will be used only during the cruise and Saturn orbit phases for monitoring the health of the subsystems and calibrating the instruments during the 6-monthly checkouts. Huygens does not perform scientific measurements before arrival at Titan and for most of the cruise the Probe is switched off. It is activated only for a 3-7 h period for the biannual checkouts. During the 22-day coast phase after separation from the Orbiter, only a timer will operate, to activate the Probe about 265 min before the predicted entry into Titan's atmosphere. Loading the value of this timer's duration and depassivating the batteries that power the Probe after separation will be the last activities initiated by command from the ground.

The Probe flight operations, and the collection of telemetered data, are controlled from a dedicated control room, the Huygens Probe Operations Centre (HPOC) at ESOC (Darmstadt, Germany). Here, command sequences are generated and transferred by dedicated communication lines to the Cassini Mission Operations Center at JPL. There, the Probe sequences are merged with commands to be sent to other subsystems and instruments of the Orbiter for uplink via NASA's Deep Space Network (DSN). Probe telecommands are stored onboard the Orbiter and forwarded to the Probe Support Equipment (PSE) at specified times (time tags) for immediate execution. Because of the great distance of Saturn from Earth (requiring up to 2.5 h for round-trip radio communication) real-time operations are not possible during the Probe descent.

Data collected by the Probe and passed to the PSE via the umbilical (during the

cruise) or the relay link (during the descent) will be formatted by the PSE and forwarded to the Orbiter's Command and Data Subsystem (CDS). The Orbiter stores all data on solid-state recorders for transmission to Earth at times when it is visible from one of the DSN ground stations. From the ground station, the data are forwarded to JPL, where Probe data are separated from other Orbiter data before being stored on the Cassini Project Database (PDB). HPOC operators access the PDB to retrieve Probe data via a Science Operations and Planning Computer (SOPC), supplied to ESOC by JPL under the terms of the interagency agreement.

Probe subsystem housekeeping data are used by ESOC to monitor the performance of the Probe, while data from the science instruments are extracted for forwarding to the investigators. During the cruise phase, these data are shipped to the scientists' home institutes by public data line or on CD-ROMs. After analysis of these data, the investigators meet the operations team to review the results of the previous checkout and to define the activities for the following checkout period. During the Saturn orbit and Probe mission phases, the investigators will be located at HPOC to expedite their access to the data and facilitate interaction with their colleagues and the Probe operators. Accommodation will be provided for the ground support equipment they need to reduce and interpret their data.

All in-flight Probe activities are prepared very carefully as any mistake could endanger its mission performance. Each checkout sequence is tested on the Probe Simulator and then on the Engineering Model (EM), both installed in HPOC. The EM has been retrofitted with flight spare computers and the instrument interfaces upgraded to flight standard. It was used as a testbed to validate all the modifications to the Probe's onboard software.

Status

Venus, Earth and Jupiter encounters

Unique science observations were made during the second Venus encounter (24 June 1999), the Earth encounter (18 August 1999) and the 6-month Jupiter flyby campaign (October 2000 to March 2001). The Saturn approach science phase began in early January 2004, providing continuous observations of the system. Result highlights are available at *http://saturn.jpl.nasa.gov*

Saturn Orbiter

After the very successful launch and injection of Cassini/Huygens on its inter-planetary trajectory, Cassini/Huygens performed four nominal planet flybys: Venus-1 (26 April 1998), Venus-2 (24 June 1999), Earth (18 August 1999) and Jupiter (30 December 2000). The flight performances of the spacecraft are excellent. The Orbiter software for the two critical sequences, the SOI manoeuvre (1 July 2004)and the Probe Relay Link (early- to mid-January 2005), were full tested in flight.

Huygens Probe

Thirteen inflight checkouts have been conducted. The payload and subsystem performance have been as expected. An end-to-end test of the Probe relay link was carried out in February 2000, using a DSN antenna to transmit a simulated Probe radio signal. This test uncovered a malfunction in the Huygens radio receivers. After intensive investigations supported by further inflight and ground tests, it was found that, owing to a design flaw, the bandwidth of the bit synchroniser of the Huygens radio receivers was too narrow. It could not cope with the expected Doppler shift from the relative displacement between the two spacecraft during the Probe mission. It would have led to significant Huygens data loss, but a change in the Orbiter trajectory and other changes in Probe operations will allow recovery of the full Probe mission.

2.5 XMM-Newton

Introduction

The XMM-Newton observatory, formerly known as the high–throughput X-ray spectroscopy mission, was launched on 10 December 1999 from Kourou, French Guiana on the first commercial launch of the Ariane-5 (V504). The mission is routinely producing high-quality data and has effectively completed its guaranteed time, AO-1 and AO-2 programmes and 7% of its AO-3 programme, which also, for the first time, includes proposals accepted in a special, large programmes, category. From 2004, annual calls for proposals will be issued around 1 September. The mission, which was originally approved for operations until end-March 2002, was approved in November 2003 by ESA's Science Programme Committee for operations up to end-March 2008.

Status

XMM-Newton is a 3-axis stabilised spacecraft with a mass of about 4 t. The satellite is dominated by a large carbon fibre telescope tube that is attached to the Service Module (SVM) at one end and to the Focal Plane Assembly (FPA) at the other. The SVM is a platform that carries all the equipment for the power, data handling and attitude & orbit control subsystems, including the structure to support the solar arrays and antennas. The satellite's attitude control loop uses a star tracker and momentum wheels, which allow for a slew rate of 90° per hour and a pointing reconstruction accuracy of a few arcsec. Gyros are used only in the case of eclipses or anomalies.

The operations efficiency in the course of 2002 reached its maximum of up to 132 000 s of science observations per revolution (the remaining 40 000 s are spent inside the radiation belts). The mission now also has a very rapid response time to Targets of Opportunity (ToO): as fast as 5.25 h. This has been put to good use a number of times when XMM-Newton performed rapid and precide follow-ups to Gamma-Ray Bursts (GRB) located by ESA's Integral.

The status of the satellite and instruments is excellent, and well in line with the design goal to operate for 10 years. Onboard consumables (e.g. power, fuel, gyros) are sufficient to operate for at least another 12 years. On the hardware side, the spacecraft is being operated on all of its prime hardware chains, and no redundancy has had to be used yet. The radiation-induced performance degradation of the instruments is in line with pre-launch expectations, and has recently been largely ameliorated by allowing the X-ray detectors to operate at lower temperatures. This detector cooling could only be done later in the mission in order to avoid possible detector contamination issues. Consequently, based on current knowledge, the instruments will last at least for the designed mission lifetime.

European Photon Imaging Cameras (PI M. Turner, Leicester University, UK)
An EPIC detector is positioned behind each of the three X-ray mirror modules. Two MOS-CCD cameras share the mirrors with the grating array, and the PN-CCD detector is located behind the fully open telescope position. The in-orbit performance of the EPIC cameras is excellent, and the degradation of the camera owing to irradiation by (mostly solar) protons is as predicted pre-launch. A decision to lower the temperature of the detectors was taken end-2002 in order to ameliorate the radiation damage. This has been very successful: not only has more than 75% of the performance degradation since launch been recovered but the rate of degradation has also decreased considerably. The EPIC cameras are particularly powerful for those sources that show weak extended X-ray emission, such as clusters of galaxies.

Reflection Grating Spectrometer (PI J. Kaastra, SRON, The Netherlands)
RGS is a powerful, large-area detector that allows XMM-Newton to take X-ray

For further information, see http://sci.esa.int/xmm

spectra with an E/ΔE of 300-700 (1st order) in the 5-35 Å (0.35-2.4 keV) soft X-ray band. The effective area for the two grating arrays is in the range of 40-200 cm^2 over this wavelength band. The instrument's performance is as predicted, and as for EPIC, it was decided at the end of 2002 to cool the detectors to a lower operational temperature. This exercise was equally successful, ameliorating a lot of the incurred radiation damage and, most importantly, dramatically decreasing the number of hot columns and hot pixels.

Optical Monitor (PI K. Mason, MSSL, UK)
OM is a powerful telescope in the 170-600 nm wavelength band, and can detect sources down to 24th magnitude in a few thousand seconds (depending on spectral type). This camera is powerful enough, both in sensitivity and positional accuracy, to allow identification of counterparts of many of the new X-ray sources detected by XMM-Newton.

The analysis of XMM-Newton data is supported by Science Analysis System (SAS) software package, which is now at version 6, being released approximately once a year. It allows data users to derive reliable and calibrated results for further analysis with standard X-ray astronomy spectral analysis packages. The derivation of accurate calibration data, and the proper incorporation of this knowledge into the SAS software, is a continuing process. The status of the calibration is now such that most (spectral) parameters can be derived to an absolute accuracy of around 2-5%, depending on the quantity.

The XMM-Newton Science Archive (XSA), based on a re-use of technology from the ISO archive, was released in March 2002. The archive allows for flexible querying and retrieving of all XMM-Newton (public) data in a highly flexible and configurable way.

In April 2003, the first version of the XMM-Newton serendipitous source catalogue (1XMM), generated by the Survey Science Centre (SSC; PI: M. Watson, Leicester, UK) was released. Most (> 80%) of the entries have not previously been reported as X-ray sources. This catalogue is expected to become a significant astronomical resource, as it is the largest catalogue of X-ray sources derived from observations with CCD energy resolution over the full 0.2-12 keV band. The catalogue contains source detections drawn from 585 EPIC observations made between 1 March 2000 and 5 May 2002. Net exposure times in these observations range from < 1000 s up to ~100 000 s. The total area of the catalogue fields is ~90 deg^2 but, taking account of the substantial overlaps between observations, the net sky area covered independently is ~50 deg^2. The catalogue contains 33 026 X-ray source detections with the highest likelihood (> 8). For these sources, the positional accuracy of the catalogue sources is generally ~0.5-2 arcsec (68% confidence radius).

Science results

XMM-Newton results continue to impact many areas of science. This is illustrated below by examples. Exciting challenges lie ahead for the mission, such as Fe-line reverberation mapping to study the immediate vicinity of accreting supermassive black holes, and studies of the hot intergalactic medium, where most of the baryons in the Universe reside. Proposals for further investigation of these and other exciting topics have been accepted for AO-3. Furthermore, from AO-3 onwards, some 15% of the available observing time is allocated to large programmes, which will be an invaluable addition to the XMM-Newton observations.

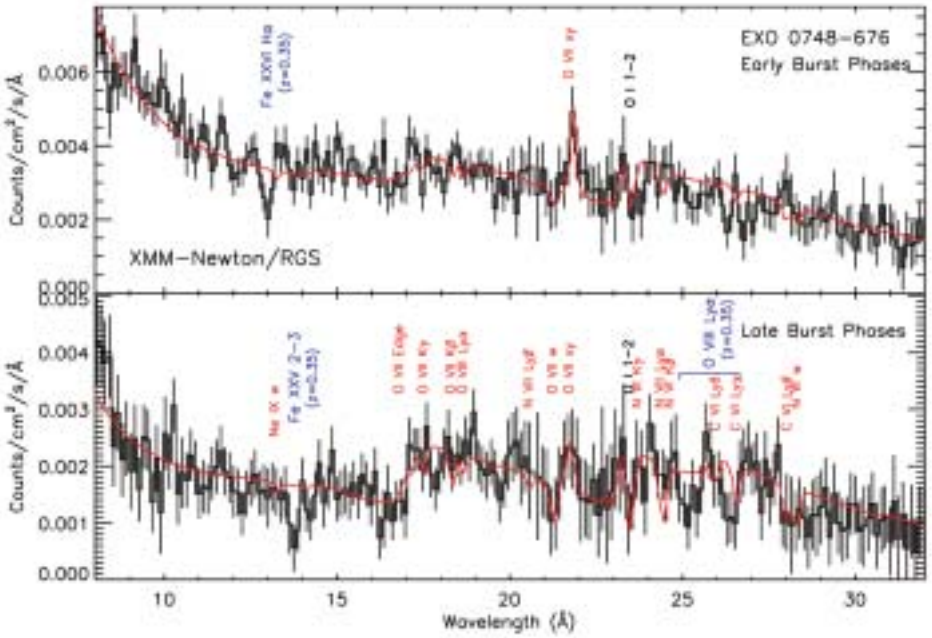

Figure 2.5.1 The RGS spectra of EXO 0748-676 for 28 type I X-ray bursts. The background-subtracted flux spectra for the early and late phases of the bursts are shown in the top and bottom panels, respectively. The data are plotted as the black histograms, with 1σ error bars derived from counting statistics. The red line is the empirical continuum, with additional O VII intercombination line emission, modulated by absorption in photoionised circumstellar material. The positions of the most prominent discrete absorption lines from the circumstellar medium are labelled in red; in the He-like spectra, 'w' signifies the n = 1-2 resonance transition, 'xy' the (unresolved) n = 1-2 intercombination transitions, while higher series members are marked Kβ, etc. Column densities in ions other than O VII are normalised to the absorption measured in O VII, assuming ionisation parameter ζ = 10, and solar abundances. The N VII Ly-α line at 24.78 Å is overpredicted, indicating a subsolar N/O abundance ratio. The black labels indicate the interstellar O 1s-2p absorption line. Blue labels indicate the photospheric absorption lines in Fe XXVI, XXV and O VIII at a redshift 0.35. The data and models have been rebinned to Δλ = 0.124 Å, which is a factor ~2.5 larger than the RGS instrument resolution.

Gamma-Ray Bursts

Through a combination of efficient planning and spacecraft performance, XMM-Newton has been able to respond quickly to targets of opportunity and be on-target some 6 h after such an initial alert. This has led to particular success for a number of GRB observations, where XMM-Newton observed delayed emission of spectral line features from hot plasma. These observations, and recent other work, have now firmly established that supernovae lie at the very heart of the GRB phenomena.

Stars

The impact from XMM-Newton has been very strong in studying X-ray emission from stars distributed all over the HR diagram, from early-type stars to cool giants. Areas of study range from understanding the outflows and winds associated with classical T-Tauri stars, where it has been possible to distinguish the X-ray emission mechanisms from weak-lined and classical T-tauri stars, to massive stars and Wolf-Rayet stars, where the absence of X-rays from WC stars and the hard tail seen in some WN stars continues to challenge existing models. Of particular importance has been the characterisation of the structure of stellar coronae at different stages of stellar evolution, including the determination of the emission measure distribution of coronal plasmas in cool stars with different levels of magnetic activity, observations of stellar flares, density diagnostics using He-like triplets, opacity effects in stellar coronae, abundance measurements and evidence for first ionisation potential effects in the coronae of very active stars.

Active Galactic Nuclei (AGN)

One of the major areas of research supported by observations with XMM-Newton has been that of AGN. For example, the Seyfert 1 galaxy MCG-6-30-15 has been observed several times and reveals that the Fe-line emission from this source can be

understood only in the context of reflection in an accretion disc around a Kerr black hole. Even energy extraction from a spinning black hole might have been detected. One of the prominent aspects discovered early on in the mission, but which is still the subject of heated debate, is the presence of either broad relativistic emission lines (as derived from the high signal-to-noise XMM-Newton data) or a dusty warm absorber (as preferred by the high spectral resolution Chandra data) in the model for the soft X-ray emission from AGN such as Mkn 766 and MCG-6-30-15.

Neutron stars

The discovery of absorption features from the surface of a neutron star and the discovery of cyclotron resonant absorption features in the spectrum of another neutron star were highly exciting results, both of which were published in Nature. The former described the discovery of gravitationally redshifted absorption features originating from the very surface of the neutron star (see Fig. 2.5.1) from which a tight constraint on the mass to radius relationship could directly be determined. This has direct significance for the nature of matter at extreme densities. The latter allowed a direct determination of the magnetic field of this neutron star, which came out much lower than expected.

Clusters of galaxies

The unique combination of high spectral resolution, throughput and sensitivity offered by XMM-Newton has broadened our knowledge of clusters of galaxies in several ways. Using the imaging spectroscopy provided by EPIC it has been possible to resolve the radial abundance and temperature gradients in the outer parts of clusters, thereby tracing the chemical and dynamical history of these clusters. The study of the buildup of clusters by infall of smaller structures has advanced through XMM-Newton observations providing important constraints for models; both through analysis of filamentary structures as a warm intergalactic medium and the study of X-ray wakes of gas stripped from infalling galaxies. Recent studies on the Coma Cluster have identified a filamentary structure whose thermodynamic state reduces the star-formation rate in the embedded spiral galaxies, providing an explanation for the presence of passive spirals observed in this and other clusters.

The deficit of cool gas, compared to the predictions of simple isobaric cooling flow models, was first detected in many cooling flow clusters by XMM-Newton. This remains a topic where considerable effort is being spent on the generation of models (involving a wide range of complex components such as conductivity and radio source mechanical energy input) to explain this feature.

XMM-Newton will continue to observe more clusters, at the faint and cosmologically distant end of the spectrum, in order to further our understanding of the formation and evolution of clusters significantly. The first measurements indicate a modest amount of cluster evolution with redshift that is consistent with standard scaling models.

Supernova remnants

Supernova explosions have a highly profound impact on the interstellar medium, both as sources of mechanical energy and heavy elements. Detailed information on these mechanisms can be derived from the study of supernova remnants. As an example, a recent study of 13 supernova remnants in the Small Magellanic Cloud (SMC) has derived a hydrogen density six times lower than that of the Large Magellanic Cloud, which has obvious consequences for the subsequent evolution of supernova remnants in the SMC.

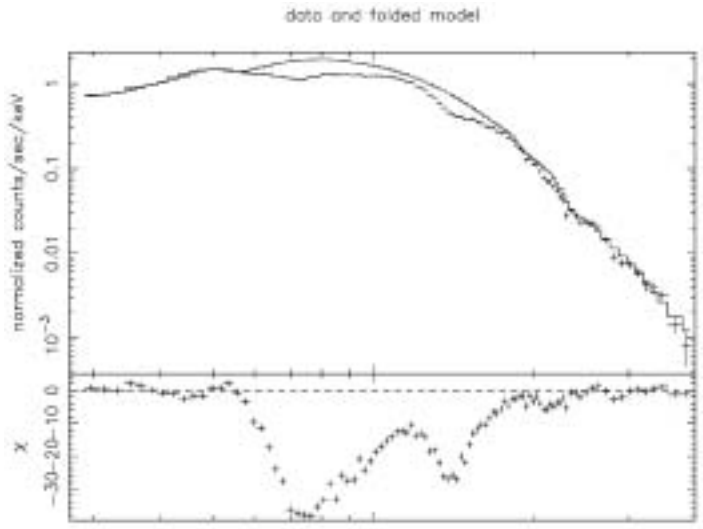

Figure 2.5.2 EPIC-pn spectrum of 1E1207.4-5209 for a total net observing time of 138.4 ks. The central energies of the three absorption features are 0.72±0.02, 1.37±0.02 and 2.11±0.03 keV. The possible fourth feature in the pn spectrum is at 2.85±0.06 keV.

X-ray background

Although the bulk of the X-ray background has been resolved through observations with both Chandra and XMM-Newton, the work continues. The classification of sources by obtaining X-ray spectra and optical data is the subject of many programmes, amongst which is the deepest XMM-Newton observation ever: 1 000 000 s on the Lockman Hole. This programme has obtained the X-ray spectra of many weak sources, and will substantially contribute to our understanding of the sources that make up the X-ray background. To reach an equivalent depth with an equal amount of spectral information in the 5-10 keV band with Chandra would require an observation 5-10 times longer.

Also in this context is the programme undertaken by the Survey Science Consortium (SSC), which is carrying out a series of serendipitous surveys in order to characterise the X-ray content of the sky through three samples of ~1000 sources each, selected at fluxes of $\sim 10^{-13}$, $\sim 10^{-14}$ and $\sim 10^{-15}$ erg cm^{-2} s^{-1}; equivalent to 10, 100 and 2000 sources per square degree, respectively.

A number of papers on XMM-Newton results were of such importance that they were also issued as press and/or news releases, and were picked up by the international media.

A paper was published in *Nature* (12 June 2003) reporting the first direct measurement of a neutron star's magnetic field. This paper reports on a long X-ray observation of the isolated neutron star 1E1207.4-5209, which, contrary to the featureless spectra observed in other sources like this, shows three distinct features, regularly spaced at 0.7, 1.4 and 2.1 keV, plus a fourth feature of lower significance, at 2.8 keV (Fig. 2.5.2). These features vary in phase with the star's rotation. The logical interpretation is that they are features from resonant cyclotron absorption, which allows the authors to calculate a magnetic field strength of 8×10^{10} G, assuming that the absorption arises from electrons.

A paper was published in *Science* (5 September 2003) reporting the discovery of two elongated parallel X-ray tails trailing the pulsar Geminga (Fig. 2.5.3). They are aligned with the object's supersonic motion, extend for ~2 arcmin and have a non-thermal spectrum produced by electron-synchrotron emission in the bow shock

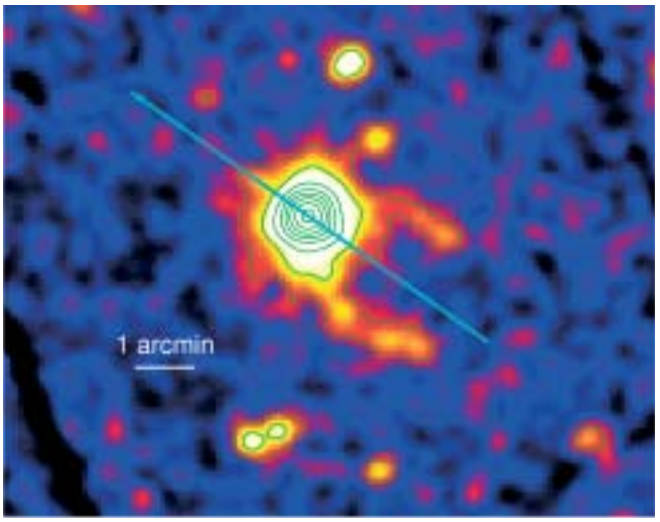

Figure 2.5.3. The XMM-Newton view of Geminga. Data from the MOS1 and MOS2 cameras have been merged and smoothed to produce the image. The emission from Geminga outshines the tails up to ~40 arcsec from the source. The tails are ~2 arcmin long and cover an area of ~2 square arcmin. They show a remarkable symmetry with respect to the pulsar proper motion direction, marked by the arrow.

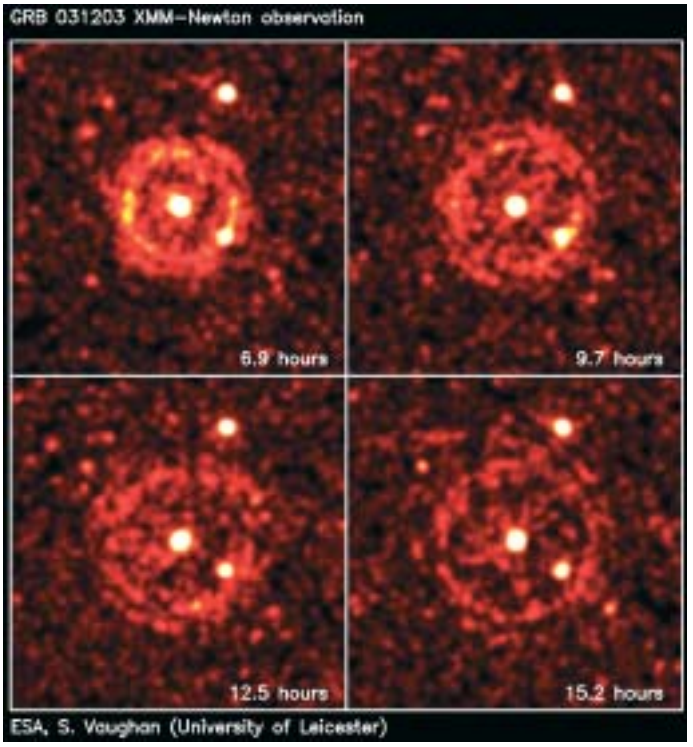

Figure 2.5.4: EPIC shows the expanding rings caused by a flash of X-rays scattered by dust in our Galaxy. The X-rays were produced by a powerful gamma burst on 3 December 2003. The slowly fading afterglow of the gamma burst is at the centre of the expanding rings. Other, unrelated, X-ray sources can also be seen. The time since the gamma-ray explosion is shown in each panel.

between the pulsar wind and the surrounding medium. Electron lifetime against synchrotron cooling matches the source transit time over the X-ray features' length. Such a first X-ray detection of a pulsar bow shock allows the pulsar electron injection energy and the shock magnetic field to be gauged, while constraining the angle of Geminga's motion and the local matter density.

On 3 December 2003, Integral observation of a GRB was followed up by XMM-Newton with its fastest response to date: within 6 h of the trigger XMM-Newton was on target and observing. This observation of GRB031203 showed a time-dependent, dust-scattered X-ray halo around the GRB source. The halo appeared as concentric ring-like structures centred on the GRB location. The expansion of the radius of these structures is consistent with small-angle X-ray scattering caused by a large column of dust along the line of sight to a cosmologically distant GRB (Fig. 2.5.4). The rings are due to dust concentrated in two distinct slabs in the Galaxy located at distances of 880 and 1390 pc, consistent with known Galactic features.

2.6 Cluster

Introduction

After 3 years of operations, the four Cluster spacecraft are making great advances in magnetospheric physics by looking for the first time at plasma structures in three dimensions. This is the first time that the Earth's magnetic field and its environment have been explored by a small constellation of four identical satellites. Results show that, with four spacecraft, a detailed 3-D view of the Sun-Earth connection processes taking place at the interface between the solar wind and the Earth's magnetic field can be obtained.

Cluster is one of the two missions (the other being SOHO) comprising the Solar Terrestrial Science Programme (STSP), the first Cornerstone of ESA's Horizon 2000 Programme. Cluster was proposed in November 1982 in response to an ESA call for proposals for the next series of scientific missions. After the failure of Ariane-5 on 4 June 1996 and the destruction of the four original satellites, Cluster was rebuilt and launched in pairs July and August 2000 on two Soyuz rockets.

In February 2002 the ESA Science Programme Committee (SPC) agreed to extend the mission by 35 months (up to end-2005). In addition, it agreed to double the amount of data acquired along each orbit using a second ground station. This greatly enhanced the scientific output by allowing continuous coverage along the orbit.

Status

The four satellites and 41 instruments (Table 2.6.1) have been working nominally since the beginning of the mission. The payload consists of magnetometers (flux gate for the static magnetic field and search coil for the magnetic waves), wire booms and electron guns to measure electric fields, and particle detectors to measure electrons and ions from a few eV to a few MeV. The mission goal is to measure the magnetospheric structures at different scales. To achieve that, about half of the spacecraft mass consisted of propellant: about 450 kg of the 600 kg was used to achieve the operational orbit of 4x19.6 R_E. The remainder is being used to modify the satellite separations (Fig. 2.6.1): four constellation manoeuvres have been made so far to create separations of 600, 2000, 100, 5000 and, since mid-2003, 250 km. A constellation manoeuvre typically takes about 1.5 months, using long thruster firings at the beginning and then smaller ones toward the end. Listed below are the 43 individual manoeuvres performed by each satellite in June-July 2003 to change the distances from 5000 km to 250 km. The manoeuvre durations are shown in minutes:

	C1	C2	C3	C4
04 Jun			34.4	
07 Jun	99.0	125.0	111.0	32.0
09 Jun	2.1	2.3	2.7	2.0
90 Jun	0.1	0.2	0.4	0.1
14 Jun	13.6	8.5	2.5	32.0
18 Jun	5.0	1.0	0.1	6.5
21 Jun	0.8	0.1	2.0	2.0
24 Jun	0.5	1.5	0.5	0.4
29 Jun	0.5	0.8	0.3	0.2
02 Jul	2.2	0.1	2.5	
07 Jul	0.1	0.1	0.1	0.1

After a manoeuvre, a few days are necessary for precise orbit determination and then to prepare the execution of the next manoeuvre. During each manoeuvre, the payloads using high voltages (ASPOC, EDI, CIS, PEACE and RAPID) are switched off to prevent any discharge in the instruments through the surrounding gas.

For further information, see http://sci.esa.int/cluster

Figure 2.6.1. Inter-spacecraft distances from launch to the end of the extended mission.

Table 2.6.1. The Cluster payload.

Acronym/Instrument	*Principal Investigator*
FGM/Fluxgate Magnetometer	A. Balogh (IC, UK)
STAFF*/Spatio-Temporal Analysis of Field Fluctuation experiment	N. Cornilleau-Wehrlin (CETP, France)
EFW*/Electric Field and Wave experiment	M. André (IRFU, Sweden)
WHISPER*/Waves of High Frequency and Sounder for Probing of Electron density by Relaxation	P. M. E. Décréau (LPCE, France)
WBD*/Wide Band Data	D.A. Gurnett (Iowa U., USA)
DWP*/Digital Wave Processing experiment	H. Alleyne (Sheffield U., UK)
EDI/Electron Drift Instrument	G. Paschmann (MPE, Germany)
CIS/Cluster-II Ion Spectrometry	H. Rème (CESR, France)
PEACE/Plasma Electron and Current Experiment	A. Fazakerley (MSSL, UK)
RAPID/Research with Adaptive Imaging Particle Detectors	P. Daly (MPAe, Germany)
ASPOC/Active Spacecraft Potential Control	K. Torkar (IWF, Austria)

* Members of the Wave Experiment Consortium (WEC)

Science highlights

One of the major advances in magnetospheric physics with Cluster is the investigation of magnetic reconnection (Fig. 2.6.2). Magnetic reconnection is believed to occur in an encounter between two opposite magnetic fields. This process is observed for astronomical objects and also for both the Sun's and the Earth's magnetospheres. The advantage of a spacecraft flying in Earth's magnetosphere is that it can measure *in situ* the key plasma parameters to help understand this complex phenomena.

For the first time, Cluster observes this phenomenon from four view points and so characterises it as never before. During a crossing of the magnetotail, the four satellites surrounded the reconnection region and detected the Hall currents when ions are decoupled from electrons. In addition, very strong electric fields were observed near the reconnection site, which could explain the acceleration of the plasma usually observed.

A consequence of the reconnection process is the release of plasmoids and flux ropes – big magnetic bubbles – which propagate from the reconnection point. Cluster is located at a maximum of 20 R_E and is therefore ideally located to study flux ropes propagating toward Earth. A recent study using the four satellites identified the speed, and the direction of propagation could be determined very accurately (mean speed about 413 km/s). In addition, the centre of the magnetotail, the plasmasheet, became thicker by about 1 R_E (6400 km) as the flux ropes passed by.

Cluster has also observed magnetic reconnection in the polar cusp, the region above the pole where particles from the solar wind enter directly into the magnetosphere and reach our atmosphere. The reconnection process accelerates ions which can then produce a bright spot in the aurora. NASA's IMAGE satellite was recording the proton aurora at the same time and detected a bright spot. This is the first time that we have observed the reconnection process *in situ* and its simultaneous effect in the ionosphere (Fig. 2.6.3).

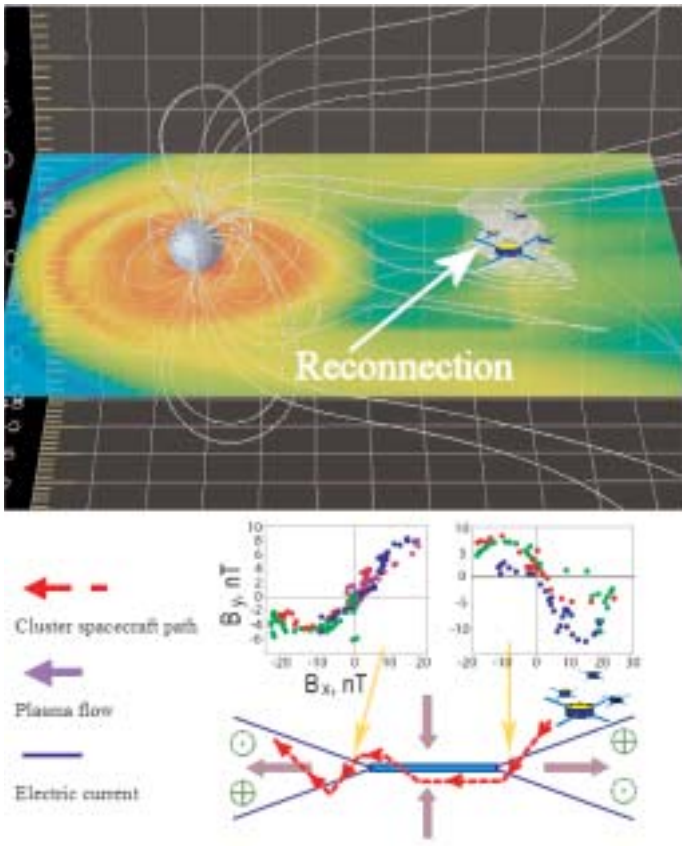

Figure 2.6.2. Simulation of magnetic reconnection in Earth's magnetosphere (top, courtesy R. Wingley, Washington Univ., USA) and Cluster's observations of the process (bottom, courtesy Runov, IWF, A).

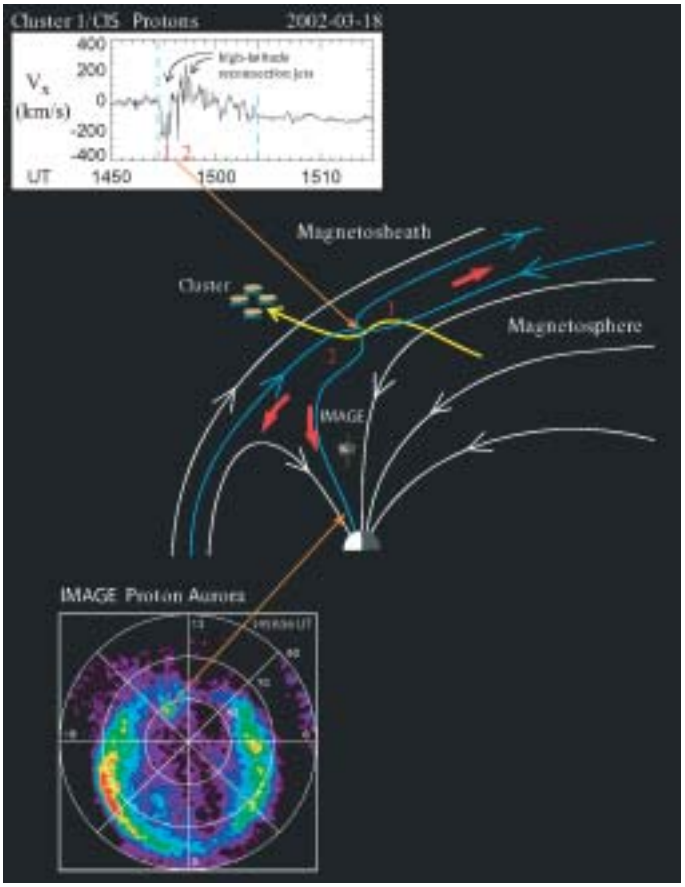

Figure 2.6.3. On 18 March 2002, the IMAGE satellite recorded an aurora that contained a dayside proton auroral spot (bottom left picture). At the same time, the Cluster quartet then passed overhead returning proton data (top left graph) that showed a magnetic reconnection was taking place and protons were leaking through Earth's magnetic shield. These protons were then being funnelled into the atmosphere along the magnetic field to form the spot.

Another science result was the precise measurement of the width of the Earth's bow shock. Shock waves are very important in planetary and astrophysical objects because they accelerate particles to very high energies that can then be detected *in situ* near the Earth or via X-rays for distant objects. The detailed study of the terrestrial bow shock is one of the mission's main objectives. Cluster allows us for the first time to measure the speed of the shock using the four satellites and then derive its thickness. A recent study on 98 bow shock crossings shows that the thickness of the shock front is best parameterised by the gyro-radius of a small population of solar wind ions trapped by, and gyrating around, the shock front itself. This is in contrast

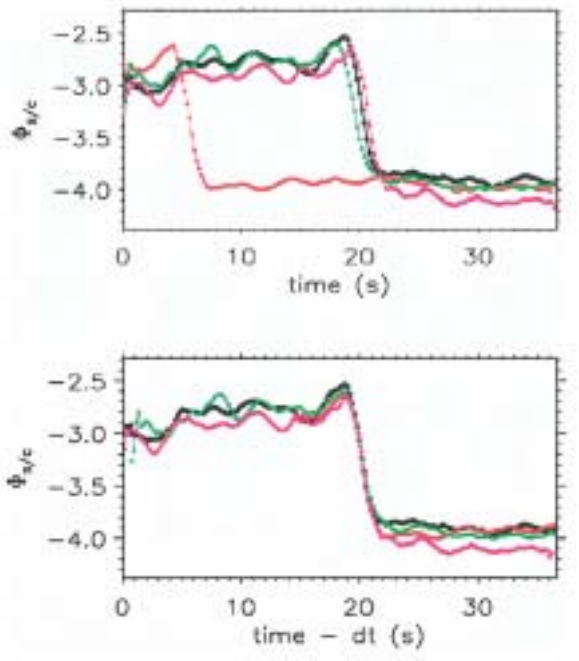

Figure 2.6.4. Smoothed spacecraft potential measurements from the four satellites (each shown as a different colour, C1 black, C2 red, C3 green and C4 magenta) at a collisionless shock (top panel). The time shift between encounters on the four satellites is used to compute the shock normal vector and speed and then its thickness. The measurements of C2, C3 and C4 are shifted with respect to C1 (bottom panel).

to earlier studies, which suggested that the shock front was best characterised by a wave in a fluid.

A very important topic where Cluster is delivering new results is surface waves observed on the flanks of the magnetosphere. During a single day, 25 crossings of the waves were observed by Cluster. The shape and motion of the waves could be fully characterised by the four satellites: speed 65 km/s and dimension 22 000 km (3.4 R_E). Like a wind blowing on a lake, these waves are produced by the solar wind blowing on the magnetosphere.

Finally, electromagnetic waves are observed to play a key role in space plasma. They are believed to be responsible for heating and acceleration of plasma and are the link between particles in the absence of collisions. A mixture of waves is usually observed in a given region but it is very difficult to distinguish between them. For the first time, all waves in the medium can be identified at a given frequency using Cluster and the k-filtering method. Remarkable results have been obtained in the magnetosheath where Alfvén, mirror and fast-mode waves could be identified very accurately.

Cluster Science Data System

The Cluster Science Data System (CSDS) is designed as a distributed system consisting of eight nationally funded and operated data centres. It makes possible the joint scientific analysis of data from all 41 instruments. The general approach is to have national data centres near the Principal Investigators (PIs) and thus near the expertise required for processing the data. A major task of CSDS is to offer products routinely, such as the Summary Parameter Data Base and the Prime Parameter Data Base. CSDS also serves to some extent as the infrastructure for the Joint Science Operations Centre (JSOC), which is a staffed facility located at the Rutherford Appleton Laboratory (UK), to support the scientific payload operations.

In most cases, the data centres produce data products on behalf of the national PI teams. Members of the Cluster science community wishing to access CSDS do so via their national data centre. In those countries not served by a national data centre, members of the Cluster community may contact the relevant PI to determine which data centre should be contacted. It should be noted that all data centres offer the same data products. Scientists from outside the Cluster community also have access to CSDS, according to the policy on data rights as agreed by the PIs. Full access can be granted to the Summary Parameters and CSDSweb.

The following products are offered:

Prime Parameter Data Base (PPDB): 65 parameters are contained in this database. The data files are written in the Common Data Format (CDF) and are held in physical units with an exhaustive set of ancillary information (or metadata). The PPDB holds data from all four spacecraft with a time resolution of 4 s. The data set is accessible by all Principal and Co-Investigators.

Summary Parameter Data Base (SPDB): 86 parameters are contained in this data base. These files are also written in the Common Data Format and are held in physical units with an exhaustive set of ancillary information. The SPDB holds only data from satellite C3 with a time resolution of 1 min. Access is not restricted.

Summary Plots: plots of summary parameters with 1 min resolution used to search for interesting events. It has been agreed that the German Data Centre will produce these plots as Postscript files centrally and distribute them inside Germany and to the other data centres. The plot information is encoded in a compact form for sending it over the network.

CSDSWeb: quicklook plots of the latest data (a few hours to a few days after acquisition) are provided from one spacecraft, including particle and wave spectrograms, as gif files. The plots cover 6 h and a full orbit (2.5 days). These data are available to the general science community.

CSDS data access has been steadily increasing since its opening on 1 February 2001. The download rate for summary and prime parameters data is now above 5 Gbytes per month and above 2 Gbytes per month for CSDSWeb. More information and data access can be found at: *http://sci2.estec.esa.nl/cluster/csds/csds.html*

Cluster Active Archive

In February 2003, the SPC agreed to develop a Cluster Active Archive (CAA) to distribute all Cluster data (including high-resolution data) to the general public. The CAA consists of a core team that will set up and maintain the archive and instrument scientists, located at the PI institutes, to prepare the data to be included in the archive. An implementation group and a steering committee are following the development of the archive. The plan is to have the data from 2001 by the end of 2004 and to continue with 2 years' worth of data included in the archive every year.

2.7 Integral

Introduction

Integral was launched on 17 October 2002 aboard a Proton vehicle from Baikonur cosmodrome. The rocket's first three stages placed Integral into a low Earth orbit from where, 50 min later, the fourth stage delivered it into the transfer orbit. A few days later, Integral used its own propulsion system for four perigee-raise burns and one apogee-adjust manoeuvre to achieve the initial operational orbit of 9 000 x 154 000 km. Operations were approved in 1993 for an initial period of 2.2 years; the design lifetime is 5 years. This ESA-led mission includes contributions from Russia (Proton) and NASA (Goldstone ground station). The mission is successfully delivering medium- to high-spatial and -spectral resolution gamma-ray observations in the 15 keV to 10 MeV energy range, as well as providing simultaneous X-ray (3-35 keV) and V-band optical monitoring.

Status

The majority of Integral observing time is available to the general astronomical community via calls for proposals. The first call, issued pre-launch in November 2001, resulted in 276 proposals that oversubscribed the available time by about a factor 19. The second call was issued in July 2003 and requested proposals for 70% of the science observing time in year-2 of operations. This call resulted in 142 proposals and a lesser, but still very large, over-subscription factor of around 8. About half of the proposals were for compact Galactic sources, a quarter for extragalactic objects and the remainder for nucleosynthesis studies and miscellaneous objects. The remaining 30% of observing time was provided to the Integral Science Working Team (ISWT) in return for their contributions to the mission. The ISWT is composed of instrument and data centre Principal Investigators, mission scientists, the Project Scientist and representatives of the US and Russian scientific communities. This 'core programme' observing time is used mainly for survey-type activities, including regular scans along the Galactic plane and deep exposures of the central radian of the Galaxy.

Status of the spacecraft and instruments is well in line with the design goal of operating for 5 years. At the current consumption rate, there is sufficient propellant for another 15 years. No unexpected degradation in the solar array or battery performance is evident, and there has been no loss of redundancy in any spacecraft system. Pointing stability and slewing accuracy comfortably exceed the requirements. The ESA Science Programme Committee recently approved an extension of Integral operations until December 2008. As part of this extension, the Integral Science Operations Centre will move from ESTEC to Vilspa.

Scientific payload

The Integral payload consists of two main gamma-ray instruments: the SPI spectrometer and the IBIS imager. Each offers both spectral and angular resolution, but they are differently optimised in order to be complementary and to achieve overall excellent performance. Recent observations show that line emissions occur on a wide range of angular and spectral extent; broader lines seem to be emitted from point-like sources and narrower lines from extended sources. Two monitor instruments provide complementary observations in the X-ray (JEM-X) and optical (OMC) wavebands to support the main instruments. A detailed description of the mission, operations and payload can be found in a special edition of *Astronomy & Astrophysics* dedicated to Integral (volume 411, November 2003).

The spectrometer, imager and X-ray monitor have a common principle of operation: they are all coded aperture mask telescopes. The coded mask technique is the key for imaging, which is all-important in separating and locating sources. It also

For further information, see http://astro.estec.esa.nl/Integral/

Table 2.7.1. Principal characteristics of the Integral scientific payload.

	SPI	*IBIS*	*JEM-X*	*OMC*
Energy range	20 keV - 8 MeV	15 keV - 10 MeV	3-35 keV	500-850 nm
Detectors/characteristics	19 Ge (each 6x7 cm) cooled @ 85K	16384 CdTe (each 4x4x2 mm); 4096 CsI (each 9x9x30 mm)	Microstrip Xe-gas detector (1.5 bar)	CCD + V-filter
Detector area (cm^2)	500	2600 (CdTe) 3100 (CsI)	2 x 500	2048 x 1024 pix
Spectral resolution	2.2 keV @ 1.33 MeV	9 keV @ 100 keV	1.3 keV @ 10 keV	–
FOV (fully coded)	16°	9x9°	4.8°	5x5°
Angular res (FWHM)	2°	12 arcmin	3 arcmin	17.6 arcsec/pix
10σ source location	1.3°	< 1 arcmin	< 30 arcsec	6 arcsec
Continuum sensitivity*	10^{-7} @ 1 MeV	$5x10^{-7}$ @ 100 keV	$1.3x10^{-5}$ @ 6 keV	18.2^{m} (10^{-3} s)
Line sensitivity*	$5x10^{-6}$ @ 1 MeV	$2x10^{-5}$ @ 100 keV	$1.7x10^{-5}$ @ 6 keV	–
Timing accuracy (3σ)	129 μs	62 μs - 30 min	122 μs	var. in units of 1 s
Mass (kg)	1309	628	65	17
Power (W)	250	220	52	12
Data rate (kbit/s)	20	57	7	2

*sensitivities are 3σ in 10^6 s, units ph cm^{-2} s^{-1} keV^{-1} (continuum) and ph cm^{-2} s^{-1} (line)

provides near-perfect background subtraction because for any particular source direction the detector pixels can be considered as being split into two intermingled subsets – those that view the source, and those for which the source is blocked by opaque mask elements. Effectively, the latter subset provides a contemporaneous background measurement for the former, made under identical conditions.

Scientific highlights

After the performance and verification phases, the observing programme began as planned in December 2002 by executing approved AO-1 open-time observations and guaranteed-time Core Programme observations. The AO-2 cycle of open-time observations began on 18 December 2003 and will last until 15 February 2005. Highlight early results are presented below; see the Integral special edition of *Astronomy & Astrophysics* for more detailed information.

Diffuse gamma-ray line emission

Measuring the properties of line emission from newly formed elements such as ^{26}Al, ^{44}Ti and ^{60}Fe is a key goal of Integral. These lines occur during explosive and hydrostatic nucleosynthesis processes in massive stars such as OB-associations, novae and supernovae. Integral's task include detailed spectroscopy and mapping of these and possible other lines.

Initial indications show that Integral is well-suited to this task. Early results

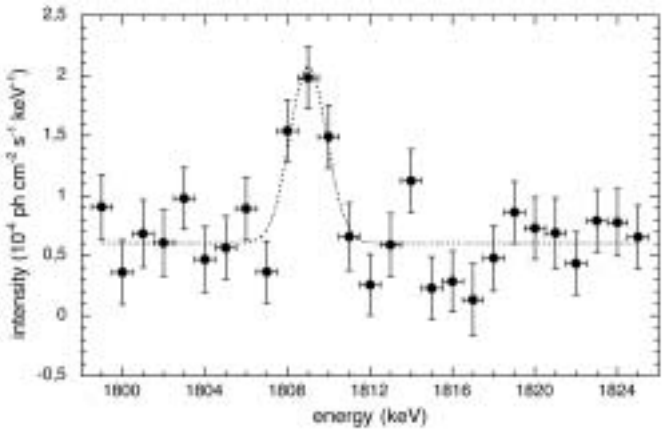

Figure 2.7.1. Spectrum of the radioactive decay of ^{26}Al (1809 keV) obtained from observations of the Galactic Centre region (Diehl et al., *A&A* 411, L451, 2003).

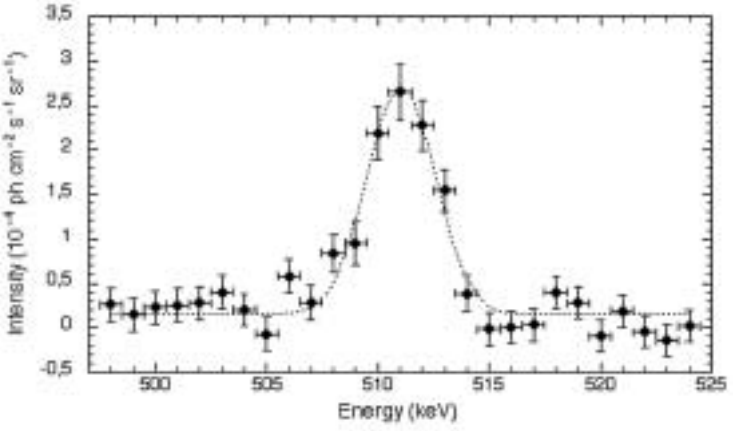

Figure 2.7.2. Spectrum of the electron-positron annhilation feature at 511 keV obtained during Galactic Centre observations (Jean et al., *A&A* 407, L55, 2003).

(Fig. 2.7.1) show that the 1809 keV radioactive decay of ^{26}Al line intensity is consistent with previous measurements, but is narrower (3.1 keV FWHM)) than the 5.4 keV FWHM line reported by the balloon-borne Gamma-ray Imaging Spectrometer.

Another high-priority target for Integral is the detailed mapping and spectroscopy of the 511 keV electron-positron annihilation feature seen from the central Galactic region (Fig. 2.7.2). An initial analysis of SPI results indicates that the 511 keV line has an intrinsic width of 2.95 keV FWHM, at the upper range of previous measurements. Detailed mapping of the morphology of the emission is providing constraints on the origin of the positrons. The line is broader than reported before, which could be explained by a different temperature regime in the annihilation environment in the interstellar medium.

Early 511 keV mapping results from SPI reveal a spherical Galactic bulge with no evidence for the disc component seen by the Oriented Scintillation Spectrometer Experiment (OSSE) on the Compton Gamma-ray Observatory (CGRO). However, with the amount of data available so far, the upper limit is still consistent with the OSSE intensity. As more observations of the Galactic centre region are performed, it is expected that Integral will produce maps of unprecedented spatial and spectral resolutions and sensitivity.

Diffuse Galactic continuum emission

Detailed maps of the central Galactic radian emission have been produced in many energy ranges between 15-40 keV and 700-1200 keV using SPI. After point source removal, these were fitted to the Galactic distributions of H I and CO emission, allowing subtraction of background components. This results in a power-law spectrum with the 511 keV line emission evident. However, the nature of the Galactic emission between 10 keV and 300 keV is a matter of debate because the relative contribution of the ISM and compact sources has not yet been determined. Recent IBIS high-resolution observations of the Galactic centre region indicate the importance of good imaging of point sources with high sensitivity, with the result that possibly most of the Galactic soft gamma-ray emission observed so far may be due to

Table 2.7.2. Principal characteristics of the Integral mission.

Launch: 17 October 2002 by Proton into orbit of 72 h, 51.6° inclination, 9 000 km perigee height, 153 000 km apogee height. Start of science operations December 2002 (nominal duration 2 years, extended mission to December 2008 approved).

Science goals: compact objects; extragalactic astronomy; stellar nucleosynthesis; galactic structure; particle processes and acceleration; identification of high-energy sources.

Science operations:
Integral Science Operations Centre (ISOC) at ESTEC (Vilspa for extended mission);
Integral Science Data Centre (ISDC) in Versoix (CH);
distribution of observing time:
1st mission year: 35% guaranteed time, 65% open time (via AO)
2nd mission year: 30% guaranteed time, 70% open time (via AO)
3rd-5th mission years: 25% guaranteed time, 75% open time (via AO)

Spacecraft:
3-axis stabilised (all errors 3σ; instruments point along x-axis, y-axis is along length of solar arrays):
absolute pointing error: 5 arcmin (y,z), 15 arcmin (x)
absolute pointing drift (10^5 s): 0.6 arcmin (y,z), 2 arcmin (x)
relative pointing error (10^3 s) : 0.3 arcmin (y,z), 1 arcmin (x)
absolute measurement error : 1 arcmin (y,z), 3 arcmin (x)
Data rate: 108 kbit/s (science telemetry)
Power (payload): 690 W
Spacecraft size: 3x4x5 m (solar arrays stowed; 16 m span deployed)
Mass: about 4000 kg at launch; 3500 kg dry; 520 kg hydrazine propellant

Operations:
Operations Centre: Mission Operations Centre (Darmstadt, D), ISOC (ESTEC)
Data transmission: S-Band, ground stations: Redu (B), Goldstone (USA)
Mission lifetime: 2 years nominal, 5 years technical design life

previously unresolved compact objects, mainly X-ray binaries. Future work will exploit the high-energy resolution, imaging response and large-scale coverage not available on previous missions.

Galactic compact sources

The Galactic Centre is a prime scientific target for Integral so significant observing is being spent on this region. Summed IBIS images in the 20-40 keV and 40-100 keV energy ranges allowed the discovery of a source (IGR J17456-2901) coincident with the Galactic Nucleus Sgr A* to within 0.9 arcmin. The source is visible up to about 100 keV with a 20-100 keV luminosity at 8 kpc of $(2.89\pm0.41)\times10^{35}$ erg/s. Although this new source cannot be unambiguously identified with Sgr A*, this is the first report of significant hard X-ray emission from the inner 10 arcmin of the Galaxy. A contribution from the Galactic super-massive black hole itself cannot be excluded. Coordinated Integral and XMM-Newton observations are planned for 2004 in order to identify the source of emission.

At the time of writing, 15 new strong high-energy galactic sources (see *http://isdc.unige.ch/~rodrigue/html/igrsources.html*) have been detected by Integral and reported in Astronomical Telegrams, IAU Circulars and similar, creating much interest in the high-energy astronomical community. Many of these sources were detected in Integral Core Programme observations such as Galactic Plane Scans

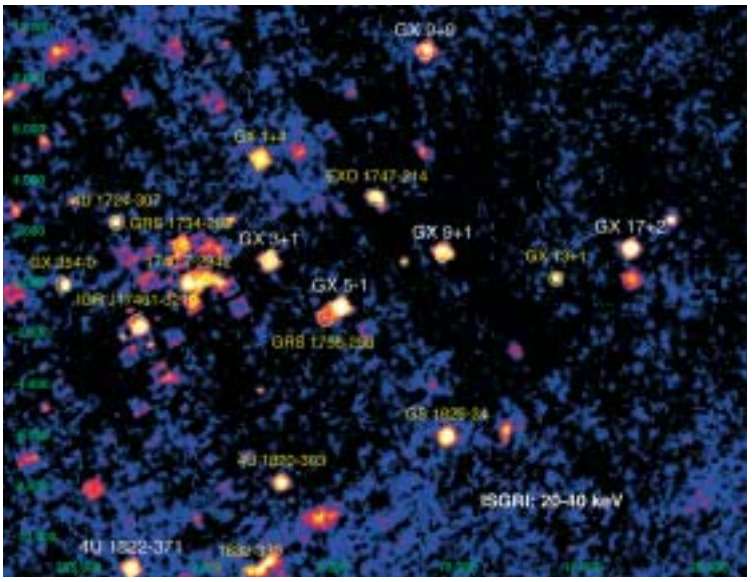

Figure 2.7.3. IBIS image of the area around the centre of our Galaxy in the energy range 20-40 keV. The image covers a region of approximately 24x30 deg. (Paizis et al., *A&A* 411, L363, 2003).

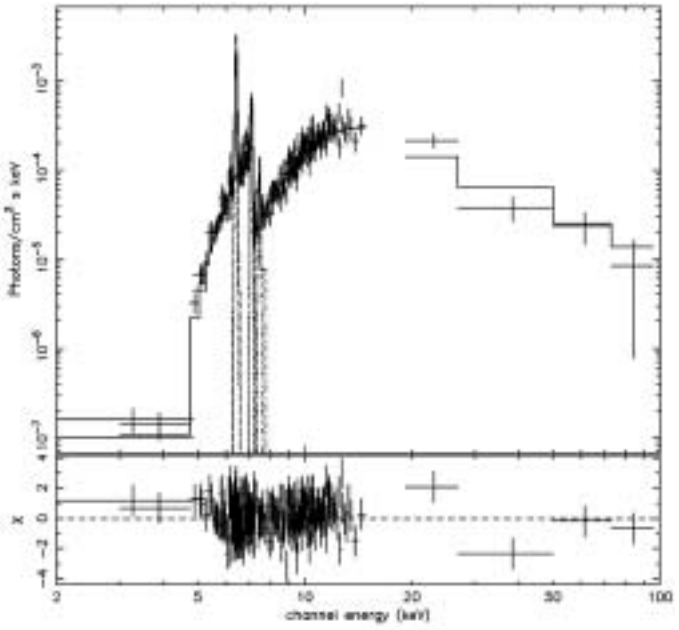

Figure 2.7.4. XMM (EPIC) and IBIS/ ISGRI photon spectra of IGR J16318-4848 along with the best fit model (an absorbed power-law continuum and three Gaussian emission lines at 6.4, 7.1 and 7.5 keV (Walter et al., *A&A* 411, L427, 2003).

(GPS) and Deep Exposure of the Central Galactic Radian (GCDE), which were designed largely to serve this purpose. Fig. 2.7.3 shows an IBIS view of the region around the Galactic Centre. The many sources visible demonstrate the richness of the Integral data.

The first of the new Integral sources, IGR J16318-4848, detected in January 2002, revealed a highly unusual, line-rich, strongly absorbed spectrum in an XMM-Newton follow-up observation. The source was hardly detectable by XMM-Newton below 5 keV due to the strong absorption, whilst being a strong source in the Integral energy range. This, and the detection of similar sources by Integral, suggests the presence of a hitherto unknown class of highly absorbed objects: 'cocooned binaries' (Fig. 2.7.4),

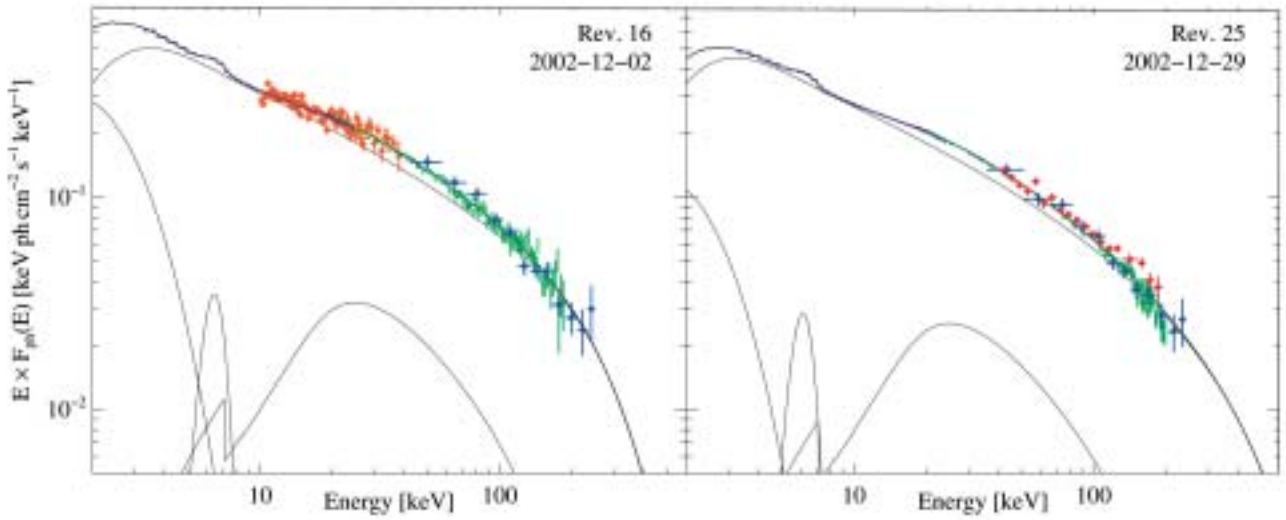

Figure 2.7.5. Spectra of the black hole Cygnus X-1 obtained from two sets of co-temporaneous Integral and R-XTE observations in December 2002. Integral imager data are shown in blue. The left panel also shows Integral X-ray monitor data in red, while the right panel shows Integral spectrometer data in red. The other data points are from R-XTE, demonstrating the good agreement between the two missions. The best-fit model for the data is shown as a solid line with the individual Comptonisation components indicated (Pottschmidt et al., *A&A* 411, L383, 2003).

predicted by F. Pacini et al. about 30 years ago. The flexible Integral observing strategy has allowed the mission to respond quickly to interesting and unexpected events. Outbursts from a number of X-ray binaries such as GRS 1915+105, XTE J16550-564, SGR 1806-20, H 1743-322 and GS 1843+009, have triggered target-of-opportunity follow-up observations.

Finally, state-of-the-art astrophysics benefits from studying objects over a wavelength range as broad as possible and simultaneously. This can be crucial in helping to understand the exact nature of the underlying physics responsible for the emission process. Integral has performed coordinated observations of a number of sources, including Cygnus X-1, GRS 1915+105 and 3C 273 (Fig. 2.7.5).

Gamma-ray bursts

Eight confirmed gamma-ray bursts (GRBs) have been observed in the fields of view of the gamma-ray instruments in 13 months of operations. This is consistent with the pre-launch estimate of about 10-12 GRBs annually. Although GRB science is a secondary objective for Integral, the mission can provide essential, rapid information in order to facilitate observations of any afterglow, or a counterpart search, at other wavelengths.

The automatic Integral burst detection software (IBAS) running at the Integral Science Data Centre in Versiox (CH), provides arcmin locations within a few tens of seconds after a GRB event. These alerts are quickly disseminated to the GRB community for follow-up observations at other wavelengths. The alert for GRB040106, with an error radius of 3.2 arcmin, was sent out only 15 s after the start of the burst (with a duration of 60 s), a record for the automatic IBAS system. One very interesting GRB observed was GRB030227. The accurate IBAS position allowed rapid follow-up observations in other wavebands. These revealed a fading magnitude +23 optical counterpart, while XMM-Newton, observing only 8 h after the burst, detected a fading X-ray counterpart with a line-rich X-ray spectrum.

Light curves (with 50 ms sampling) of around one GRB per day are provided by the SPI anti-coincidence system, which is sensitive essentially to the full sky. The precise timing provided is combined with measurements from other missions in the Interplanetary Network to provide accurate GRB positions.

2.8 Mars Express

Introduction

Mars Express was launched on 2 June 2003 from Baikonur cosmodrome aboard a Soyuz-Fregat vehicle. After a 7-month journey, it was inserted into Mars orbit on 25 December 2003. A week before arrival, preparations began for separating the lander: Mars Express was placed on a trajectory that allowed Beagle 2, which had no propulsion system of its own, to enter the martian atmosphere for a direct descent to the planned landing site on Isidis Planitia at 10.6˚N / 90.74˚E. Beagle 2 was released on 19 December and should have landed during 25 December. Contact was attempted by the NASA Mars Odyssey orbiter, several Earth-based radio telescopes and later with the Mars Express orbiter itself, but no signal was ever received.

ESA provided the launcher, orbiter, mission operations and part of Beagle 2, the rest of the lander being funded by a UK-led consortium of space organisations. The orbiter's instruments were provided and funded by scientific institutions throughout the ESA Member States. Other countries, including the USA, Russia, Poland, Japan and China, are also participating in various scientific capacities. The ground segment includes the Mission Operations Centre (MOC) at ESOC, Darmstadt, Germany, and ESA's deep-space ground station at New Norcia in Western Australia. Support from NASA's Deep Space Network (DSN) is helping to increase the scientific data return. The orbiter was built by Astrium in Toulouse (F) as prime contractor, and involved a large number of other European companies as subcontractors.

Status

Mars Express began to return its first scientific measurements and results before the mapping orbit was reached on 28 January 2004. The orbiter's operational performance is very good, and payload commissioning is progressing. The early orbits offer the best opportunity for optimised observing conditions (illumination, targets of interest, distance to the Sun, lack of eclipses) and therefore maximum science return. During this early phase of operations, primarily dedicated to instrument checkout and calibration, scientific observations of the planet and its environment are being acquired. The orbiter went through its maximum eclipse durations (up to 94 min per orbit) in late February to early March 2004. After the very rapid rise in eclipse duration, there will be a slow reduction until August 2004, permitting an increase of the science operations.

Payload commissioning started in early January and will take until April 2004, ending with deployment of MARSIS, the subsurface sounding radar/altimeter on 20 April. The initial mission duration will be one martian year (687 days), but an extension of an additional martian year is planned.

Scientific operations

The orbiter records all of the scientific data gathered by its own experiments, and then transmits them to Earth during the periods of ground station visibility. The volume of data being downlinked will vary throughout the year from less than 1 Gbit/day to about 6 Gbit/day. The Mars Express Project Scientist Team (PST) and the Principal Investigators (PIs) have compiled a Master Science Plan (MSP) scheduling the acquisition of science data by Mars Express in a way that is consistent with the scientific objectives for the mission and the resources available during the various periods of observation. The MSP forms the basis of all payload operations planning during the various phases of the mission.

The high-level scientific planning is performed by the Science Operations Working Group, which includes the PST and representatives of all PI teams. As one of several players involved in the science operations, the Payload Operations Service (POS) established at the Rutherford Appleton Laboratory (UK), is supporting the PST, the

For further information, see http://sci.esa.int/marsexpress

Table 2.8.1. The scientific objectives of Mars Express.

Orbiter
- Global high-resolution (10 m) photogeology
- Super-resolution imaging at 2 m pix^{-1} of selected areas
- Global mineralogical mapping at 100 m resolution
- Global atmospheric circulation and mapping of composition
- Subsurface structure at km-scale down to the permafrost
- Surface-atmosphere interactions
- Interaction of the upper atmosphere with the solar wind

Lander
- Geology of landing site
- Organic and inorganic chemistry
- Exobiology (search for life signatures)
- Meteorology

Table 2.8.2. The Mars Express scientific experiments.

Expt. Code	*Instrument*	*Principal Investigator*	*Participating Countries*
Orbiter			
HRSC	Super/High-Resolution Stereo Colour Imager	G. Neukum	D, F, RU, US, FIN, I, UK
OMEGA	IR Mineralogical Mapping Spectrometer	J.P. Bibring	F, I, RU
PFS	Atmospheric Fourier Spectrometer	V. Formisano	I, RU, PL, D, F, E, US
MARSIS	Subsurface-Sounding Radar/Altimeter	G. Picardi & J. Plaut	I, US, D, CH, UK, DK
ASPERA	Energetic Neutral Atoms Analyzer	R. Lundin & S. Barabash	S, D, UK, F, FIN, I, US, RU
SPICAM	UV and IR Atmospheric Spectrometer	J.L. Bertaux	F, B, RU, US
MaRS	Radio Science Experiment	M. Paetzold	D, F, US, A
MARESS	Lander Communications Relay	E. Flamini	I
Lander			
Beagle-2	Suite of imaging instruments, organic and inorganic chemical analysis, robotic sampling devices and meteo sensors	C. Pillinger	UK, D, F, HK, CH

Table 2.8.3. Mars Express Interdisciplinary Scientists.

Orbiter

Space environment and coordination between Mars Express and Nozomi
K. Maezawa, ISAS, JPN

Atmosphere and surface-atmosphere interactions
F. Forget, LMD/CNRS, Paris, F

Geological evolution
G.G. Ori, Int. Research School of Planetary Sciences, Università d'Annunzio, Pescara, I

Geodesy and cartography
T.C. Duxbury, JPL, USA

Lander

Astrobiology
R. Amils, CAB-Centro de Astrobiologia Torrejon de Ardoz, E

Geochemistry
E.K. Gibson, NASA Johnson Space Center, Houston, TX, USA

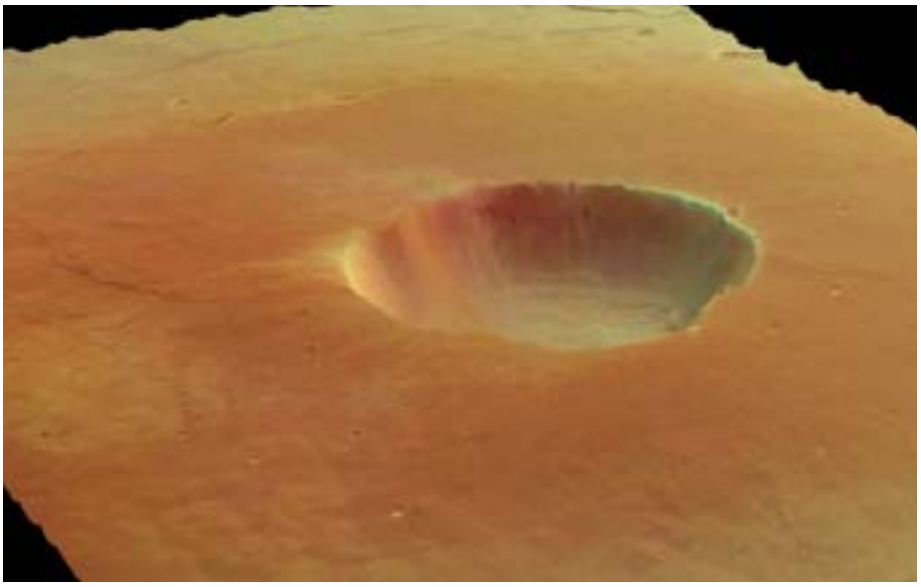

Figure 2.8.2. An overhead view of the complex caldera at the summit of Olympus Mons, the highest volcano in our Solar System. Olympus Mons has an average elevation of 22 km and the caldera has a depth of about 3 km. This is the first high-resolution colour image of the complete caldera. It was recorded by HRSC from a height of 273 km during orbit 37 of Mars Express, on 21 January 2004. The image is about 102 km across (resolution 12 m per pixel) and is centred at 18.3°N / 227°E; south is at the top.

Figure 2.8.1 (facing page). This 3-D oblique view of the summit caldera of Albor Tholus, a volcano in the Elysium region, was recorded by HRSC on 19 January 2004. The caldera has a diameter of 30 km and depth of 3 km; the volcano has a diameter of 160 km and height of 4.5 km. This is geologically interesting, because the caldera depth is similar to the volcano's height, which is unusual on Earth. On the far left rim of the caldera, a bright 'dust fall' seems to flow from the surrounding plateau into the caldera.

PIs and the MOC at ESOC. The POS has been responsible, under a contract from ESA, for the development, implementation, testing and operations of the system and tools to support the science operations. The PST and POS both interface with the MOC and PIs.

Scientific highlights

High-resolution, down to 10-12 m/pixel (HRSC) and 2-4 m/pixel (SRC), stereo and colour images have been taken and processed, as well as multi- and hyper-spectral visible and near-IR measurements from the OMEGA imaging spectrometer and the PFS and SPICAM spectrometers. The ASPERA instrument is also in good health and taking measurements of the martian environment. Radio science data have been collected using both the ESA New Norcia and NASA DSN ground stations.

These first scientific data are among the highest spatial and spectral resolutions ever delivered from Mars orbit. Most of the observations made so far took place near pericentre and covered a variety of essential surface features and targets of interest such as volcanic terrains (Tharsis Montes, Elysium Mons, Hecates Tholus), chaotic terrains near Valles Marineris, Isidis Planitia with the Beagle 2 landing site, the NASA Spirit and Opportunity landing sites (Gusev Crater and Meridiani), and polar

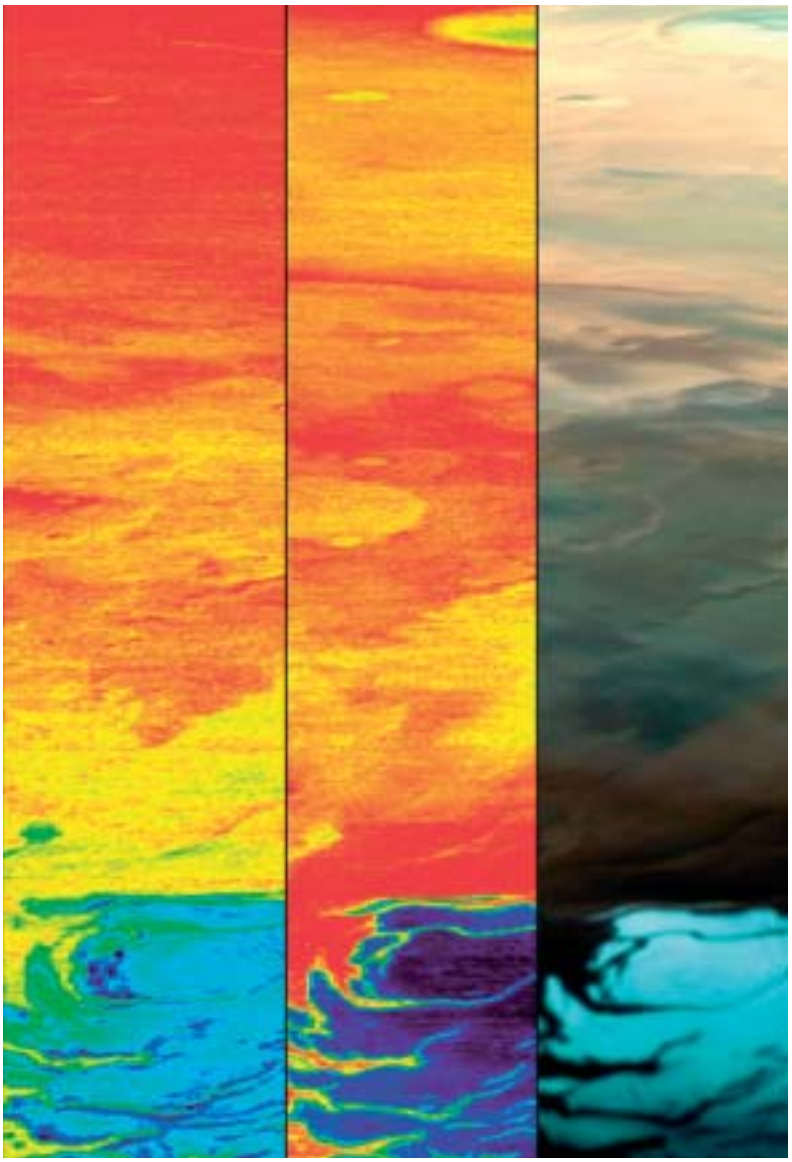

Figure 2.8.3. OMEGA observed the southern polar cap of Mars on 18 January 2004 in all three bands. At right is the visible image; centre is the carbon dioxide ice; left is the water ice.

areas. The focus of the mission is being extended to global coverage and image mosaic construction.

The first imaging and spectroscopic data sets returned by the orbiter already provide important new information about the martian surface, in particular about chaotic regions, outflow channels, the crustal dichotomy boundary, and volcanic and erosional features. As an example, analysis of OMEGA data acquired over the southern polar cap has revealed the existence of trapped water ice along with carbon dioxide ice. The science return will complement previous data, results and scientific interpretations dealing with surface mineralogy and rock and soil compositional variations, the nature of volcanic surface materials, the occurrence of aqueous mineralisation, the dust transport and accumulation processes, and the geologic and climatic processes.

2.9 SMART-1

Introduction

SMART-1, the first of the Small Missions for Advanced Research in Technology series in ESA's Scientific Programme, was launched from Kourou, French Guiana by Ariane-5 on 27 September 2003. 42 min after lift off, SMART-1 (Figs. 2.9.1 & 2.9.2) was released into a geostationary transfer orbit of 654 x 35 885 km, inclined at 7°.

The SMART missions were introduced into ESA's science programme to prepare the technology for future Cornerstone missions. SMART-1 is designed mainly to demonstrate innovative and key technologies for future deep-space science missions, with the potential to reduce the size and cost of propulsion systems while increasing manoeuvring flexibility and the mass available for scientific instrumentation. The first technology to be demonstrated on SMART-1 is Solar Electric Primary Propulsion (SEPP), a highly efficient and lightweight propulsion system that is ideal for long-duration deep-space missions. The propulsion system of SMART-1 consists of a single ion engine fuelled by 82 kg of Xe and powered by solar energy. This plasma thruster design is based on the 'Hall effect' and can accelerate ions to speeds up to 16 km/s. It delivers 70 mN of thrust with a specific impulse 5-10 times better than traditional chemical thrusters. The low thrust levels are compensated for by very long thrust intervals – months to years, instead of the minutes for typical chemical engines.

A wide range of other new technologies are being demonstrated in addition to SEPP: a Li-Ion modular battery package, new-generation high-data-rate deep-space communications in the X- and Ka-bands (KaTE), and techniques enabling spacecraft to determine their positions autonomously in space as a step towards fully autonomous navigation. The principal characteristics of the spacecraft are summarised in Table 2.9.1.

Scientific objectives

In synergy with the technology objectives, the science objectives for the lunar investigations include studies of the origin of the Earth-Moon system, accretional processes that led to the formation of planets, the chemical composition and evolution of the Moon, geophysical processes (volcanism, tectonics, cratering, erosion, deposition of ices and volatiles) for comparative planetology, and high-resolution

Figure 2.9.1. SMART-1 in lunar orbit.

For further information, see http://sci.esa.int/smart-1/

Table 2.9.1. The SMART-1 payload experiments.

Expt. Code	*Investigation Type*	*Main Investigator*	*Team Co-Is*	*Description of Experiment*
AMIE	Principal Investigator	J.L. Josset (CH)	F, NL, I, ESA	5.3° FOV miniaturised CCD-camera, with 4 fixed filters and micro-Data Processing Unit for Moon multi-band imaging. 1.8 kg, 9 W
Laser-link	Guest Technology Investigator	Z. Sodnik (ESA)		Demonstration of a deep-space laser link with ESA Optical Ground Station; sub-aperturing techniques for mitigating atmospheric distortion. Uses AMIE
OBAN	Guest Technology Investigator	F. Ankersen (ESA)		Validation of On-Board Autonomous Navigation algorithm by planetary bodies tracking. Uses star trackers and AMIE images
SPEDE	Principal Investigator	W. Schmidt (FIN)	FIN, S, ESA, USA	Langmuir probes measure spacecraft potential and plasma environment. Support to Electric Propulsion monitoring. 0.7 kg,1.2 W
RSIS	Guest Science Investigator	L. Iess (I)	USA, D, UK, F, ESA, S	Radio-science experiment monitors the Electric Propulsion. Uses KATE and AMIE
SIR	Technology Investigator	U. Keller (D)	D, UK, CH, I, IRL	Miniaturised near-IR (0.9-2.4 µm) grating spectrometer for lunar surface mineralogy studies. 1.7 kg, 2.5 W
D-CIXS/ XSM	Technology Investigator	M. Grande (UK) J. Huovelin (FIN)	FIN, S, E, I, F, ESA, USA	Compact X-ray spectrometer for mapping lunar chemical and variations of X-ray objects. 3.3 kg, 13 W
EPDP	Technology Investigator	G. Noci (I)	I, ESA, FIN, A	Multi-sensor package for monitoring the Electric Propulsion; plasma environment characterisation. 2.3 kg, 18 W
KATE	Technology Investigator	R. Birkl (D)	ESA, UK	X/Ka-band Telemetry, Tracking & Control package, demonstrates telecommunication and tracking 5.2 kg, 18 W

Table 2.9.2. Principal characteristics of the SMART-1 spacecraft.

Stabilisation: 3-axis, zero momentum
Attitude control: autonomous star tracker, Sun sensor, rate sensor gyro, reaction wheels, reaction control hydrazine system, thruster engine gimbals
Mass: 350 kg at launch
Size: 1 m cube, 14 m from tip-to-tip of solar arrays
Propellants: 82 kg of xenon and 4 kg of hydrazine
Power: two solar wings of three panels each; total area 10 m^2, generating 1950 W @ 1 AU. Supported by 5 Li-ion batteries totalling 600 Wh storage
Telemetry data rate: S-band 62 Kbit s^{-1}, X-band: 2 Kbit s^{-1} (from lunar orbit), Ka-band 120 Kbit s^{-1}
Onboard memory: redundant 4 Gbit solid-state mass memory
Primary propulsion: Stationary Plasma Thruster PPS-1350, nominal 70 mN thrust at 1350 W inlet power and Specific Impulse of 16 000 Ns kg^{-1}

Figure 2.9.2. SMART-1 attached to its Ariane launch vehicle.

mapping. SMART-1 carries seven instruments (Table 2.9.2) with which 10 experiments will be performed during the mission. Part of the payload monitors the electric propulsion and spacecraft environment, and tests novel spacecraft and instrument technologies:

— the diagnostic instruments include SPEDE, the spacecraft potential plasma and charged particles detector, to characterise the spacecraft and its environment, together with EPDP, a suite of sensors monitoring secondary thrust-ions, charging and deposition effects;
— KaTE supports radio science (RSIS) to monitor the acceleration provided by the electric propulsion and is used as a test bed for turbo-code techniques to improve the return of scientific data;
— RSIS, a set of radio-science and technology investigations, aimed at characterising the X/Ka-band deep-space communication channels and demonstrating a method for measuring the libration of the Moon from orbit by using high-resolution images from AMIE, and accurate orbit determination by tracking in Ka-band in preparation for BepiColombo.

The remote-sensing instruments for imaging and spectrometry are all highly miniaturised:

— D-CIXS, a compact X-ray spectrometer based on novel Swept Charge Device (SCD) detectors and micro-collimator optics, to perform lunar geochemistry, by fluorescence mapping of the major rock-forming elements (Mg, Si, Al, O, Fe), and to monitor bright X-ray sources during cruise;
— XSM, an X-ray solar monitor, to observe variations in the Sun from activity and flares, and to serve in the calibration of the D-CIXS determination of absolute lunar elemental abundances;
— SIR, a miniaturised quasi-monolithic point-spectrometer, is the first-ever near-IR

Figure 2.9.3. The Moon imaged by AMIE on 29 January 2004.

lunar spectrometer to survey the distribution of the main minerals in the lunar crust;

— AMIE, a miniature camera based on 3-D integrated electronics, imaging the Moon in four spectral bands defined by thin-film filters, and supporting three guest investigations: Laser-Link, a demonstration of acquisition of a deep-space laser-link from the ESA Optical Ground Station at Tenerife; OBAN, the demonstration of an autonomous navigation tool; and RSIS for the in-orbit measurement of lunar libration.

Status

By the end of January 2004, the spacecraft had completed more than 200 orbits, with all functions normal. It had accumulated more than 1700 h of thrust, using 27.1 kg of Xe, which provided a velocity increase of about 1.22 km/s. It was in a highly elliptic orbit with a perigee of 14 312 km and an apogee of 59 491 km and an orbital period of 24 h 53 min. This orbit was optimised to limit the length of the eclipses in March 2004. After 4 months of regular passages through the near-Earth radiation belts and suffering heavily from energetic particle events, SMART-1 has reached a much quieter environment. With the ion engine off for most of the month, February 2004 was used to commission the payload. A first test image of the Moon was obtained by AMIE on 18 January (Fig. 2.9.3). The efficiency of the electric propulsion system and the higher level of electric power available (resulting from low solar cell degradation and lower power consumption) means that SMART-1 will be able to arrive at the Moon earlier than Spring 2005, as was anticipated at launch, and will not require the lunar swing-bys. Lunar capture will occur either in mid-November or mid-December 2004, with the spacecraft reaching its final orbit about 6 weeks later. After capture, it will fly over the lunar north pole, aiming at a point of closest approach above the south pole, so achieving a wide polar orbit. During the following weeks, the ion engine will gradually reduce the size and duration of the orbit, to improve the view of the lunar surface. In early 2005, the mission will enter its nominal 6-month science phase.

2.10 Double Star

Introduction

The collaboration between China and ESA on Cluster began in 1992 when China proposed to set up a Data Centre to distribute Cluster data. Since then, several Chinese scientists have been hosted in Europe at ESA establishments and Principal Investigator (PI) institutes and have become Co-Investigators on the Cluster mission. In 1997, the Chinese Centre for Space Science and Applied Research (CSSAR) presented the Cluster Science Working Team (SWT) with their new magnetospheric Double Star Programme (DSP) and invited the Cluster PIs to participate in the payload; six Cluster PIs provided their instrument flight spare models.

A major milestone was reached in July 2001 when ESA and the Chinese National Space Administration (CNSA) signed the DSP agreement of cooperation. ESA's aims in this first collaboration with China are to provide unique opportunities for European space plasma scientists, to increase the scientific return of DSP by acquiring 4 h of data per day, to support the refurbishment/rebuilding of the European instruments, to coordinate the scientific operations of the European instruments on DSP, and to help in the pre-integration of the European instruments in Europe.

Within 2.5 years, TC-1 (Tan Ce: Explorer) was launched from Xichang in Southern China, on 29 December 2003 (Fig. 2.10.1) into a 570 x 78 970 km, 28.5° orbit. Owing to over-performance by the upper stage, the apogee is about 12 000 km higher than planned, but this should not affect the scientific objectives. Furthermore, the Earth's bow shock, which was not included in the original scientific objectives, will now be observed. Preliminary estimates indicate that the number of conjunctions with Cluster have decreased slightly, which would be compensated for by the longer time interval of the individual conjunctions.

TC-2, scheduled for launch on 20 July 2004, is aimed at a 700 x 39 000 km polar orbit. Its instruments will concentrate on the physical processes over the magnetic poles and the development of auroras.

Status

Commissioning of TC-1 and its instruments (Table 2.10.1) began in early January 2004. The first operation was deployment of the solid boom carrying the magnetometer. However, the other boom, carrying the search coil (STAFF/DWP), did not deploy but it does not affect the satellite's stability and the spin axis is, as planned, close to the north ecliptic pole. The STAFF/DWP sensor is close to the spacecraft and suffering from interference; the PI team is changing the software to reduce the noise. FGM began commissioning on 8 January and its electronics completed check-out in 4 days. Data acquisition then began to calibrate the instrument.

PEACE (electron detector) started electronics tests on 20 January and is working nominally. Some software tuning was required to optimise the onboard compression algorithm. Increased solar activity (M6.1 flare) beginning 21 January meant that an interplanetary shock arrived at Earth on 22 January at 01:35 UT. The increased pressure of the solar wind (more than five times the usual) produced a significant compression of the magnetosphere. The bow shock was pushed towards Earth and passed TC-1 at 12.6 R_E according to preliminary PEACE data. The Cluster satellites were also in the solar wind and observed the interplanetary shock; the combined readings allowed this event to be well-studied.

ASPOC entered commissioning on 24 January and emerged 5 days later with all four ion emitters working perfectly. This instrument will keep TC-1 'grounded' and measure low-energy particles. HIA, the hot ion analyser, began check-out on 4 February. The 2 days of electronics checks verified that all components were in perfect shape. Then high voltages were raised slowly to around 1500 V and the first

For further information, see http://sci.esa.int/doublestar

Figure 2.10.1. Launch of the first Double Star satellite, TC-1, on 29 December 2003 at 19:06 UT.

Table 2.10.1. Double Star payload.

Instrument	*PI*
Equatorial satellite	
Active Spacecraft Potential Control (ASPOC)	K. Torkar, IWF, Graz, A
Fluxgate Magnetometer (FGM)	C. Carr IC, UK
Plasma Electron and Current Exp. (PEACE)	A. Fazakerley, MSSL, Dorking, UK
Hot Ion Analyser (HIA), sensor 2 of CIS	H. Reme, CESR, Toulouse, F
part of Spatio-Temporal Analysis of Field Fluct.(STAFF) + Digital Wave Processor (DWP)	N. Cornilleau/H. Alleyne, CETP, Velizy, F & Sheffield U., UK
High Energy Electron Detector (HEED)*	W. Zhang & J.B. Cao, CSSAR, China
High Energy Proton Detector (HEPD)*	J. Liang & J.B. Cao, CSSAR, China
Heavy ion detector (HID)*	Y. Zhai & J.B. Cao, CSSAR, China
Polar satellite	
Neutral Atom Imager (NUADU)	S. McKenna-Lawlor, Ireland U., IRL
Fluxgate Magnetometer (FGM)	T. Zhang, IWF, A
Plasma Electron and Current Exp. (PEACE)	A. Fazakerley, MSSL, Dorking, UK
Low Energy Ion Detector (LEID)*	Q. Ren & J.B. Cao, CSSAR,China
Low Frequency Electromagnetic Wave detector (LFEW)*	Z. Wang & J.B. Cao, CSSAR, China
High Energy Electron Detector (HEED)*	W. Zhang & J.B. Cao, CSSAR, China
High Energy Proton Detector (HEPD)*	J. Liang & J.B. Cao, CSSAR, China
Heavy ion detector (HID)*	Y. Zhai & J.B. Cao, CSSAR, China

*instrument built by China

ions were detected on 9 February. Calibration continued to 13 February, when the instrument was declared fully functional.

The instruments were further calibrated and the data distribution system commissioned in time for the commissioning review on 10 March, following which TC-1's nominal mission operation phase could begin.

Data distribution system

The Double Star Data System (DSDS) was set up to coordinate the scientific operations of the European instruments and distribute the data to all scientific users. The European Payload Operation Services (EPOS) at RAL (UK) is coordinating the scientific operations of the European instruments (except NUADU, operated by China). It interacts with the PIs and the Double Star and Operations Centre in China. In addition, EPOS is distributing planning data to the scientific community and developed the Double Star data management system. The data system comprises four data centres, in Austria, China, France and the UK. The satellites send data to the ESA ground station at Villafranca (E) and the Chinese stations in Beijing and Shanghai. They are then decommutated in China and sent to the PIs team via the Austrian centre. A dedicated VPN line is used for the data traffic between Europe and China. Once in the PI institutes, the raw data are processed and calibrated and then distributed to the four data centre for access by the scientific community.

2.11 Rosetta

Introduction

Ariane V158 lifted off precisely on schedule at 07:17:51 UT on 2 March 2004 carrying the Rosetta spacecraft to start the 10-year journey to Comet 67P/Churyumov-Gerasimenko. This was a year after the original launch date for the mission to Comet 46P/Wirtanen. In January 2003, Rosetta and its payload were ready for launch, but the failure of the new Ariane-5 ECA launcher on its maiden flight on 11 December 2003 grounded the vehicle family and Wirtanen moved out of range. The Project Team, in close cooperation with the Flight Dynamics Team at ESOC, studied possible options for a new mission. Comet P67/Churyumov-Gerasimenko was the only target that could be reached using the original launcher (Ariane-5G+), did not require any modification to the spacecraft or payload, and did not extend the mission duration by more than 2 years.

Intensive observations of the new target began immediately. Hubble Space Telescope observations showed a nucleus radius of 2 km. A major concern was whether the Philae lander could cope with the higher touchdown speed of about 1 m/s, in contrast to the 0.5 m/s for the 600 m radius of Wirtanen. Studies and tests demonstrated that only a minor modification was required for the landing gear. In April 2003, the Rosetta Science Team approved the new mission scenario, which provides at least the same potential scientific return as the original baseline. The principal mission milestones are:

Launch	2 March 2004
Earth Gravity Assist #1	March 2005
Mars Gravity Assist	March 2007
Earth Gravity Assist #2	November 2007
Asteroid Steins flyby	September 2008
Earth Gravity Assist #3	November 2009
Asteroid Lutetia flyby	July 2010
Enter/exit hibernation	July 2011/January 2014
Rendezvous manoeuvre	May 2014
Start global mapping phase	August 2014
Lander delivery	November 2014
Perihelion passage	August 2015
End of mission	December 2015

Background

The International Rosetta Mission was approved in November 1993 by ESA's Science Programme Committee as the Planetary Cornerstone Mission in the Agency's Horizon 2000 long-term space science programme. The prime scientific objective of the mission is to study the origin of comets, the relationship between cometary and interstellar material, and its implications with regard to the origin of the Solar System. The measurements to be made in support of this objective are:

— global characterisation of the nucleus, determination of dynamic properties, surface morphology and composition;
— determination of the chemical, mineralogical and isotopic compositions of volatiles and refractories in a cometary nucleus;
— determination of the physical properties and interrelation of volatiles and refractories in a cometary nucleus;
— study of the development of cometary activity and the processes in the surface layer of the nucleus and the inner coma (dust/gas interaction);
— global characterisation of asteroids, including the determination of dynamic properties, surface morphology and composition.

For further information, see http://sci.esa.int/rosetta

Table 2.11.1. The Rosetta Orbiter payload.

Acronym	*Objective*	*Principal Investigator*
Remote Sensing		
OSIRIS	Multi-colour imaging NAC (Narrow Angle Camera) 2.35×2.35° WAC (Wide Angle Camera) 12×12° (250-1000 nm)	H.U. Keller, MPI fur Aeronomie, Katlenburg-Lindau, Germany
ALICE	UV spectroscopy (70-205 nm)	A. Stern, Southwest Research Institute, Boulder, Colorado, USA
VIRTIS	VIS/IR mapping spectroscopy (0.25-5 µm)	A. Coradini, IASFC-CNR, Rome, Italy
MIRO	Microwave spectroscopy (1.3 & 0.5 mm)	S. Gulkis, NASA-JPL, Pasadena, CA, USA
Composition Analysis		
ROSINA	Neutral gas and ion mass spectroscopy. Double-focusing, 12-200 amu, m/Δm~3000. Time-of-flight, 12-350 amu, m/Δm~2500 including Neutral Dynamics Monitor	H. Balsiger, Univ. of Bern, Switzerland
COSIMA	Dust mass spectrometer (SIMS, m/Δm~2000)	J. Kissel, MPI für Aeronomie, Lindau, Germany
MIDAS	Grain morphology (Atomic Force Microscope, nm resolution)	W. Riedler, Space Research Inst., Graz, Austria
Nucleus Large-scale Structure		
CONSERT	Radio sounding, nucleus tomography	W. Kofman, LPG, Grenoble, France
Dust Flux, Dust Mass Distribution		
GIADA	Dust velocity and impact momentum measurement, contamination monitor	L. Colangeli, Oss. Astronomico di CapodiMonte Naples, Italy
Comet Plasma Environment, Solar Wind Interaction		
RPC	Langmuir probe, ion and electron sensor, flux-gate magnetometer, ion composition analyser, mutual impedance probe	A. Eriksson, Swedish Inst. of Space Physics, Uppsala, Sweden; J. Burch, Southwest Research Inst., San Antonio, Texas, USA; K-H. Glassmeier, TU Braunschweig, Germany; R. Lundin, Swedish Inst. of Space Physics, Kiruna, Sweden; J.G. Trotignon, LPCE/CNRS, Orleans, France; C. Carr, Imperial College London, UK
RSI	Radio science experiment	M. Pätzold, Univ. of Cologne, Germany

Direct evidence of the constitution of cometary volatiles is particularly difficult to obtain, as the constituents observable from Earth and even during the flybys of Comet Halley in 1986 result from physico-chemical processes such as sublimation and interactions with solar radiation and the solar wind. What we know today about cometary material from those earlier missions and ground-based observations does, however, demonstrate the low degree of evolution of cometary material and hence its tremendous potential for providing unique information about the make-up and early evolution of the solar nebula.

The study of cometary material presents a major challenge because of the very characteristics that make it a unique repository of information about the formation of the Solar System, namely its high volatiles and organic-material contents. A funda-

Table 2.11.2. The Rosetta Lander payload.

Acronym	*Instrument*	*Principal Investigator*
APXS	Alpha-p-X-ray Spectrometer	R. Rieder, MPI Chemistry, Mainz, D
SD2	Sample Acquisition System	A. Ercoli-Finzi, Polytecnico, Milano, I
COSAC	Gas Chromatograph/Mass Spectrometer	H. Rosenbauer, MPAe, Lindau, D
PTOLEMY	Evolved gas analyser	I. Wright, Open Univ., UK
CIVA ROLIS	Rosetta Lander imaging system	J.P. Bibring, IAS, Orsay, F; S. Mottola, DLR Berlin, D
SESAME	Surface Electrical and Acoustic Monitoring Experiment, Dust Impact Monitor	D. Möhlmann, DLR Cologne, D; W. Schmidt, FMI, SF; I. Apathy, KFKI, H
MUPUS	Multi-Purpose Sensor for Surface and Sub-surface Science	T. Spohn, Univ. of Münster, D
ROMAP	RoLand Magnetometer and Plasma Monitor	U. Auster, DLR Berlin, D; I. Apathy, KFKI, H
CONSERT	Comet nucleus sounding	W. Kofman, LPG, Grenoble, F

mental question that the Rosetta mission has to address is, to what extent can the material accessible for analysis be considered representative of the bulk of the material constituting the comet, and of the early nebular condensates that constituted the cometesimals 4.57×10^9 years ago? This representativeness issue has to be addressed by first determining the global characteristics of the nucleus, namely its mass, density and state of rotation, which can provide us with clues as to the relationship between the comet's outer layers and the underlying material.

The dust and gas activity observed around comets, as well as its rapid response to insolation, guarantees the presence of volatiles at or very close to the surface in active areas. Analysing material from these areas will therefore provide information on both the volatiles and the refractory constituents of the nucleus. The selection of an appropriate site for the surface-science investigations should be relatively straightforward, given the mission's extensive remote-sensing observation phase and the Rosetta Orbiter advanced instrumentation that covers a broad range of wavelengths.

The dust-emission processes are induced by very low density gas outflows and thus should preserve the fragile texture of cometary grains. These grains can be collected at low velocities (a few tens of m/s) by the spacecraft after short travel times (of the order of minutes). This will minimise alterations induced by any interaction with solar radiation. Similarly, gas analysed in jets or very close to the surface should yield reliable information on the volatile content of the cometary material in each source region.

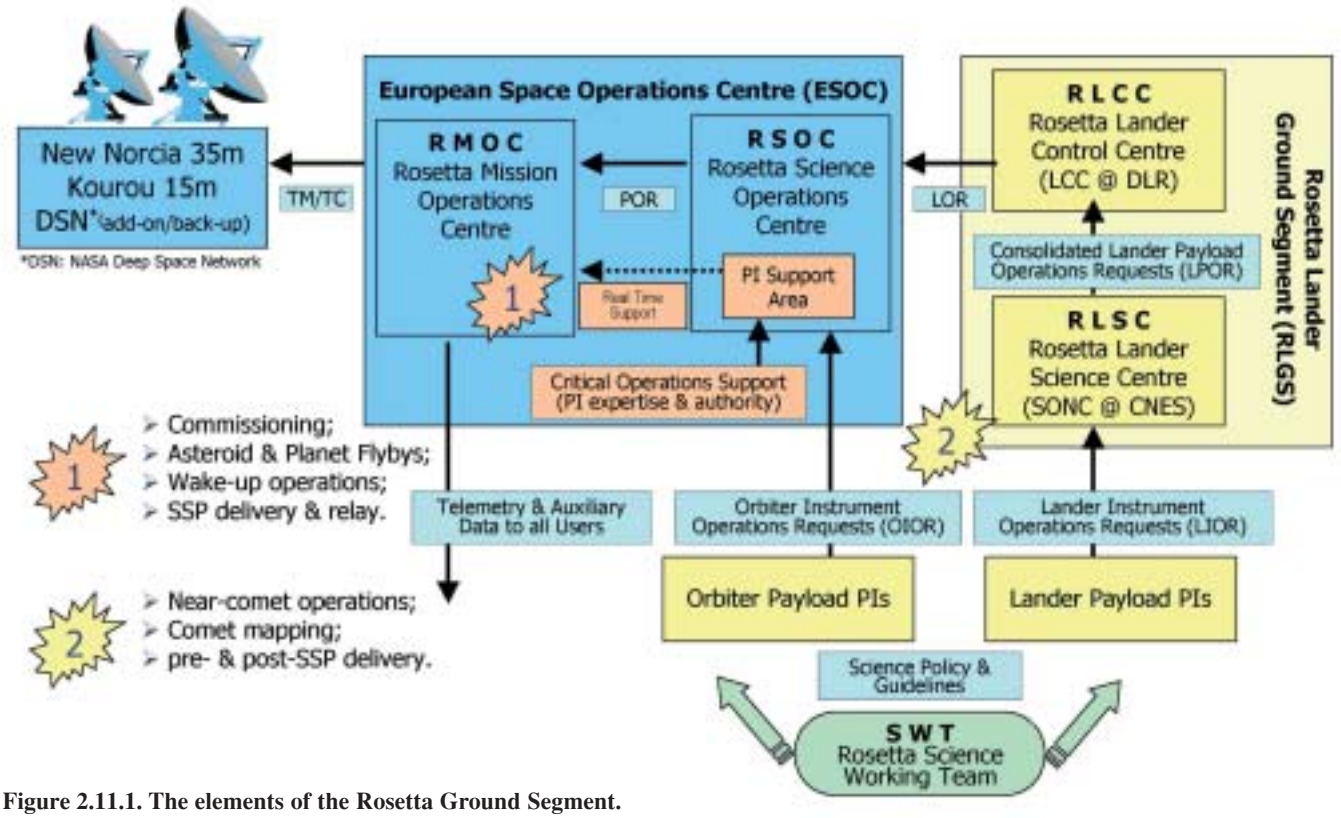

Figure 2.11.1. The elements of the Rosetta Ground Segment.

Science operations

Figure 2.11.2. ESA's 35 m Deep Space Antenna at New Norcia, Western Australia.

Rosetta is a Principal Investigator (PI)-type mission, i.e. the individual Experiment Teams are responsible for defining the science operations timelines for their individual instruments (Tables 2.11.1 & 2.11.2). These requests are coordinated and merged into the Science Operations Plans by the Rosetta Science Operations Centre (RSOC), in ESA's Research and Scientific Support Department in ESTEC, Noordwijk, The Netherlands. For key mission phases (commissioning, nucleus rendezvous, lander delivery), RSOC is collocated with the Rosetta Mission Operations Centre (RMOC) at ESOC, in Darmstadt, Germany (Fig. 2.11.1). ESOC is operating and controlling the spacecraft throughout the mission, working through the Agency's 35 m Deep Space Antenna at New Norcia in Western Australia (Fig. 2.11.2).

The Rosetta Science Data Archive will be prepared by RSOC in collaboration with the Primitive Bodies Node of the Planetary Data System at the University of Maryland.

Five Interdisciplinary Scientists have been nominated for a limited period to support the mission's implementation:

— M. Fulchignoni, DESPA, Observatoire de Paris, France, to develop physico-chemical models of the possible target asteroids in order to provide the Rosetta Project and the Rosetta Science Working Team with a reference data set;

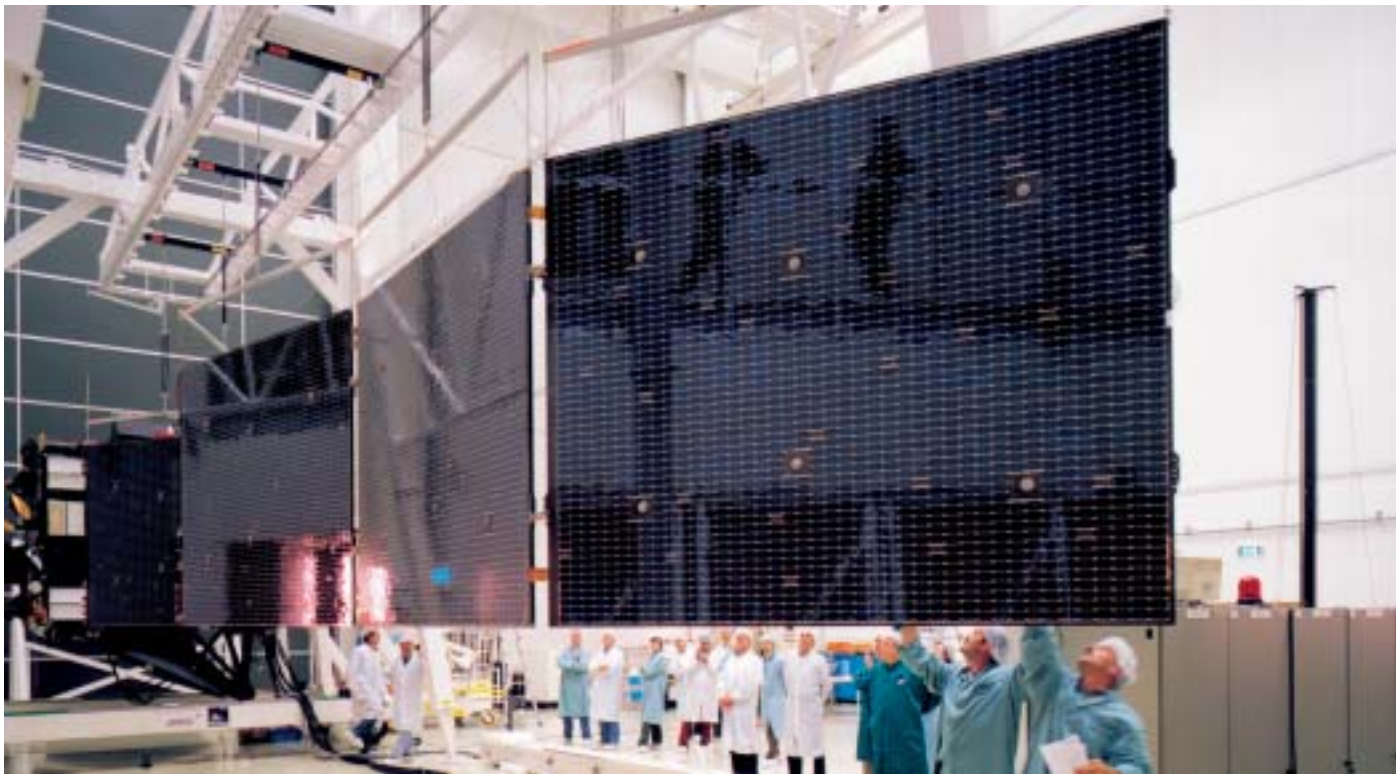

Figure 2.11.3. The Rosetta Proto-Flight Model during solar array deployment test at ESTEC.

Table 2.11.3. Rosetta spacecraft characteristics.

Spacecraft
3-axis stabilisation
Highly autonomous (two star trackers, Sun sensors, navigation cameras)
Three laser gyro packages
S/X-band up and downlink
Data transmission rates: 5-20 kbit/s (depending on geocentric distance)
Solid State Mass Memory: 25 Gbit
Solar Arrays (LILT-cells, low intensity, low temperature cells) to provide 400 W @ 5.2 AU
Size: box shaped, 2.5×2.5×2 m, all instruments body-mounted
Launch mass: ~3000 kg
Propellant: ~1670 kg bipropellant monomethyl hydrazine (MMH), nitrogen tetroxide (NTO)
Mission lifetime: 11 years

— P. Weissman, NASA-JPL, Pasadena, California, USA, to provide thermo-physical modelling of the cometary nucleus and of the inner coma of comets;
— R. Schulz, ESA RSSD, to liaise with the astronomical community and to derive a basic characterisation of the target comet from ground-based observations;
— E. Grün, MPI für Kernphysik, Heidelberg, Germany and M. Fulle, Trieste Astronomical Observatory, Italy, to provide empirical 'engineering models' for the nucleus dust environment in order to establish a reference data set for the Rosetta Project and the Rosetta Science Teams.

Status

After the successful launch, spacecraft commissioning operations began immediately. The first instrument to be switched on was COSIMA, the dust mass spectrometer, on 7 March. Rosetta is sharing usage of ESA's Deep Space Antenna in New Norcia with Mars Express so, to optimise the science return for that mission, the commissioning activities are divided into three phases during 2004 and will be formally completed by a Commissioning Review in October 2004.

3. Missions in Post-Operations/Archival Phase

3.1 ISO

Introduction

ESA's Infrared Space Observatory (ISO) made almost 30 000 scientific observations in its 2.5-year operational lifetime, which ended in May 1998. Employing its four sophisticated and versatile scientific instruments ISO provided astronomers with diverse data of unprecedented sensitivity at IR wavelengths of 2.5-240 µm. Infrared light penetrates the obscuring dust that hides much of the Universe from inspection at visible wavelengths; light of these wavelengths originates from bodies and material that are cool and distinct from the energetic sources of visible light, like stars. These cool sources are of fundamental importance. A rich variety of atomic, ionic, molecular and solid-state spectral features trace the chemistry and evolution of the cold gas and dust from which stars form, and which they in turn enrich with the heavy elements produced during their nuclear burning and terminal phases. New generations of stars and planets form from the enriched interstellar medium, revealing their presence first through the IR emission associated with proto-stellar and proto-planetary sources. Most of the star formation in the history of the Universe is revealed through the IR emission of the heated dust clouds that would otherwise hide it from view.

The mission resulted from a proposal made to ESA in 1979. After a number of studies, ISO was selected in 1983 as the next new start in the ESA Scientific Programme. Following a Call for Experiment and Mission Scientist Proposals, the scientific instruments were selected in mid-1985. The two spectrometers, a camera and an imaging photo-polarimeter jointly covered wavelengths from 2.5 µm to around 240 µm with spatial resolutions ranging from 1.5 arcsec (at the shortest wavelengths) to 90 µm (at the longer wavelengths). The satellite design and main development phases started in 1986 and 1988, respectively, with Alcatel (Cannes, F; formerly Aerospatiale) as prime contractor. ISO was launched perfectly in November 1995 by an Ariane-44P and all went very smoothly in orbit. At 12 µm, ISO was a thousand times more sensitive and had a hundred times better angular resolution than IRAS. Routine scientific operations began in February 1996 and continued until April 1998, with limited operations continuing through May. All data were reprocessed with the end-of-mission calibration to populate the first homogeneous ISO Data Archive, which opened to the community in December 1998. By August 1999, all data had entered the public domain.

Through the ensuing 4 years of the post-operations phase, ESA's ISO Data Centre developed and refined the ISO Data Archive to offer the ISO data to the worldwide astronomical community, and, together with the National Data Centres in various member states and in the US (see footnote p76), worked to fill the archive with the best systematically processed and calibrated data products that could be achieved for the huge ISO database. These products allow users to select data sets of interest for deeper study with interactive analysis tools. ISO's Legacy Archive, containing this reference product set, was released at the end of February 2002.

During ISO's Active Archive Phase, which is running from January 2002 to December 2006, the ISO Data Centre continues to work with active National Data Centres in The Netherlands, Germany and the UK to support the community in its use of the ISO data and to leave behind a homogeneous archive as a legacy to future generations of astronomers, especially those preparing and interpreting Herschel observations. Particular focus is placed on systematic reduction of selected observing modes and on the opportunity represented by the growing mass of published ISO data to gather into the archive the refined data products upon which astronomers have based their published work. In this way, we will fill the archive with immediately reusable refined data products, so preparing the ISO archive for its role as part of a system of interoperable archives forming the 'virtual telescopes' of the future.

For further information, see http://www.iso.vilspa.esa.es

Table 3.1.1. Principal characteristics of the ISO instruments.

Instrument/ PI	*Participating countries*	*Main function*	*Wavelength (μm)*	*Spectral resolution*	*Spatial resolution*	*Outline description*
ISOCAM (C. Cesarsky, CEN-Saclay, F)	F, GB, I, S, USA	Camera and polarimetry	2.5-17	Broadband, narrow-band and circular variable filters	Pixels of 1.5, 3, 6 & 12 arcsec	Two channels, each with a 32×32-element detector array
ISOPHOT (D. Lemke, MPI für Astronomie, Heidelberg, D)	D, DK, E, GB, IRL, SF, USA	Imaging photopolarimeter	2.5-240	Broadband and narrowband filters Near-IR grating spectrometer (R~90)	Variable from diffraction-limited to wide-beam	Three subsystems: 1. multi--band, multi-aperture photopolarimeter (3-125 μm) 2. far-IR camera (50-240 μm) 3. spectrophotometer (2.5-12 μm)
SWS (Th. de Graauw, Lab. for Space Research, Groningen, NL	B, D, NL, USA	Short-wavelength spectrometer	2.5-45	1000 across wavelength range and 2×10^4 for 12-44 μm	14×20 and 20×44 arcsec	Two gratings and two Fabry-Perot interferometers
LWS (P. Clegg, Queen Mary College, London, UK	F, GB, I, USA	Long-wavelength spectrometer	43-195	200 and 10^4 across wavelength range	1.65 arcmin	Grating and two Fabry-Perot interferometers

ISO science

ISO continues to deliver ground-breaking results in all areas of astronomy. The vast scientific potential still locked in the ISO archive was evidenced in the symposium 'Exploiting the ISO Data Archive – Infrared Astronomy in the Internet Age' organised by the ISO Data Centre in Sigüenza, Spain, in June 2002 (ESA SP-511). Through new calibration tools, more than the science goals of the original proposals are being reached. A number of archival projects are also being undertaken, involving systematic analysis of large data sets, unveiling new findings and pushing the development of classification studies. Astromineralogy, a new field of research opened by ISO, calls for more laboratory measurements to interpret the wealth of spectroscopic observations of a variety of astronomical objects. ISO permitted comparison of stellar spectra with cometary spectra, which revealed parallels between the chemical composition of dust in our Solar System and dust around other stars. Now, more similarities are being found between asteroids and minerals spectra. Numerous results on the chemistry of the interstellar-medium have been obtained by ISO, such as the ubiquity of water and of the probably-organic substances that give rise to broad features in IR spectra of a huge range of astronomical objects, from protostars to galaxies. More identification of molecular species and elements have been made in the last 2 years. Figure 3.1.1 shows the most massive molecular cloud in our Galactic Center, Sagittarius B2, the richest spectrum ever recorded by any space telescope in the far-IR, obtained with ISO's Long Wavelength Spectrometer. Many signatures from different molecular species have been detected in this spectrum, the 'Rosetta Stone' of ISO's far-IR spectra, some of them for the first time in the interstellar medium. Deeply embedded star-forming regions (obscured at visible wavelengths) delivered complex spectra, encouraging the development of

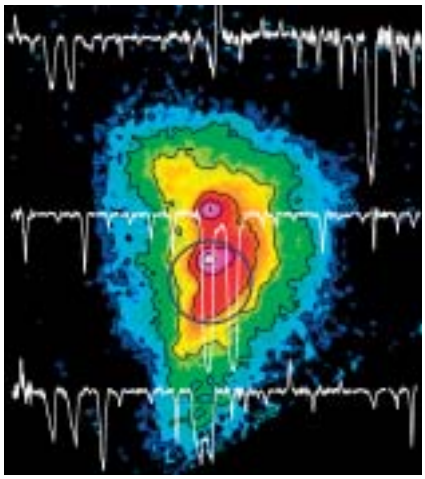

Figure 3.1.1. The Fabry-Perot LWS spectrum of Sagittarius B2, the most massive molecular cloud in the Galactic Centre. Many lines from different molecular species have been detected in this spectrum. The fundamental rotational transitions of light molecules (H_2O, OH, CH, NH, ...), the high J transitions of polyatomic species (NH_3, HCN, CO, ...), the vibrational bending modes of non-polar molecules (C_3, C_4, ...) and the fine structure lines of many atoms, some of them for the first time in the interstellar medium. The spectrum is superimposed on to a 350 µm CSO image of Sgr B2. (ESA/LWS and Javier Goicoechea et al. (CSIC, Madrid, Spain) and Caltech Submillimeter Obs. and Lis D.C.))

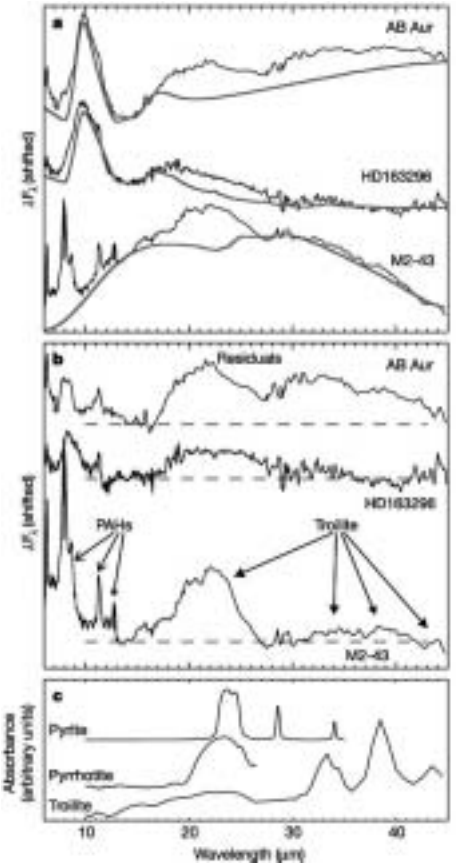

Figure 3.1.2. IR spectra of stars showing a pronounced 23.5 µm feature from iron sulphide grains. a: the mid-IR spectra of the young stars AB Aurigae, HD163296 and the evolved star M2-43. The grey lines in the AB Aur and HD163296 spectra represent model fits to the full ISO spectra using amorphous silicates, metallic Fe and carbonaceous material. The grey line in the M2-43 spectrum is a fit to the continuum using amorphous carbon and MgS. b: residuals after subtracting the models from the observed ISO spectra. c: IR spectra of troilite (FeS) and of pyrite (FeS2) calculated from optical constants, and of pyrrhotite (Fe1-xS) from laboratory measurements. Noted are the major resonances of FeS at 23, 33 and 38 µm in the residual spectrum of M2-43. (ESA/SWS and Keller et al.)

laboratory studies to establish an inventory of detected material in ice form. Around new-born stars, sulphur has been detected for the first time, an important result as it reconciles the fact that sulphur is on average an abundant element in the Galaxy. Figure 3.1.2 shows the detection by ISO's Short Wavelength Spectrometer of iron sulphide grains in the protoplanetary disc of young stellar objects.

A number of systematic studies of stellar samples were also conducted, such as the investigation on the time variation observed in water-vapour bands from oxygen-rich Mira variables (interpreted as originating from two layers), and of the last stages of stellar evolution (a rapid process ending up in a planetary nebula).

Improved processing of ISOPHOT data unveiled spectacular images of a number of galaxies, in unprecedented detail. Previously isolated quasars are now merged into a single evolutionary picture, based on the measurements of their spectral energy distribution (Fig. 3.1.3). New catalogues have been published, such as of detected sources in a survey of the inner Galaxy made with ISOCAM (the ISOGAL programme), or galaxies from the Serendipity Survey made with ISOPHOT.

Deep observations made with ISOCAM of different regions of the sky (Fig. 3.1.4), free from nearby sources, have yielded similar counts of detected primordial galaxies, explaining most of the observed diffuse background of IR light, which had previously puzzled astronomers, and represents a major advance in charting the global history of star formation in the Universe, and a major advance in determining the relative

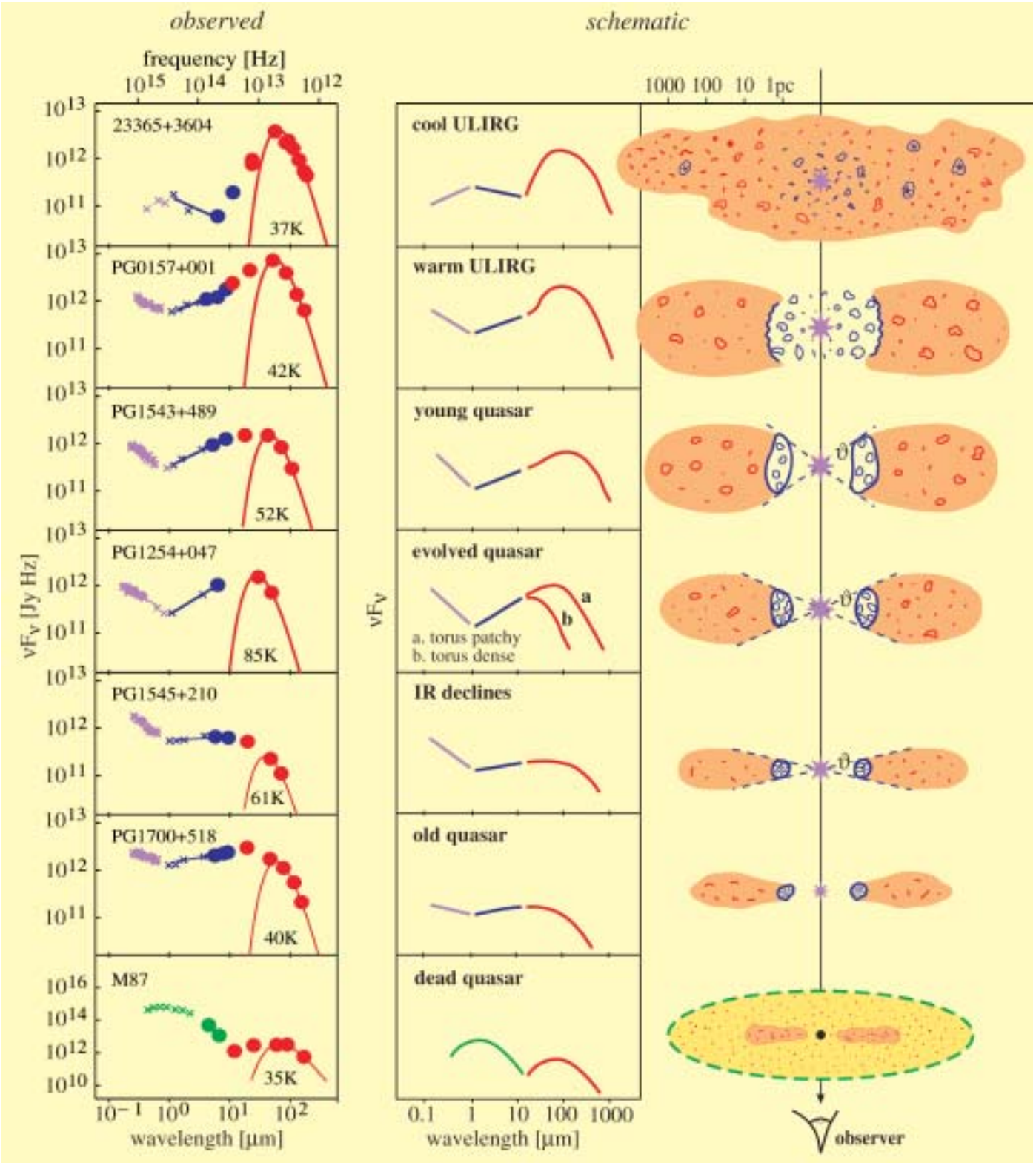
observed
schematic
frequency [Hz]
23365+3604
37K
PG0157+001
42K
PG1543+489
52K
PG1254+047
85K
PG1545+210
61K
PG1700+518
40K
M87
35K
vFν [Jy Hz]
wavelength [μm]
cool ULIRG
warm ULIRG
young quasar
evolved quasar
a
b
a. torus patchy
b. torus dense
IR declines
old quasar
dead quasar
vFν
wavelength [μm]
1000 100 10 1pc
observer

Figure 3.1.3. A complete ISO view of Palomar-Green (PG) quasars, based on 64 IR spectral energy distributions between 5 µm and 200 µm. Not only are coarse IR differences between Ultra-Luminous IR Galaxies (ULIRGs) and quasars seen, known from earlier IRAS studies, but also the details and a possible evolution of the dust distribution and emission even among the optically-selected Palomar-Green quasar sample. During such an evolution, the dust distribution rearranges, settling more and more into a torus/disc-like configuration. During the evolution, the Active Galactic Nuclei strength grows, then stays high and finally declines. A 'dead quasar' remains as a relict, with a starved black hole sitting in a bright host galaxy.
(ESA/PHT and Haas et al. (MPIA, Heidelberg, D))

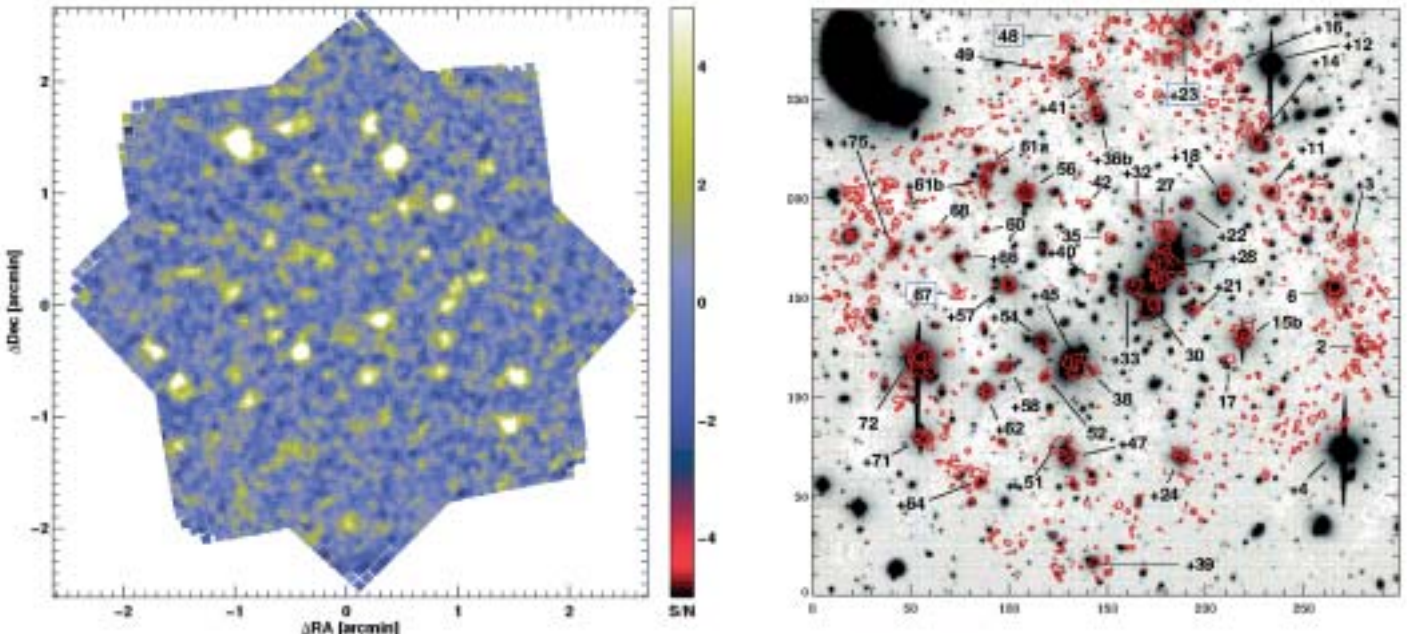

Figure 3.1.4. The deepest surveys by ISO at 6.7 µm. Left: The SSA13 field, where 65 sources were detected down to 6 µJy. The field is 16 arcmin square. Right: contours of an ISOCAM 7 µm image of Abell 2390 overlaid on a KPNO R-band image. Boxes around a number indicate a Chandra source; circles a SCUBA source. This is one of four gravitationally lensing galaxy clusters from which deep mid-IR counts of the background lensed galaxy population have been derived. Nearly 200 mid-IR sources have been extracted from the 100 sq. arcmin surveyed. Often optically very faint, they are heavily dust-obscured objects and reveal star-formation rates in some cluster galaxies more than an order of magnitude higher than those derived from optical data. The two independent studies, conducted on different fields on the sky and with different techniques in the same CAM filter, yield similar integrated galaxy counts accounting for most of the diffuse IR background, in fair agreement with evolutionary models of the early Universe.
(ESA/CAM, Sato et al. (a) and Metcalfe et al. (b))

importance in the Universe of energy generation by stars and energy generation by processes of accretion of matter onto black holes.

This wide sweep of discovery affirms ISO's place at the forefront of spaceborne astronomy missions. The expected results and the surprises from ISO continue to be produced at the substantial rate of 140 papers/year. In May 2003 ISO reached its 1000th publication. At the time of writing, about half of the time spent on scientific observations still awaits to be exploited.

ISO Data Archive (IDA)

ISO performed around 30 000 science observations. Allowing for observations made in the parallel and serendipity modes (observational modes in which an instrument could observe while another instrument was prime), almost 150 000 data sets were recorded. Since ISO was operated as an observatory with four complex instruments, the resulting data are very heterogeneous. The data underwent extensive processing, including validation and accuracy analysis. In total, around 400 GBytes of data are stored on magnetic disks. To serve these data to the user community, a sophisticated archive has been developed by ISO Data Centre with continuous and fruitful cooperation between users and developers to provide a unique state-of-the-art astronomical data archive. In addition to the observational data products, the archive also contains satellite housekeeping data, software tools, documentation and externally derived products.

The IDA is based on an open and flexible three-tier architecture: Data Products and Database: Business Logic: and User Interface. An important consideration was to separate the stored data from their final presentation to the user. The Business Logic and the User Interface were developed entirely in JAVA and XML, which allows the IDA to be accessible from any platform and from the most popular web browsers. This has facilitated its reuse for other ESA archive projects (such as XMM-Newton, Integral and Planetary Missions).

A textual and visual presentation of the data is offered to users to aid them in selecting observations for retrieval through FTP. One of the main features is the provision of browse products or quick-look data associated with each observation. These enable users to make informed decisions as to which observations they want to download for detailed astronomical analysis.

By March 2004, more than 1500 astronomers had registered as users. IDA supports easy-to-make but powerful queries against all ISO data. The quick-look images and on-line visualisation tools aid users in the selection of products for data retrieval through a 'shopping basket' mechanism familiar to anyone who has made commercial purchases via the web. After email notification that their request has been serviced, users make fast data retrieval by FTP. A direct download facility is also available.

Off-line products

Every ISO observation has been run through an automatic data-analysis pipeline called Off-Line Processing (OLP), to generate standard data products. The automatic data products passed through several generations, until at the end of ISO Post Operations and in the first months of the Active Archive Phase in early 2002 a final full reprocessing of all ISO data was performed, producing the ISO Legacy Archive. All products were put on hard disk, superseding previous product versions.

Interactive analysis tools

All interactive analysis tools, including a number of software packages offered to the community for reduction and analysis of ISO data, are archived. These include: ISOCAM Interactive Analysis (CIA); ISOPHOT Interactive Analysis (PIA); Observers' SWS Interactive Analysis (OSIA); LWS Interactive Analysis (LIA); and ISO Spectroscopic Analysis Package (ISAP). They are obtainable through the ISO WWW page or directly from the responsible software groups.

Documentation

Extensive explanatory and technical support documentation is archived. This includes the five volumes of the *ISO Handbook* (now released in their final form as SP-1262), gathering all the information needed to make efficient use of ISO data, and extensive

technical documentation, tracing and explaining the experience of the instrument teams as they worked to understand the calibration of their instruments. Together with the ISO Data Products, the body of explanatory and support documentation is called the ISO Explanatory Library. The calibration legacy of ISO is extensively documented in ESA SP-511.

Highly Processed Data Products (HPDP)
While the automatic processing pipeline copes well with a number of instrumental artifacts, the products can still be improved 'by hand' through interactive analysis tools or improved algorithms.

The ISO Data Archive has been enhanced with a facility to enrich its contents continuously through ingestion of the resulting reduced data and associated catalogues and atlases. These are highly visible for use by the general user. A campaign is now ongoing to gather data sets from the scientific community. In parallel, a number of projects have been undertaken to purge products further associated with essential observing modes from the remaining instrumental artifacts. Many of these products can already be easily queried and retrieved from the archive.

Virtual observatory

A Virtual Observatory (VO) is a collection of interoperating data archives and software tools that use the Internet to form a scientific research environment in which astronomical research programmes can be conducted. In much the same way as a real observatory consists of telescopes, each with a collection of unique astronomical instruments, the VO consists of a collection of data centres, each with unique collections of astronomical data, software systems and processing capabilities.

The ISO archive incorporated many, and growing, elements of interoperability with other popular astronomical archives. Target names entered into the IDA user interface are resolved with searches in the NED or SIMBAD databases. Individual observations in the ISO database are linked to related publications listed in the ADS database maintained by Harvard. ADS in turn links publications to ISO data sets upon which they are based. Searches in the Strasbourg-based CDS/Vizier archive link targets to any existing ISO data for that target, and at NASA's IPAC, tools allow overlap of ISO and IRAS target fields to be visualised. The ad-hoc implementation of these interoperability elements has now evolved into a system complying with the new standards set by the Virtual Observatory international community. ISO has been one of the first archives to be part of the European Virtual Observatory prototype, as demonstrated in January 2004.

Conclusions

ISO has made, and continues to make, ground-breaking contributions to all areas of astronomy, from Solar System studies, to the limits of cosmology and the history of the Universe. The mission itself was technically extremely successful, with several key aspects of the technology substantially outperforming their specifications (e.g. cryostat hold time, and attitude and orbit control accuracy and stability). Beyond that, the challenge of serving the huge body of ISO results to the astronomical community in a user-friendly way stimulated the development of an innovative data archive, pioneering many aspects of interoperability, and leading the way towards the virtual observatories of the future. Its contents are being constantly upgraded, with more 'readily-usable' products.

One of the major keys to success of the active archive phase will be the knowledge, skills and continuity of expertise of the people involved. The ESA ISO Data Centre

at Villafranca has built up a unique set of experience around the archive, the data and the related community support, together with the detailed expertise on all four instruments that is necessary to support the general European community. Retention of these core skills and knowledge will continue to enable the community to get the most out of ISO and will, additionally, build a bridge in ESA's planning towards future missions, especially Herschel.

Footnote to p69: the Data Centres responsible for ISO User Support were or are (Centres continuing to operate into the Active Archive Phase are marked with *):

ISO Data Centre at ESA, Vilspa in Spain*
Five Specialist National Data Centres (NDCs) :
French ISO Centres, SAp/Saclay and IAS/Orsay, France; ISOPHOT Data Centre at MPIA, Heidelberg, in Germany*; Dutch ISO Data Analysis Centre at SRON, Groningen, NL*; ISO Spectrometer Data Centre at MPE in Munich, D*; UK ISO Data Centre at RAL, Oxford, UK*
plus, in the USA: ISO Support Center at NASA's IPAC, on CalTech campus.

4. Projects Under Development

4.1 Herschel

Introduction

The Herschel Space Observatory is a multi-user observatory-type mission that will provide observation opportunities for the entire astronomical community in the relatively poorly explored 57-670 µm part of the far-IR and sub-mm range of the electromagnetic spectrum. Herschel is the fourth of the original Cornerstone missions in the ESA Horizon 2000 science plan.

Scientific objectives

Herschel (Fig. 4.1.1) is the only space facility dedicated to the far-IR and sub-mm part of the spectrum. It has the potential for discovering the earliest epoch proto-galaxies, revealing the cosmologically evolving AGN/starburst symbiosis, and unravelling the mechanisms involved in the formation of stars and planetary system bodies. A major strength of Herschel is its photometric mapping capability for performing unbiased surveys related to galaxy and star formation. Redshifted ultraluminous IRAS galaxies (with spectral energy distributions that peak in the 50-100 µm range in their rest frames) as well as class 0 proto-stars and pre-stellar objects in our own and nearby galaxies peak in the Herschel 'prime' band. Herschel is also well-equipped to perform spectroscopic follow-up observations to characterise further particularly interesting individual objects.

The key science objectives emphasise the formation of stars and galaxies, and the interrelation between the two. Example observing programmes with Herschel will include:

— deep extragalactic broadband photometric surveys in the 100-600 µm Herschel 'prime' wavelength band and related research. The main goals will be a detailed investigation of the formation and evolution of galaxy bulges and elliptical galaxies in the first third of the present age of the Universe;
— follow-up spectroscopy of especially interesting objects discovered in the survey. The far-IR/sub-mm band contains the brightest cooling lines of interstellar gas, which give very important information on the physical processes and energy production mechanisms (e.g. AGN *vs.* star formation) in galaxies;
— detailed studies of the physics and chemistry of the interstellar medium in galaxies, both locally in our own Galaxy as well as in external galaxies, by means of photometric and spectroscopic surveys and detailed observations. This includes implicitly the important question of how stars form out of molecular clouds in various environments;
— observational astrochemistry (of gas and dust) as a quantitative tool for understanding the stellar/interstellar lifecycle and investigating the physical and chemical processes involved in star formation and early stellar evolution in our own Galaxy. Herschel will provide unique information on most phases of this lifecycle;
— detailed high-resolution spectroscopy of a number of comets and the atmospheres of the cool outer planets and their satellites.

From experience, it is also clear that the discovery potential is significant when a new capability is being implemented for the first time. Observations have never been performed in space in the prime band of Herschel. The total absence of even residual atmospheric effects – enabling both a much lower background for photometry and full wavelength coverage for spectroscopy – and a cool low-emissivity telescope open up a new part of the phase-space of observations. Thus, a space facility is essential in this wavelength range and Herschel will be breaking new ground.

For further information, see http://astro.esa.int/herschel

Figure 4.1.1. The Herschel satellite in orbit. Clearly visible are the passively cooled telescope behind its protective sunshade, the superfluid helium cryostat containing the science instruments, and the service module. (Alcatel Space Industries)

Figure 4.1.2. Herschel's primary mirror blank, shown just after the brazing together of 12 individual SiC segments to form a monolithic structure was completed in late 2003. This mirror blank will now be ground, polished and coated in the course of 2004. (EADS Astrium)

Table 4.1.1. Herschel scientific payload.

Acronym	*Instrument*	*Principal Investigator*
PACS	camera/spectrometer, ~57-205 µm	A. Poglitsch, MPE, Garching (D)
SPIRE	camera/spectrometer, ~200-670 µm	M. Griffin, U. Cardiff (UK)
HIFI	high-res heterodyne spectrometer	Th. de Graauw, SRON, Groningen (NL)

Table 4.1.2. Principal characteristics of the Herschel mission.

Type of mission: far-IR and sub-mm observatory; 4th ESA Cornerstone mission
Science goals: star and galaxy formation, interstellar medium physics and chemistry, solar system body studies
Telescope: 3.5 m-diameter Cassegrain telescope of silicon carbide
Spacecraft: 3-axis spacecraft with superfluid helium cryostat for instrument focal plane unit cooling
Size: height 7.5 m x width 4 m, launch mass 3 t
Science data rate: 130 kbit/s average production rate
Lifetime: 3 years of routine science operations
Operational orbit: Lissajous orbit around L2
Launch: dual launch (with Planck) on Ariane-5 in 2007

Telescope and science payload

In order to exploit fully the favourable conditions offered by being in space Herschel will need a precise, stable, low-background telescope, and a complement of capable scientific instruments. The telescope (Fig. 4.1.2) will be passively cooled (placing it outside the cryostat maximises its size), while the instrument focal plane units will be housed inside a cryostat, containing superfluid helium below 1.7K. The bolometer arrays in PACS and SPIRE will be cooled to approximately 300mK using dedicated instrument-provided sorption coolers.

The Herschel telescope must have a total wavefront error (WFE) of less than 6 µm, corresponding to diffraction-limited operation at about 90 µm. It must also have a very low emissivity in order to minimise the background signal, and the whole optical chain must be optimised for high straylight rejection. Protected by a fixed sunshade, the telescope will radiatively cool to an operational temperature in the vicinity of 80K. The design is a classical Cassegrain with a 3.5 m diameter primary and an 'undersized' secondary. The telescope will be provided by EADS Astrium (Toulouse, F) and will be constructed almost entirely of silicon carbide (SiC). It will have a primary mirror made of 12 segments brazed together to form a monolithic mirror that will be polished to the required accuracy, providing positive control of the overall WFE driver.

The scientific payload consists of three instruments (Table 4.1.1), which will be provided by consortia led by Principal Investigators (PIs) in return for guaranteed observing time; they are:

Photodetector Array Camera and Spectrometer (PACS)
PACS is a camera and low- to medium-resolution spectrometer for wavelengths up to

about 205 µm. It employs in total four detector arrays: two bolometer arrays for photometry and two photoconductor arrays for spectroscopy. PACS can be operated either as photometer, fully sampling a field of view of 1.75 x 3.5 arcmin on the sky simultaneously in two broadband colours (either of the 60-85 µm or 85-130 µm bands plus the 130-210 µm band), or as an integral field line spectrometer covering just under 1 arcmin square on the sky with a resolution of ~1500.

Spectral and Photometric Imaging REceiver (SPIRE)
SPIRE is a camera and low- to medium-resolution spectrometer for wavelengths longer than about 200 µm. It comprises an imaging photometer and a Fourier Transform Spectrometer (FTS), both of which use bolometer detector arrays. There is a total of five arrays: three dedicated for photometry and two for spectroscopy and spectrophotometry. As a photometer, it covers a large 4 x 8 arcmin field of view that is imaged in three colours (centred on 250, 360 and 520 µm simultaneously, and in spectroscopy a field approximately 2.6 arcmin across with resolution of order 100.

Heterodyne Instrument for the Far Infrared (HIFI)
HIFI is a heterodyne spectrometer. It offers very high velocity resolution spectroscopy using auto-correlator and acousto-optical spectrometers, combined with low noise detection using superconductor-insulator-superconductor (SIS) and hot electron bolometer (HEB) mixers. Five dual polarisation SIS mixer bands cover the frequency range 490-1250 GHz, and two HEB bands cover 1410-1910 GHz. HIFI covers a single pixel on the sky, and builds up images either by raster scanning or by on-the-fly mapping.

Spacecraft and in-orbit operations

Herschel's configuration, shown in Fig. 4.1.1, is based on the well-proven ISO cryostat technology. It is modular, consisting of the 'extended payload module' (EPLM) comprising the superfluid helium cryostat (housing the optical bench with the instrument focal plane units) which supports the telescope, the sunshield/shade, and payload associated equipment; and the service module (SVM), which provides the infrastructure and houses the warm payload electronics.

An industrial consortium led by Alcatel Space Industries (Cannes, F) as prime, with EADS Astrium (Friedrichshafen, D) responsible for the EPLM, and Alenia Spazio (Torino, I) for the SVM, and a host of subcontractors from all over Europe, are building the spacecraft. Arianespace will provide the launch services in Kourou. For a summary of principal mission characteristics see Table 4.1.2.

An Ariane-5 launcher, shared by Planck, will inject both satellites into a transfer trajectory towards the second Lagrangian point (L2) in the Sun-Earth system. They will then separate from the launcher, and subsequently operate independently from orbits of different amplitude around L2, which is situated 1.5 million km away from the Earth in the anti-sunward direction. It offers a stable thermal environment with good sky visibility. Since Herschel will be in a large orbit around L2, which has the advantage of not costing any orbit injection delta-V, its distance to the Earth will vary within 1.2-1.8 million km. Herschel will take about 4 months to reach the operational orbit. For the first couple of weeks after launch, while cooldown and outgassing take place, the telescope will be kept warm by heaters to prevent it acting as a cold trap for the outgassing products. It will then cool down, and it is envisaged that the opening of the cryostat door (thus providing 'first light') will take place around 5-6 weeks after launch. Commissioning and performance verification will take place enroute towards L2, followed by a science demonstration phase. Once

these crucial mission phases have been accomplished, Herschel will begin routine science operations.

Science operations

Herschel will be a multi-user observatory open to the general astronomical community. It will perform routine science operations for a minimum of 3 years, until depletion of the helium. The available observation time will be shared between guaranteed time (one third) owned by contributors to the Herschel mission (mainly by the PI instrument consortia), and open time allocated to the general community (including the guaranteed time holders) on the basis of calls for observing time. The initial call for observing proposals is planned to be issued in 2005.

The scientific operations will be conducted in a novel decentralised manner. The operational ground segment comprises six elements:

— Herschel Science Centre (HSC), provided by ESA;
— three dedicated Instrument Control Centres (ICCs), one for each instrument, provided by the respective PI;
— the Mission Operations Centre (MOC), provided by ESA;
— the NASA Herschel Science Center (NHSC), provided by NASA.

The HSC acts as the interface to the science community and outside world in general, supported by the NHSC (primarily) for the US science community. The HSC provides information and user support related to the entire life-cycle of an observation, from calls for observing time, the proposing procedure, proposal tracking, data access and data processing, as well as general and specific information about using Herschel and its instruments.

All scientific data will be archived and made available to the data owners. After the proprietary time has expired for a given data set, the data will be available to the entire astronomical community in the same manner as they were previously available only to the original owner. The accumulated experience from earlier observatory missions (particularly ISO and XMM-Newton) is being used in the implementation of the infrastructure by ESA and the PIs together. An important conclusion is to build one single system that evolves over time, rather than having separate systems for different mission phases. The first functional version of this system is already being used in connection with instrument level tests.

Status and schedule

Following an Invitation to Tender (ITT) procedure, the industrial contract for Herschel (and Planck) spacecraft for phases B, C/D, and E1 was awarded, and phase B began, in April 2001. The first major review, the System Requirements Review (SRR), took place in the autumn 2001. Following the SRR, the industrial consortium was formed by the selection of subcontractors, which has involved in excess of 100 procurement activities. Further design work has been conducted in parallel with the procurement. The next major step, the Preliminary Design Review (PDR) was performed in autumn 2002. Starting in spring 2004, the Critical Design Review (CDR) of the spacecraft payload module will take place, to be followed by the CDR at satellite level in the autumn.

The PIs were selected in 1998; the initial instrument deliveries will take place in 2004, when the cryogenic qualification models (CQMs) will be delivered for integration and testing using a Herschel cryostat mock-up manufactured from existing ISO hardware, and avionics models (AVMs) for testing together with the SVM. Many

subsystems of the instrument flight models (FMs) are currently being manufactured; the assembly of the FMs will start after delivery of the CQMs.

The telescope activity was started in mid-2001, and the Mid-Term Review (MTR) was held in November 2001, paving the way for the telescope CDR in April 2002. The telescope is now being manufactured for delivery in 2005.

The current planning envisages a series of milestones, including instrument and telescope FM deliveries in 2005, to be followed by spacecraft integration and extensive system-level ground testing, leading to the launch in 2007.

4.2 Planck

Scientific goals

In late 1992, the COBE team announced the detection of intrinsic temperature fluctuations in the Cosmic Background Radiation Field (CBRF), observed on the sky at angular scales larger than ~10°, and at a brightness level $\Delta T/T \sim 10^{-5}$. More recently, in February 2003, the WMAP team announced results on scales of about 15 arcmin with a similar sensitivity (see *http:///lambda.gsfc.nasa.gov* for detailed descriptions of both COBE and WMAP). These fluctuations have been interpreted as due to differential gravitational redshift of photons scattered out of an inhomogeneously dense medium; they thus map the spectrum of density fluctuations in the Universe at a very early epoch. This long-sought result establishes the Inflationary Big Bang model of the origin and evolution of the Universe as the theoretical paradigm. However, in spite of the importance of the COBE and WMAP measurements, many fundamental cosmological questions remain open. Building on the pioneering work of COBE and WMAP, the main objective of the Planck mission is to map the fluctuations of the CBRF with an accuracy that is set by fundamental astrophysical limits, allowing these fundamental questions to be effectively addressed.

Mapping the fluctuations of the CBRF with high angular resolution and high sensitivity would give credible answers to such issues as: the initial conditions for structure evolution, the origin of primordial fluctuations, the type of potential that drove inflation, the existence of topological defects, the nature and amount of dark matter, and the nature of dark energy. Planck will set constraints on theories of particle physics at energies higher than 10^{15} GeV, which cannot be reached by any conceivable experiment on Earth. Finally, the ability to measure to high accuracy the angular power spectrum of the CBRF fluctuations will allow the determination of fundamental cosmological parameters such as the density parameter Ω_0, and the Hubble constant H_0, with an uncertainty of a few percent.

The observational goal of the Planck mission is to mount a single space-based experiment to survey the whole sky with an angular resolution as high as 5 arcmin, a sensitivity approaching $\Delta T/T \sim 10^{-6}$, and covering a frequency range that is wide enough to encompass and deconvolve all possible foreground sources of emission. The main scientific result of the mission will be an all-sky map of the fluctuations of the CBRF. In addition, the sky survey will be used to study in detail the very sources of emission that contaminate the cosmological signal, and will result in a wealth of information on the dust and gas in both our own Galaxy and extragalactic sources. One specific notable result will be the measurement of the Sunyaev-Zeldovich effect in many thousands of galaxy clusters, leading for example to the determination of cluster bulk velocities over scales of ~300 Mpc out to a redshift of ~1 with a velocity uncertainty of ~50 km/s.

Planck payload

The Planck payload consists of a 1.5 m-diameter offset telescope, with a focal plane shared by clusters of detectors in nine frequency bands covering the range 30-900 GHz. The three lowest frequency bands (up to ~70 GHz) consist of HEMT-based receivers actively cooled to ~20K by an H_2 sorption cooler. The higher frequency bands employ arrays of bolometers cooled to ~100mK; the H_2 sorption cooler provides pre-cooling for a Joule-Thomson 4K stage, to which a dilution refrigerator is coupled. The characteristics and goal performance of the Planck instruments are shown in Table 4.2.1.

The satellite will be placed into a Lissajous orbit around the L2 point of the Earth-Sun system. At this location, the payload can point continuously in the anti-Sun direction, thus minimising potentially confusing signals from thermal fluctuations and stray-light entering the detectors through far side-lobes. From L2, Planck will carry

For further information, see http://www.rssd.esa.int/Planck

Figure 4.2.1. The current configuration of the Planck satellite, as developed by Alcatel Space (F).

out two complete surveys of the full sky, for which it requires about 14 months of observing time. The spacecraft will be spin-stabilised at 1 rpm. The viewing direction of the telescope will be offset by 85° from the spin axis, so that the observed sky patch will trace a large circle on the sky.

Planck is a survey-type project, developed and operated as a PI mission. The payload will be provided by two PI teams, who will also man and operate two Data Processing Centres, which will process and monitor the data during operations, and reduce the final data set into the science products of the mission. All-sky maps in the nine frequency bands will be made publicly available one year after completion of the mission, as well as a first-generation set of maps of the CBRF, Sunyaev-Zeldovich effect, dust, free-free and synchrotron emission. The time-series of observations (after calibration and position reconstruction) will also eventually be made available as an on-line archive.

Status

Planck was selected in late 1996 as the third Medium Mission (M3) of ESA's Horizon 2000 Scientific Programme, and is now part of its Cosmic Vision Programme. At the time of its selection, Planck was called COBRAS/SAMBA; after the mission was approved, it was renamed in honour of the German scientist Max Planck (1858-1947), winner of the Nobel Prize for Physics in 1918. Planck will be launched together with the Herschel far-IR and sub-mm observatory in February 2007.

Starting in 1993, a number of technical studies laid the basis for the issue in September 2000 of an Invitation to Tender (ITT) to European industry for the procurement of the Herschel and Planck spacecraft. From the submitted proposals, a single prime contractor, Alcatel Space (F), was selected in early 2001 to develop both

Table 4.2.1. Planck instrument performance goals.

Telescope	1.5 m (projected aperture) offset; shared focal plane; system emissivity ~1% Viewing direction offset 85° from spin axis; field of view 8°									
Instrument	LFI			HFI						
Centre Frequency (GHz)	30	44	70	100	143	217	353	545	857	
Detector Technology	HEMT LNA arrays			Bolometer arrays						
Detector Temperature	~20K			0.1K						
Cooling Requirements	H_2 sorption cooler			H_2 sorption + 4K J-T stage + Dilution cooler						
Number of Detectors	4	6	12	8	12	12	12	4	4	
Bandwidth (GHz)	6	8.8	14	33	47	72	116	180	283	
Angular Resolution (FWHM arcmin)	33	24	14	9.5	7.1	5	5	5	5	
Average $\Delta T/T$ per pixel (14 months, 1σ, 10^{-6} units)	2.0	2.7	4.7	2.5	2.2	4.8	14.7	147	6700	
Average $\Delta T/T$ (polarisation) per pixel (14 months, 1σ, 10^{-6} units)	2.8	3.9	6.7	4.0	4.2	9.8	29.8			

spacecraft. Alcatel Space is supported by two major subcontractors: Alenia Spazio (Torino, I) for the Service Module and Astrium GmbH (Friedrichshafen, D) for the Herschel Payload Module; and by many other industrial subcontractors from all ESA member states. The detailed definition work began in June 2001, and is now advanced. The current design of Planck is shown in Fig. 4.2.1.

In early 1999, ESA selected two consortia of scientific institutes to provide the two Planck instruments: the Low Frequency Instrument will be developed and delivered to ESA by a consortium led by R. Mandolesi of the Istituto di Astrofisica Spaziale e Fisica Cosmica (CNR) in Bologna (I); the High Frequency Instrument will be provided to ESA by a consortium led by J.-L. Puget of the Institut d'Astrophysique Spatiale (CNRS) in Orsay (F). More than 40 European institutes, and some from the USA, are collaborating on the development, testing and operation of these instruments, as well as the ensuing data analysis and exploitation. The capabilities of the instruments are described in Table 4.2.1.

In early 2000, ESA and the Danish Space Research Institute (DSRI, Copenhagen) signed an Agreement for the provision of the two reflectors that constitute the Planck telescope. DSRI leads a consortium of Danish institutes, and together with ESA has subcontracted the development of the Planck reflectors to Astrium GmbH (Friedrichshafen), who are manufacturing the reflectors using state-of-the-art carbon fibre technology.

In parallel, the instrument development has proceeded largely according to

schedule, in spite of a number of financial difficulties during 2002, which at the time of writing have been largely resolved. Some hardware subsystems are already being manufactured and tested. The first deliveries of instrument qualification models are expected in early 2004, with the flight models due in mid-2005.

4.3 Venus Express

Introduction

Venus Express, an orbiter to study the atmosphere, plasma environment and surface of Venus, was proposed to ESA in response to the March 2001 Call for Ideas for reuse of the Mars Express platform. A strict schedule was imposed, aiming at a launch date in 2005, with a strong recommendation to include instruments already available, in particular as flight-spare units from Mars Express and Rosetta. A Mission Definition Study was conducted during mid-July to mid-October 2001. Venus Express was eventually recommended for selection by the science programme advisory committees on the strength of its excellent scientific value. On 11 July 2002, although the payload funding was still not fully in place, ESA's Science Programme Committee unanimously approved the start of work on Venus Express. On 5 November 2002, ESA made its final decision on the payload complement and therefore to proceed with the mission. Industrial and payload activities started in mid-July. Venus Express will be by far the fastest developed scientific project implemented by ESA.

Mission overview

Venus Express is to be launched from Baikonur, Kazakhstan, by a Soyuz equipped with a Fregat upper-stage in October-November 2005, on a direct transfer trajectory to Venus. The transfer duration is about 150 days. An orbit insertion manoeuvre will place the spacecraft in a highly elliptical 5-day orbit around Venus. An apocentre lowering manoeuvre will put the spacecraft in its final 24 h polar orbit, with a pericentre altitude of 250-350 km and an apocentre altitude of 66 000 km. Scientific observations will be split between the pericentre region, where high-resolution studies of small-scale features will be carried out, and near-apocentre and intermediate observations, where global features will be studied. The data will be transmitted to ground during the 8 h following the pericentre pass each orbit. ESA's second Deep Space Tracking station at Cebreros, Spain, presently under construction, will be used as the nominal ground station for control and data down-link. The other 35 m station, at New Norcia, Australia, will be used during mission-critical operations and for radio science support during dedicated campaigns at certain phases of the mission. A nominal mission duration of 2 Venus sidereal days (486 Earth days) is planned, with the possibility to extend the mission for another 2 Venus days.

Scientific goals

The main goal of the mission is to carry out a comprehensive study of the atmosphere of Venus and to study to some detail the plasma environment and the interaction between the upper atmosphere and the solar wind. Several aspects of the surface and surface-atmosphere interactions will also be studied. In order to organise properly the topics to be studied and to ensure that the full potential of the mission is realised, seven Science Themes have been defined, each with its own detailed set of objectives:

— atmospheric dynamics;
— atmospheric structure;
— atmospheric composition and chemistry;
— cloud layers and hazes;
— radiative balance;
— surface properties and geology;
— plasma environment and escape processes.

Addressing these themes to a proper depth will enable solutions to many of the fundamental questions still open for Venus. These include: what is the mechanism of the global atmospheric circulation; what are the mechanisms and the driving force

For further information, see http://sci.esa.int/venusexpress

Table 4.3.1. The Venus Express scientific payload.

Code	*Technique*	*PI & Co-PI*
ASPERA	Plasma analyser. Energetic neutral atom imager	PI: S. Barabash (IRF-Kiruna, Sweden) Co-PI: J.-A. Sauvaud (CESR/CNRS, Toulouse, France)
MAG	Magnetometer	PI: T. Zhang (IFW, Graz, Austria)
PFS	High-resolution IR Fourier spectrometer	PI: V. Formisano (IFSI- Frascati, Italy)
SPICAV	UV & IR atmospheric spectrometer for solar/stellar occultations and nadir observations	PI: J.-L. Bertaux (SA/CNRS, Verrières-le-Buisson, France) Co-PI: O. Korablev (IKI, Moscow, Russia) Co-PI: P. Simon (BIRA-IASB, Brussels, Belgium)
SOIR	High-resolution solar occultation channel	Co-PI: D. Nevejans (BIRA-IASB, Brussels, Belgium)
VeRa	Radio occultation instrument	PI: B. Häusler (Universität der Bundeswehr, München, Germany) Co-PI: M. Pätzold (Univ. Köln, Germany)
VIRTIS	UV-visible-IR imaging and high-resolution spectrometer	Co-PI: P. Drossart (CNRS/LESIA & Observatoire de Paris, France) Co-PI: G. Piccioni (IASF-CNR, Roma, Italy)
VMC	Wide-angle Venus Monitoring Camera	PI: W. Markiewicz (MPAe, Katlenburg-Lindau, Germany)

behind the atmospheric super-rotation; what are the chemical composition and its spatial and temporal variations at the short and long term; what is the role of the cloud layers and the trace gases in the thermal balance of the planet; what is the importance of the greenhouse effect; how can the origin and the evolution of the atmosphere be described; what has been and what is the role of atmospheric escape for the present state of the atmosphere; what role does the solar wind play in the evolution of the atmosphere; is there still active volcanism and seismic activity on Venus? Resolving these issues is of crucial importance for understanding the long-term evolution of climatic processes on the sister planets Venus, Earth and Mars, and will significantly contribute to general comparative planetology.

Venus Express will provide a breakthrough by fully exploiting the near-IR atmospheric windows over the night side, discovered in the 1980s, through which radiation from the lower atmosphere and even the surface escapes to space. The mission will also tackle open questions on the plasma environment, focusing on non-thermal atmospheric escape.

Scientific payload

As there were strict requirements on the payload – they had to be available to match the challenging schedule of the mission – the list of potential instruments was restricted. The obvious candidates were the spare models from the Mars Express and Rosetta projects. After detailed assessment, three Mars Express and two Rosetta instruments were chosen, enhanced with a new miniaturised 4-band camera and a new magnetometer (with heritage from the Rosetta lander). In addition, a very high-resolution solar occultation spectrometer was added to one of the original Mars Express instruments. This resulted in an instrument complement able to sound the entire atmosphere from the surface to 200 km altitude by combining different spectrometers, an imaging spectrometer and a camera, covering the UV to thermal-IR range, along with a plasma analyser and a magnetometer. Radio science will use the

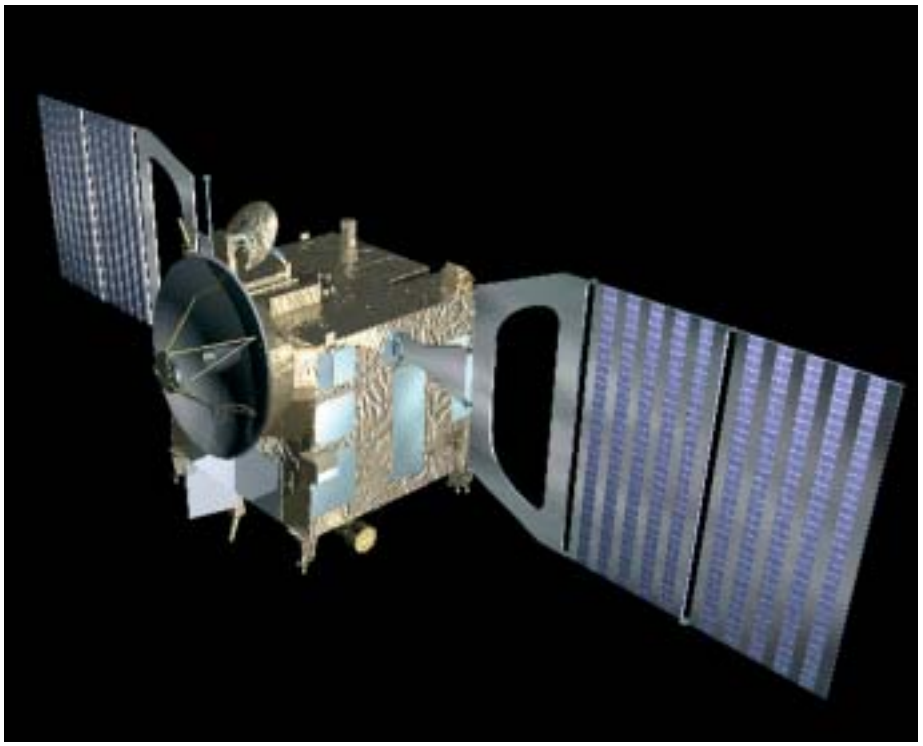

Figure 4.3.1. The Venus Express spacecraft in fully operational configuration. As the solar input at Venus is significantly higher than at Mars, the solar panels are shorter.

communication link to Earth enhanced with an ultra-stable oscillator, for high-resolution vertical investigations. The elements of the scientific payload are listed in Table 4.3.1. As it turns out, despite the limitations in choice, the payload is close to optimised for the mission, and all aspects of the objectives will be addressed to a proper depth.

Spacecraft

The spacecraft (Fig. 4.3.1) is derived from the Mars Express design and reuses most subsystems without modifications. The major differences are in the thermal control system, which has been redesigned in order to cope with the much higher heat input from the Sun and the higher albedo of the planet itself. For the same reason, the solar panels have been completely redesigned: they are based on high-temperature GaAs cells and have a total area about half the size of the Mars Express panels.

The X-band telemetry rate will vary according to the Earth distance, with a minimum rate giving at least 500 Mbit of science data per orbit. An S-band channel is also provided for near-Earth communications and radio science investigation.

The main spacecraft dimensions, excluding the solar panels, are 1.7 x 1.7 x 1.4 m and the total launch mass is about 1270 kg, of which 550 kg is propellant.

Status

All engineering models of the payload have been delivered and successfully tested on the electrical function and verification bench. The flight models are being assembled and tested; delivery for integration on the spacecraft is planned for late spring to early summer 2004. The spacecraft structure has been manufactured and the combined propulsion system has been integrated (Fig. 4.3.2). Final assembly of the spacecraft

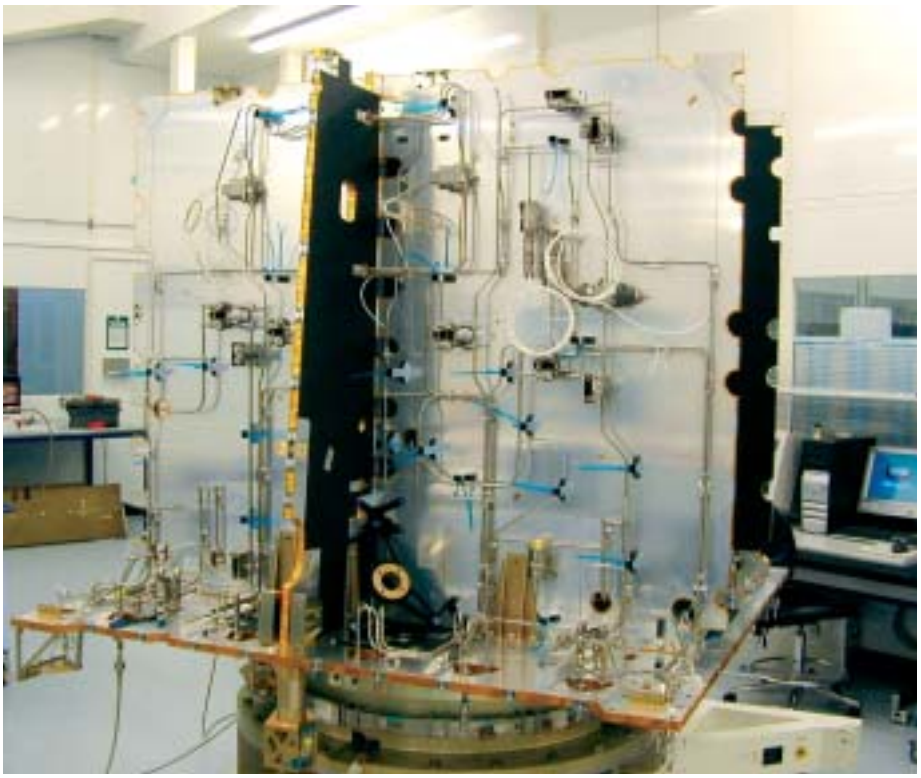

Figure 4.3.2. The main spacecraft structure during integration of the propulsion system, at Astrium Ltd, Stevenage (UK).

and payload will be finished by October 2004, when the system function verification and environmental testing begins. This will include exposure to a representative solar input at Venus of 2600 W/m^2.

Prime contractor for the spacecraft is Astrium-EADS, Toulouse (F) and the subcontractor for Assembly Integration and Verification is Alenia Spazio, Turin (I).

4.4 Contributions to Nationally-led Missions

4.4.1 COROT

COROT is a small mission for asteroseismology and planet-finding funded mainly by CNES, with substantial contributions from the ESA Science Programme, Austria, Belgium, Germany, Italy, Spain and ESA/RSSD. COROT will be the third mission in the CNES small-mission series based upon the Proteus multi-mission platform, and is due to be launched in mid-2006. It is the first attempt to perform accurate asteroseismic observations, as well as to detect rocky planets. Both goals require the accuracy of space-based photometry.

The COROT payload is composed of an off-axis afocal parabolic system (two mirrors), with a 27 cm-diameter, f/4 telescope, giving a 2.8 x 2.8° field of view. The camera comprises two separate elements, with two CCDs each: one for the asteroseismic observations and the other for the planet finding. The planet-finding camera includes a dispersive element (prism) that allows the collection of colour-resolved light curves. ESA has financed the procurement of the telescope optics (which include an afocal dioptric telescope and a refractive objective assembly), and is supporting the Assembly, Integration and Verification of the payload.

The COROT observing programme will include the detailed asteroseismic study (with very high frequency resolution) of a dozen of bright stars (V = 6-9), the asteroseismic study (with lower accuracy) of some hundred fainter stars, and the search for planets on a much larger number (~10 000) of fainter stars (V = 11-16.5).

ESA's participation in COROT was approved by the Science Programme Committee in October 2000. In return for the ESA contribution, scientists in ESA member countries will have access to the COROT scientific data, through an open Announcement of Opportunity issued in 2002.

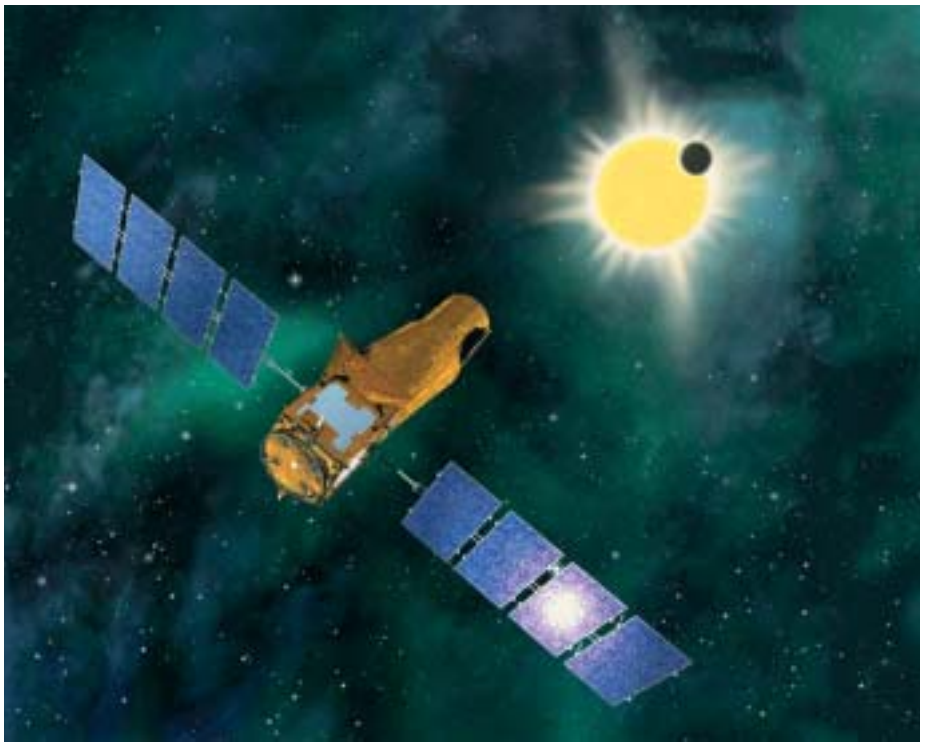

Figure 4.4.1.1. The COROT spacecraft in orbit, pointed towards a planetary transit.

For further information, see http://corot.astrsp-mrs.fr

4.4.2 Microscope

Microscope (MICROSatellite à traînée Compensée pour l'Observation du Principe d'Equivalence) will be the first mission to test the Equivalence Principle (EP) in space. It is aimed at testing the EP to 1 part in 10^{15}, 2-3 orders of magnitude more precise than is possible on the ground or with lunar-laser ranging. This test is of fundamental importance for our understanding of gravity. A violation of the EP would place severe restrictions on the validity of General Relativity; a confirmation of the EP up to the level of 1 part in 10^{15} would provide strong constraints for theories that attempt to unify General Relativity with the other fundamental interactions.

The payload comprises two differential electrostatic accelerometers, one testing a pair of materials A-A (to provide an upper limit for systematic errors), the other testing a pair of materials A-B (the EP test proper). The test masses are freely-floating concentric cylinders of about 500 g each; material A is platinum, material B is titanium. As the satellite orbits the Earth, the Earth's gravity pulls on the test masses. Because the test masses are constrained to one-dimensional motion any EP violation signal would be periodic at orbital frequency. The signal is the force that is required to keep the test masses in a pair centred on each other. During flight, the spacecraft rotates about its long axis at a small multiple of the orbital frequency in order to spectrally shift the science signal from orbit-fixed systematic error sources. One major error source for an EP test in space is test-mass charging due to penetrating charged particles (cosmic rays, solar protons, radiation belt particles in particular as the satellite traverses the South Atlantic Anomaly). In the Microscope experiment, the problem of test-mass charging has been eliminated by grounding the test masses through a thin gold wire.

The 3-axis stablised 193 kg satellite is planned for launch in November 2007 on a shared Dnepr rocket into a Sun-synchronous, quasi-circular orbit at about 700 km altitude. The drag by the residual atmosphere at orbital altitude and solar radiation pressure will be compensated by a system of proportional Field Emission Electric Propulsion (FEEP) thrusters. A total of 12 thrusters (four 3-thruster clusters), each with a thrust authority of 150 µN will be employed. Their noise level must not exceed 0.1 $\mu N/Hz^{1/2}$ at frequencies > 0.1 Hz to provide the required drag-free performance of $3x10^{-10}$ m s^{-2} $Hz^{-1/2}$ in the measurement bandwidth. The FEEP thrusters also serve as actuators for fine attitude control. After the nominal mission of up to one year, prolonged lifetime tests with eventually degrading FEEP thrusters are proposed to maximise the in-orbit operational experience with this novel electric propulsion system on its first spaceflight.

Microscope is a CNES/ESA collaboration: ESA's share is the procurement of the FEEP thrusters. In return, ESA will have full access to all FEEP thruster flight data, which provide a valuable technology test in space for a whole suite of future astronomy and fundamental physics space missions.

In the course of re-evaluating their scientific programme, CNES stopped payload development funding at ONERA from March 2002 until November 2003 and funding for industrial contracts in 2003. At the end of April 2003, CNES confirmed the continuation of the Project. The System Requirements Review (equivalent to a Project Phase-A Review) was held in November and December 2003. In January 2004 the Project Phase-B kicked off. The Project Preliminary Design Review (PDR) will be held at the end of Phase-B, in December 2004. The FEEP thruster PDR took place in June 2003, with a delta PDR in July to close out open issues. An extended (2000 h desirable) FEEP thruster system lifetime test is planned for 2004.

4.4.3 Astro-F

Astro-F, under development by ISAS/JAXA, is the second Japanese space mission for infrared astronomy. It will make an all-sky survey with better sensitivity, spatial resolution and wider wavelength coverage than IRAS. Astro-F has a 67 cm-diameter telescope cooled down to 6K and will observe in the wavelength range 1.8-200 µm. An M5 rocket will place the satellite into a Sun-synchronous polar orbit at 745 km altitude. The target launch date is August 2005.

ESA is collaborating with JAXA/ISAS in order: to increase the scientific output of the mission by capturing all of the possible data (impossible with the baselined single ground station in Japan); to make observing opportunities available to the European community; to accelerate the production of the sky catalogues, which will be extremely valuable in the exploitation of the Herschel and Planck missions. In brief, the cooperation involves ESA provision of tracking and scientific data processing support in return for observation time and accelerating public access to the mission's far-IR sky catalogues.

For tracking support, the top-level documents concerning requirements and implementation plans for the use of the Kiruna ground station have been signed off by all parties and implementation is well underway. In June 2003, a radio-frequency compatibility test was successfully carried out in ESOC with ISAS participation. Regarding pointing reconstruction and distribution of observing time to the ESA astronomical community, an overall implementation plan has been agreed and implementation has begun, with regular detailed interactions between the ESA team at Vilspa and ISAS personnel.

4.4.4 Astro-E2

Astro-E2 will be Japan's fifth X-ray astronomy satellite. The mission is being developed at ISAS/JAXA, together with a number of US and Japanese institutes. The planned launch date is early 2005 from the Kagoshima Space Centre on an M5 rocket. Astro-E2 will cover the energy range 0.4-700 keV with three instruments. An imaging X-ray micro-calorimeter (XRS) will provide ~6 eV FWHM energy resolution in the energy range 0.4-10 keV, and four CCDs (XIS) will provide high-sensitivity imaging in the same range. Above 10 keV, the non-imaging hard X-ray detector (HXD) will provide spectral and timing information.

Following a month-long check-out and a 6 month interval when the data belong to the Astro-E2 Science Working Group, a Guest Investigator Programme will begin. ISAS/JAXA have offered participation by European astronomers in this programme; RSSD are coordinating this participation and an Announcement of Opportunity is expected around May 2004.

5. Missions under Definition

5.1 BepiColombo

Introduction

BepiColombo, the latest planetary mission of ESA's Cosmic Vision programme, is devoted to the exploration of Mercury and its environment, with the aim of understanding the process of planetary formation and evolution in the hottest part of the proto-planetary nebula as well as understanding the similarities and differences between the magnetospheres of Mercury and Earth. The mission will be carried out as a joint project between ESA and JAXA (Japan Aerospace Exploration Agency). The baseline mission consists of two spacecraft: the Mercury Planetary Orbiter (MPO) and the Mercury Magnetospheric Orbiter (MMO), launched together on a Soyuz-Fregat. ESA is responsible for MPO, and JAXA for MMO. In addition to the launcher, ground segment and MPO operations, ESA will also provide the Solar Electric Propulsion Module (SEPM) and the Chemical Propulsion Module (CPM) for delivering the two spacecraft to Mercury and insertion into their dedicated orbits.

In May 1993, a mission to Mercury was proposed to ESA in response to a Call for Ideas. It was selected as a Cornerstone candidate in the Horizons 2000 scientific programme of the Agency in 1996. On 15 October 2000, ESA's Science Programme Committee (SPC) approved BepiColombo (MPO, MMO and a Mercury Surface Element, MSE) as ESA's 5th Cornerstone mission, with launch in 2009/2010. At that time, the mission scenario foresaw MPO and MMO launched separately, on two Soyuz-Fregats, within the same launch window. However, during this study phase it turned out that a third launch vehicle was required for MSE. The severe reduction in the science budget after the Ministerial Conference in November 2001 caused the MSE to be dropped from the mission baseline.

Between 1 October 2002 and 30 June 2003, BepiColombo went through a reassessment with the aim of maximising the scientific performance by optimising the payload complement, while attempting to reduce costs and programmatic risk. The preferred mission scenario that emerged was to launch MPO/MMO together on a single launcher (a Soyuz-Fregat 2-1B, offering higher launch capability) in mid-2012. To achieve this ambitious goal with adequate resource margins, the MPO payload resources, particularly mass, had to be significantly reduced while ensuring the mission's scientific competitiveness was enhanced. This has been achieved by defining, from the analysis of the science objectives, the corresponding payload complement and resulting instrument requirements. An optimised reference payload suite was defined in which instruments share common functions and resources, producing improved science performance at significantly lower cost. On 6 November 2003 the SPC approved the BepiColombo mission with the MPO/MMO complement as a part of the reconstructed Cosmic Vision programme. A novel payload selection procedure for MPO was approved at the same meeting; it deviates from the classical, competitive Announcement of Opportunity process but is tailored to the needs of the mission.

On the JAXA side, the Mercury Exploration Working Group (MEWG) was formed in June 1997 under the Steering Committee for Space Science (SCSS) in the former Institute of Space and Astronautical Science (ISAS) to investigate a mission to Mercury. MEWG published the Japanese plan based on a spinning Mercury orbiter with chemical propulsion and multiple Venus and Mercury flybys. The possibility of collaboration with BepiColombo was discussed for the first time during the meeting of the Inter-Agency Consultative Group (IACG) in November 1999. Following the approval of BepiColombo as ESA's 5th Cornerstone, MEWG was reformed for the investigation of an MMO as part of BepiColombo. The International Mercury Exploration Mission as part of BepiColombo was approved by the SCSS in January 2002, followed by the formal approval of the Space Activities Commission in June 2003.

For further information, see http://sci.esa.int/bepicolombo

Scientific objectives

Mercury is an extreme of our planetary system. Since its formation, it has been subjected to the highest temperature and has experienced the largest diurnal temperature variation of any object in the Solar System. It is the closest planet to the Sun and has the highest uncompressed density of all planets. Solar tides have influenced its rotational state. Its surface was altered during the initial cooling phase and its chemical composition may have been modified by bombardment in its early history. Mercury therefore plays an important role in constraining and testing dynamical and compositional theories of planetary system formation. Only NASA's Mariner-10 has returned data from Mercury. Three flybys in 1974-1975 obtained images of somewhat less than half of the surface and discovered the unexpected magnetic field that is, though weak, strong enough to stand off the solar wind and form the magnetosphere. Although these data have been fully exploited, many gross features remain unexplained. Many conclusions are still speculative and have evoked a great number of new questions. The BepiColombo Science Advisory Group outlined the general scientific objectives of the mission:

— exploration of Mercury's unknown hemisphere;
— investigation of the geological evolution of the planet;
— understanding the origin of Mercury's high density;
— analysis of the planet's internal structure and search for the possible liquid outer core;
— investigation of the origin of Mercury's magnetic field;
— study of the planet's magnetic field interaction with the solar wind;
— characterisation of the surface composition;
— identification of the composition of the radar bright spots in the polar regions;
— determination of the global surface temperature;
— determination of the composition of Mercury's vestigial atmosphere (exosphere);
— determination of the source/sink processes of the exosphere;
— determination of the exosphere and magnetosphere structures;
— study of particle energisation mechanisms in Mercury's environment;
— fundamental physics: verification of Einstein's theory of gravity.

The complexity of these fundamental objectives hampers their straightforward translation into required payload – none can be achieved through measurements by any single instrument. Therefore, additional information was gathered to provide a concise quantification of the intended goals of the mission in terms of actual derived scientific quantities. Out of this assessment, involving experts from the wide scientific community in addition to the BepiColombo Science Advisory Team, the BepiColombo MPO Reference Payload emerged:

— High Resolution Camera;
— Stereo Camera;
— Limb Pointing Camera;
— Visible-Near-IR Mapping Spectrometer;
— Thermal-IR Spectrometer/Radiometer;
— Laser Altimeter;
— UV Spectrometer;
— X-ray Spectrometer;
— Solar X-ray Monitor;
— Gamma-ray-Neutron Spectrometer;
— Radio Science Experiment, Accelerometer;

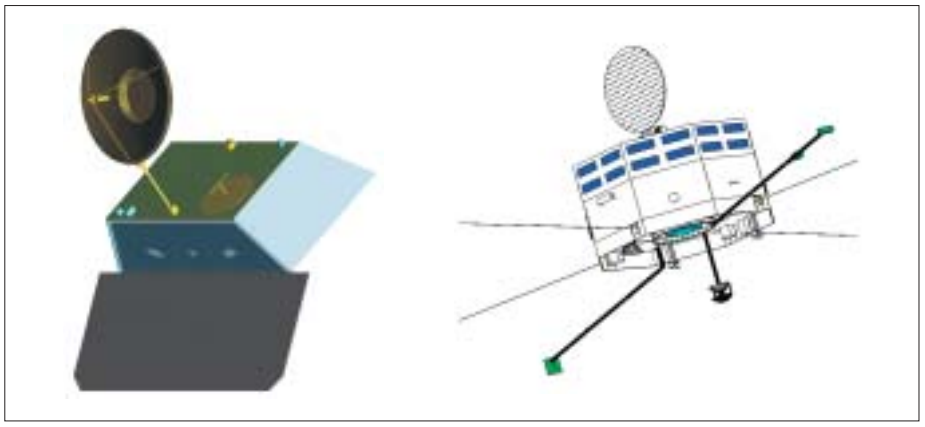

Figure 5.1.1. MPO (left) and MMO (right) of BepiColombo.

— Magnetometer;
— Neutral Particle Analyser;
— Miniature Plasma Analyser;
— Planetary Ion Camera.

Similar activities were conducted by international science teams, consisting of Japanese and European scientists, in coordination with ISAS/JAXA, to produce the MMO Reference Payload:

— Electron Spectrum Analyser;
— Mass Spectrum Analyser;
— Solar Wind Analyser;
— High-Energy Particles Analyser;
— Energetic Neutral Atoms Imager;
— Magnetometer;
— Plasma Wave Instrument;
— Mercury Dust Monitor;
— Mercury Imaging Cameras (surface, and Na and K atmosphere).

Mission scenario

In the baseline scenario, MPO and MMO are launched together on a single Soyuz-Fregat 2-1B in mid-2012. The transfer to Mercury employs Solar Electric Propulsion for a travel time of 4.2 years. Upon arrival the Solar Electric Propulsion Module is jettisoned and the Chemical Propulsion Module provides Mercury capture and orbit insertion. ESA is responsible for the cruise operations up to the delivery of the orbiters at their destinations, plus MPO operations and data acquisition. JAXA is responsible for MMO operations around Mercury. Fig. 5.1.1 shows the MPO and MMO concept configurations.

Mercury Planetary Orbiter
MPO is a 3-axis-stabilised and nadir-pointing module with an operational lifetime of at least an Earth year. It has one axis aligned with the nadir direction for continuous observation of the planet. Its low-eccentricity polar orbit (400 x 1500 km) will provide excellent spatial resolution over the entire surface. MPO's reference payload

does not consist of self-standing instruments, each with its own supporting subsystems, but rather of scientific sensors (‘instrument front-ends’) that share common functions and resources for their back-ends.

Mercury Magnetospheric Orbiter
MMO is a spinning spacecraft to be placed in a 400 x 12 000 km polar orbit, with an operational life of at least an Earth year. Its instruments focus on the study of fields, waves and particles in Mercury’s environment. The 15 rpm spin-stabilisation facilitates the azimuth scan of the particle detectors and the deployment of wire electric antennas. The spin axis will be almost perpendicular to the equator. The orbit is polar and highly elliptic; its major axis lies in the equatorial plane to permit a global exploration of the magnetosphere up to a distance of nearly 6 planetary radii from the Mercury’s centre.

Status

At the end of 2003, ESA asked for an International Payload Review Committee to assess the model payload that resulted from the reassessment phase in 2003, and to recommend the definitive reference payload for MPO. Based on their recommendation, the Request for Proposal for MPO was issued on 27 February 2004, with the responses due on 15 May 2004.

5.2 Gaia

Introduction

After a detailed concept and technology study during 1998-2000, Gaia was selected as a confirmed mission within ESA's scientific programme in October 2000, with a launch date of 'not later than 2012'. It was confirmed by ESA's Science Programme Committee following a re-evaluation of the science programme in June 2002, and reconfirmed following another re-evaluation of the programme in November 2003. A launch date of mid-2010 is currently targeted.

Scientific goals

Gaia will rely on the proven principles of ESA's Hipparcos mission to solve one of the most difficult yet deeply fundamental challenges in modern astronomy: to create an extraordinarily precise 3-D map of about a billion stars throughout our Galaxy and beyond. In the process, it will map their motions, which encode the origin and subsequent evolution of the Galaxy. Through comprehensive photometric classification, it will provide the detailed physical properties of each star observed: characterising their luminosity, temperature, gravity and elemental composition. This massive stellar census will provide the basic observational data to tackle an enormous range of important problems related to the origin, structure and evolutionary history of our Galaxy – a kind of 'Humane Genome Project' for astronomy.

Gaia will achieve this by repeatedly measuring the positions of all objects down to V = 20 mag. Onboard object detection will ensure that variable stars, supernovae, burst sources, micro-lensed events and minor planets will all be detected and catalogued to this faint limit. Final accuracies of 10 μarcsec at 15 mag, comparable to the diameter of a human hair at a distance of 1000 km, will provide distances accurate to 10% as far as the Galactic Centre, 30 000 light years away. Stellar motions will be measured even in the Andromeda Galaxy.

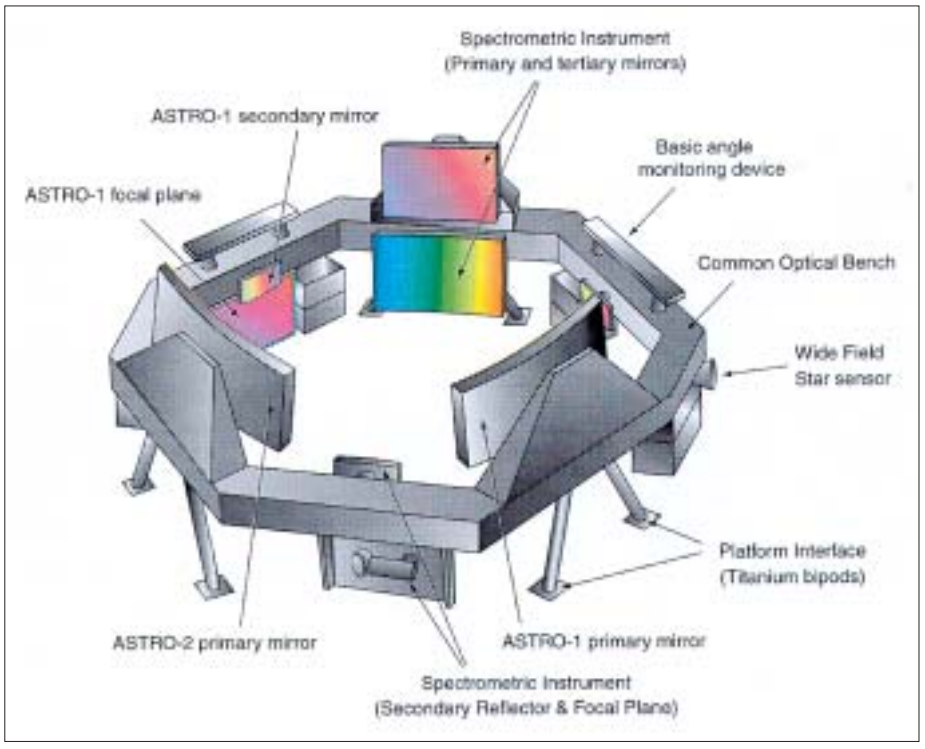

Figure 5.2.1. The GAIA payload comprises two astrometric viewing directions, and the radial velocity/spectroscopic instrument, suspended on a common stable platform. The instrument scans the sky by spinning about an axis perpendicular to the supporting ring structure.

For further information, see http://www.rssd.esa.int/Gaia

Table 5.2.1. Gaia vs. Hipparcos capabilities.

	Hipparcos	*GAIA*
Magnitude limit	12	20 mag
Completeness	7.3 - 9.0	~20 mag
Bright limit	~ 0	~3-7 mag
Number of objects	120 000	26 million to V = 15
		250 million to V = 18
		1000 million to V = 20
Effective distance limit	1 kpc	1 Mpc
Quasars	none	~500 000
Galaxies	none	10^6 - 10^7
Accuracy	~1 milliarcsec	4 µarcsec at V = 10
		10 µarcsec at V = 15
		200 µarcsec at V = 20
Broadband photometry	2-colour	4-colour to V = 20
Medium band photometry	none	11-colour to V = 20
Radial velocity	none	1-10 km/s to V = 16-17
Observing programme	pre-selected	onboard and unbiased

Gaia's expected scientific harvest is of almost inconceivable extent and implication. Its main goal is to clarify the origin and history of our Galaxy, by providing tests of the various formation theories, and of star formation and evolution. This is possible because low-mass stars live for much longer than the present age of the Universe, and therefore retain in their atmospheres a fossil record of their detailed origin. The Gaia results will precisely identify relics of tidally-disrupted accretion debris, probe the distribution of dark matter, establish the luminosity function for pre-main sequence stars, detect and categorise rapid evolutionary stellar phases, place unprecedented constraints on the age, internal structure and evolution of all stellar types, establish a rigorous distance-scale framework throughout the Galaxy and beyond, and classify star-formation and kinematical and dynamical behaviour within the Local Group of galaxies.

Gaia will pinpoint exotic objects in colossal and almost unimaginable numbers: many thousands of extrasolar planets will be discovered, and their detailed orbits and masses determined; tens of thousands of brown dwarfs and white dwarfs will be identified; some 100 000 extragalactic supernovae will be discovered and details passed to ground-based observers for follow-up observations; Solar System studies will receive a massive impetus through the detection of many tens of thousands of new minor planets; inner Trojans and even new trans-Neptunian objects, including Plutinos, may be discovered. Gaia will follow the bending of starlight by the Sun and major planets, over the entire celestial sphere, and therefore directly observe the structure of space-time (the accuracy of its measurement of General Relativistic light bending may reveal the long-sought scalar correction to its tensor form). The PPN parameters gamma and beta will be determined with unprecedented precision. New

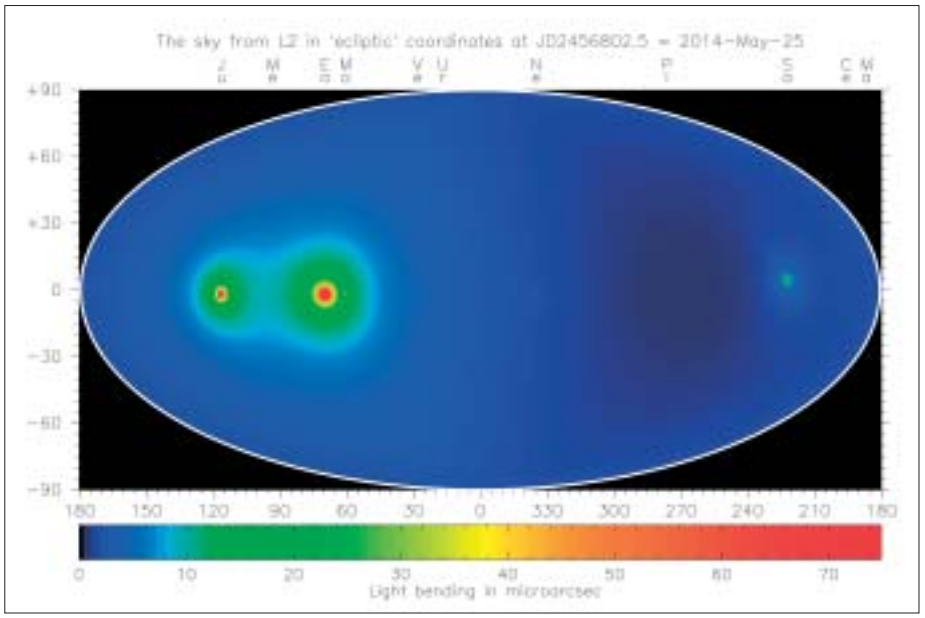

Figure 5.2.2. The amplitude of the relativistic light bending terms due to the presence of the various Solar System objects, as seen by Gaia from its L2 orbit. The sky is shown in ecliptic coordinates, and the dominant effect of the Sun's gravitational field has been suppressed. At the epoch simulated (May 2014), the effects of Jupiter, the Earth, Moon and Saturn can be clearly seen. All planets as well as other Solar System objects, including the four Galilean moons of Jupiter, and the most massive minor planets, will have a measurable effect on the Gaia observations. (Courtesy J. de Bruijne).

constraints on the rate of change of the gravitational constant, and on gravitational wave energy over a certain frequency range, will be obtained.

The spacecraft

Gaia will carry the demonstrated Hipparcos principles into orders of magnitude improvement in terms of accuracy, number of objects, and limiting magnitude, by combining them with state-of-the-art technology. It will be a continuously scanning spacecraft, accurately measuring 1-D coordinates along great circles, and in two simultaneous fields of view, separated by a well-defined and well-known angle. These 1-D coordinates are then converted into the astrometric parameters in a global data analysis, in which distances and proper motions 'fall out' of the processing, as does information on double and multiple systems, photometry, variability, metric, planetary systems, etc. The payload is based on a large CCD focal plane assembly, with passive thermal control, and natural short-term (3 h) instrument stability arising from the sunshield, selected orbit and robust payload design.

The telescopes are of moderate size, with no specific design or manufacturing complexity. The system fits within a Soyuz-Fregat launch configuration, without deployment of any payload elements (moving from an Ariane to a Soyuz launch was one of the results of the 2002 redesign effort). A Lissajous orbit at L2 is the adopted operational orbit, from where about 1 Mbit/s of data is returned to the single ground station throughout the 5-year mission. The 10 μarcsec accuracy is evaluated through a comprehensive accuracy assessment programme; this remarkable accuracy is possible partly by virtue of the (unusual) instrumental self-calibration achieved through the data analysis on-ground. This ensures that final accuracies essentially reflect the photon noise limit for localisation accuracy, exactly as achieved with Hipparcos.

One of the objectives of the Concept and Technology Study completed in 2000 was to identify the areas of technology where further development is required before

moving into Phase-B, scheduled to start in early 2005. About 15 well-identified key technology areas were identified, including the CCD/focal plane development, silicon carbide mirrors, onboard data handling, and antenna design. All of these activities are now underway, and should lead to full confidence in the required technology by the end of 2004. Noteworthy progress in 2003 was the detailed design review of the primary mirror, leading to the start of the manufacturing of a prototype SiC primary mirror in early 2004. Detailed design of the focal plane assembly is proceeding intensively, with the first custom-made Gaia CCDs being manufactured by e2v in late 2003.

Scientific organisation and progress

During 2001, a scientific organisation structure was put in place for the period until the start of Phase-B. About 280 European scientists are now working on various preparatory aspects of Gaia, ranging from the instrument design, through to the data processing, the treatment of specific objects (such as variable and multiple stars), and the optimisation of the photometric and radial velocity instruments. A group of about 12 scientists forms the Gaia Science Team, charged with advising ESA on all aspects of the scientific development and conduct of Gaia, and chaired by the ESA Project Scientist.

About 16 working groups, under the direction of leaders and coordinated by the science team, are responsible for the study and development of the various scientific aspects of the mission. Considerable progress has been made in many areas during the last 2 years. One very challenging task is to design the medium-band photometric system capable of classifying and physically characterising the billion objects observed: for example, determining their temperatures, surface gravity, reddening and metallicity. One working group is charged with the optimisation and development of the radial velocity instrument, where the challenge is to establish the characteristics of an instrument optimally designed to determine radial velocities for as many objects as possible (down to 17-18 mag), and to derive spectral characteristics at the same time. The relativity working group has made considerable progress in defining the principles underlying the derivation of a reference system deeply affected by gravitational light bending where, for example, effects due to the Sun, Jupiter, the other planets and even the more massive minor planets, will be observable at the microarcsec level. One group is actively assessing the observability and detectability of Solar System objects, including Near-Earth Objects; another is assessing the detectability of transient events such as microlensing, supernova and gamma ray bursts.

A key activity where much early effort has been devoted is to establish the feasibility of the Gaia data analysis procedure. The task is large and daunting: over its 5-year mission, Gaia will deliver some 100 TByte of data, and will require processing power of order 10^{20} floating point operations. Given that the data are effectively ‘tangled’ in time and position on the sphere, the data analysis problem is extremely challenging, even taking realistic assumptions about data processing capabilities extrapolated 10 years into the future. A prototype system has been set up, which is capable of ingesting a realistic but simplified telemetry stream, detecting and matching up observations of the same objects observed days, weeks or months apart, and subjecting them to an iterative adjustment in which the stellar parameters, satellite attitude and calibration parameters are estimated. The present study aims at the solution of simulated observations of about a million stars distributed over the celestial sphere. Activities will continue under the present study contract until the end of 2004.

5.3 LISA Pathfinder

Introduction

LISA Pathfinder (formerly SMART-2) is intended to demonstrate the key technologies for the ESA/NASA collaborative LISA mission. To this end, LISA Pathfinder will accommodate a LISA Technology Package (LTP), provided by European institutes and industry, and a Disturbance Reduction System (DRS) that is very similar to the LTP and has the same goals but is provided by US institutes and industry.

Mission goals

The mission goals for the LTP can be summarised as:

— demonstrating drag-free and attitude control in a spacecraft with two proof masses in order to isolate the masses from inertial disturbances. The aim is to demonstrate the drag-free system with a performance on the order of 10^{-14} m $s^{-2}/\sqrt{Hz}$ in the bandwidth 10^{-3}-10^{-1} Hz. The LISA requirement in the same band is 10^{-15} m s^{-2} /√Hz;
— demonstrating the feasibility of performing laser interferometry in the required low-frequency regime with a performance as close as possible to 10^{-12} m/√Hz in the frequency band 10^{-3}-10^{-1} Hz, as required for the LISA mission;
— assessing the longevity and reliability of the capacitive sensors, thrusters, lasers and optics in the space environment.

As the environment on the LISA Pathfinder spacecraft will be comparatively noisy (in terms of temperature fluctuations and residual forces), the technology demonstrator is aimed at meeting specifications that are about a factor 10 more relaxed than necessary for LISA.

LISA Technology Package

The LTP represents one arm of the LISA interferometer, in which the distance between the two proof masses is reduced from 5 million km to 20 cm. As in LISA, the proof masses fulfil a double role: they serve as optical references (mirrors) for the interferometer and as inertial references for the drag-free control system.

The LTP drag-free control system consists of an accelerometer (or inertial sensor), a propulsion system and a control loop. The two identical proof masses (46 mm cubes) are housed in individual vacuum cans (Fig. 5.3.1). Capacitive sensing in three dimensions measures the displacement of the cubes with respect to their housing. These position signals are used in a feedback loop to command µN proportional thrusters to enable the spacecraft to remain centred on the proof mass. Field Emission Electric Propulsion (FEEP) thrusters will be used as actuators.

Although the proof masses are shielded from non-gravitational forces by the spacecraft, cosmic rays and solar flare particles can significantly charge them, leading to electrostatic forces. A system of fibre-coupled UV lamps will discharge the proof masses at regular intervals. As surface effects on the proof masses can cause electrostatic forces, the proof masses have to be coated very carefully to avoid contamination. In order not to damage the coating during launch, a caging mechanism is used to maintain the proof masses in a safe position during launch.

Using two proof masses, the reference point for the drag-free system can be chosen to be on each of the two masses or at any point between. Having two also allows verification of the performance of the drag-free control loop with the second proof mass by sensing its movements relative to the spacecraft (or the first proof mass) while the spacecraft follows the first proof mass.

The position of the proof masses with respect to the spacecraft or each other is

For further information, see http://sci.esa.int/lisa

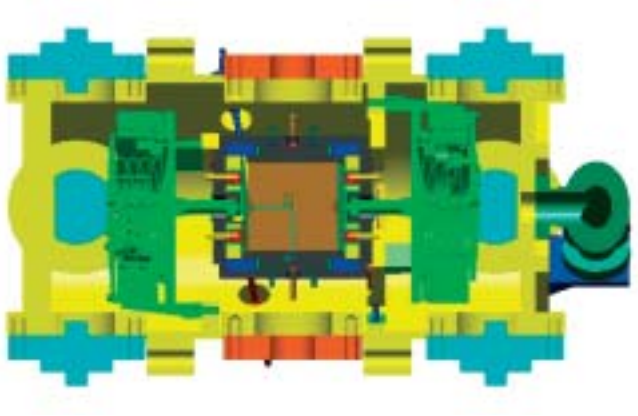

Figure 5.3.1. The proof masses at the core of the LTP are surrounded by positioning, sensing and caging systems within their vacuum enclosure.

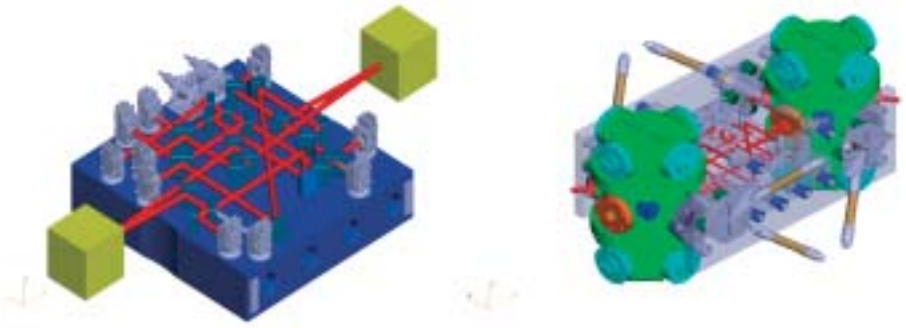

Figure 5.3.2. Left: the LTP Optical Bench. The path of the laser light is shown in red, the two proof masses are show in yellow. Right: the LTP Assembly.

measured by an interferometric system that is capable of picometre precision in the frequency band 10^{-3}-10^{-1} Hz (Fig. 5.3.2). The outcome of ongoing technology development contracts will decide upon the exact realisation of the interferometric measurement system. The remaining temperature fluctuations aboard the spacecraft require the use of materials with very small coefficients of thermal expansion. As the dynamic range needed is comparatively large (up to 10 mm), a heterodyne interferometer is favoured.

Disturbance Reduction System

The Disturbance Reduction System (DRS) is a NASA-supplied system with the same mission goals as LTP but using slightly different technology. Its exact design will be determined by studies but the baseline foresees two inertial sensors and an interferometric readout similar to that planned for LTP. The thrusters for the drag-free control system will be different from the FEEPs: DRS is based on colloidal thrusters that use ionised droplets of a colloid accelerated in an electric field to provide propulsion.

Launch & orbit

LISA Pathfinder will be launched by a small European vehicle into a geostationary transfer orbit. From there, it will use its own propulsion module to reach its operational orbit around the L1 point about 1.5 million km from the Earth towards the Sun (Fig. 5.3.3). The exact orbital parameters are subject to a trade-off: a larger orbit (about 750 000 km radius) allows a ‘free-injection’ strategy, saving propellant and

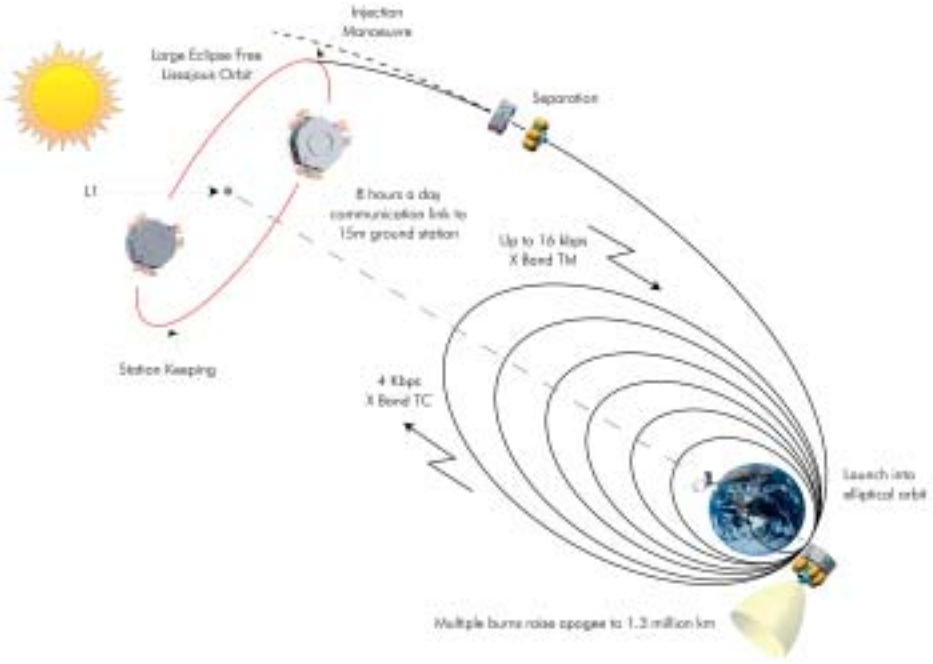

Figure 5.3.3. Transfer from low-Earth elliptical orbit to an orbit around L1. Total transfer time is 4 months.

mass; a tighter orbit (about 120 000 km radius) facilitates communications with Earth. The orbit is chosen so that it fulfils the stringent requirement of the LTP and DRS with respect to thermal stability and gravitational disturbances.

The launch of LISA Pathfinder is planned for early 2008. Following the transfer, initial set-up and calibration phases, the in-flight demonstration of the LISA technology will take place in the second half of 2008 (90 days LTP, 70 days DRS, 20 days joint operations), providing timely feedback for the development of the LISA mission.

Status

During the Definition Phase (Phase-A/B1, September 2001 to July 2002), two parallel studies were carried out by Astrium (UK) and CASA (E) as prime contractors. These studies assumed a variety of mission scenarios (with and without the DRS, with and without a Darwin Technology Package) involving one or two spacecraft. This phase was followed by an Extended Definition Phase (November 2002 to June 2003), during which two parallel studies were carried out by the same prime contractors, but now focusing on only one mission scenario: LISA technology (LTP and DRS) and only one spacecraft. In mid-2003, Astrium (UK) was selected as the prime contractor for the Implementation Phase (Phase-B2/C/D). As this phase could not be started immediately, the Extended Definition Phase was continued until January 2004 with only Astrium (UK) as prime. Since February 2004, LISA Pathfinder has been in the Implementation Phase.

In November 2003, ESA's Science Programme Committee (SPC) decided that the long-term space science plan will include LISA Pathfinder, subject to affordable cost-at-completion and formally secured LTP payload funding. Final formal approval of the LISA Pathfinder mission is expected at the June 2004 SPC meeting, after signature of the Multilateral Agreement by ESA and those national funding agencies making contributions to the LTP.

5.4 LISA

Scientific goals

Gravitational waves are a necessary consequence of Einstein's theory of General Relativity. They cause a shrinking and stretching of space-time and therefore modify the distance between freely-falling test masses. Their strength can be expressed in terms of the strain, the relative change in distance caused by a gravitational wave. In contrast to the familiar electromagnetic waves, they are by nature quadrupole waves.

Predicted in 1916 by Einstein and proved in the late 1950s to be observable, there is no direct evidence for their existence, although there is indirect evidence from the famous Hulse-Taylor binary pulsar (PSR1913+16): its orbital period is decaying due to the loss of orbital energy to gravitational waves at exactly the rate predicted by General Relativity. Efforts to detect gravitational waves in the high-frequency range (frequencies from 10 Hz to the kHz range) on the ground with bar detectors and small interferometers have been made since the 1960s. The construction of several large ground-based interferometers with increased sensitivity is now well underway; one is already fully operational (TAMA, in Japan), others in their final (LIGO, a US project with two sites in Hanford, Washington and Livingston, Louisiana, GEO600, a British-German collaboration, near Hannover, Germany) or advanced (VIRGO, an Italian-French project near Pisa, Italy) stages of construction. Full operation of most of the first-generation ground-based detectors is expected within a few years.

The primary objective of the LISA (Laser Interferometer Space Antenna) mission is the detection and observation of gravitational waves from massive black holes (MBHs) and galactic binaries in the frequency range 10^{-4}-10^{-1} Hz (Fig. 5.4.1). This low-frequency range is inaccessible to ground-based interferometers because of the background of local gravitational noise and because ground-based interferometers are limited in length to a few kilometres.

Ground-based interferometers can in principle observe the bursts of gravitational radiation emitted by galactic binaries during the final stages (lasting minutes or seconds) of coalescence when the frequencies are high and the amplitudes and frequencies both increase quickly with time. However, the improvement of theoretical knowledge over the last few years has shown that the signal-to-noise ratio, though still slightly uncertain, is expected to be marginal for first-generation detectors. Only

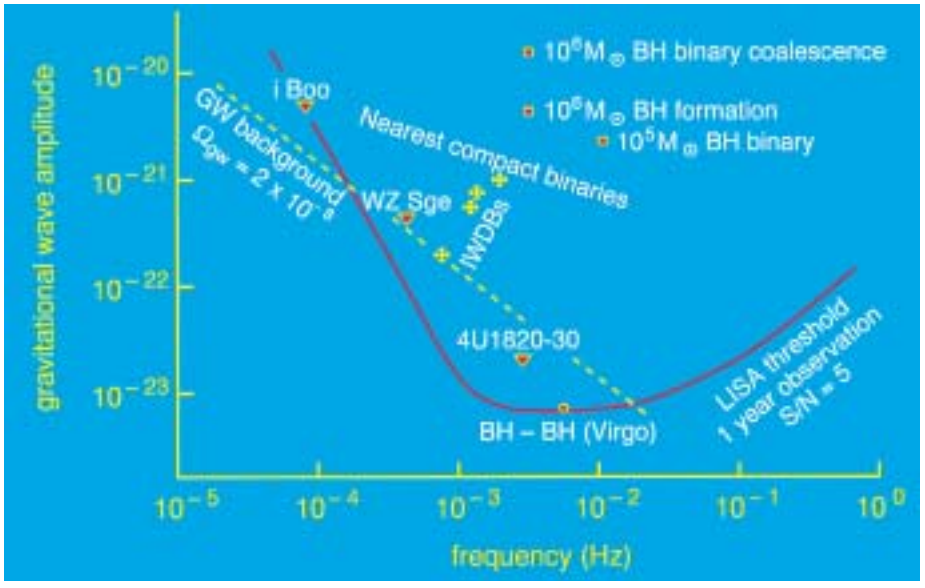

Figure 5.4.1. The target sensitivity curve of LISA and the strengths of expected gravitational-wave sources.

For further information, see http://sci.esa.int/lisa

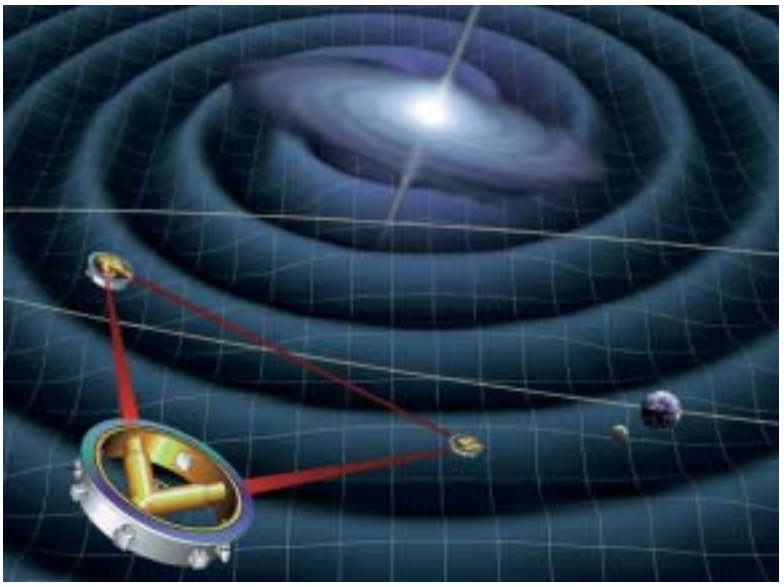

Figure 5.4.2. Orbital configuration of the three LISA spacecraft.

second-generation detectors, to be commissioned after 2005, are expected to achieve reliable detection of those important astrophysical sources. Coalescences of MBHs are detectable only in space owing to the very low frequencies involved.

In the low-frequency band of LISA, sources are well-known and signals are stable over long periods (many months to thousands of years). LISA will detect signals from numerous sources with signal-to-noise ratios of 50-1000 for MBHs, which will allow determination of the internal parameters of their source such as position and orientation. LISA will complement the operation of the second-generation ground-based interferometers, giving a full coverage of the frequency spectrum, from a tenth of a mHz to the kHz region.

Configuration

The LISA mission comprises three identical spacecraft positioned 5 million km apart in an equilateral triangle. LISA is basically a giant Michelson interferometer in space with a third arm to give independent information on the two polarisations of gravitational waves and for redundancy. The distance between the spacecraft (the armlength of the interferometer) determines the frequency range in which observations can be made with LISA. The centre of the triangular formation is in the plane of the ecliptic, 1 AU from the Sun and trailing the Earth by approximately 20°. The plane of the triangle is inclined at 60° with respect to the ecliptic, which means that the triangular formation of the spacecraft is maintained throughout the year, with the triangle appearing to counter-rotate about the centre of the formation once per year (Fig. 5.4.2).

The position of the formation 20° behind the Earth is a result of a trade-off between minimising the gravitational disturbances from the Earth-Moon system and the communications needs. While going farther away would further reduce the disturbances, the larger distance would require larger antennas or higher transmitter power.

While LISA can be described as a Michelson interferometer, the actual implementation is somewhat different from a ground-based interferometer. The laser

Figure 5.4.3. Cutaway view of one of the three identical LISA spacecraft. The main structure is a ring with a diameter of 1.8 m and a height of 0.48 m. The top of the spacecraft is covered by a solar cell array, removed here to allow a view of the Y-shaped payload.

light going out from the centre spacecraft to the other corners is not directly reflected back because very little would be received that way. In an analogy to a radio-frequency transponder scheme, the laser on the distant spacecraft is instead phase-locked to the incoming light, generating a return beam of full intensity. The transponded light from the far spacecraft is received by the centre spacecraft and superposed with the onboard laser light that serves as the local oscillator in a heterodyne detection. As this entwines laser frequency noise with a potential gravitational wave signal, the signal from the other arm is used to take out the laser frequency noise and obtain the pure gravitational wave signal.

Even at a distance of 50 million km from Earth, the remaining gravitational disturbances of the Earth, Moon and the large planets are sufficient to cause relative velocities of the spacecraft of up to 20 m/s so that, in the course of a year, the distance between the spacecraft changes by many thousands of kilometres. The relative velocity causes the transponded light to be Doppler-shifted by up to 20 MHz. The resulting signal is well outside the LISA detection band and can be removed by onboard data processing.

Each spacecraft has a launch mass of about 460 kg (including contingency), which includes the payload, ion drive, propellants and spacecraft adapter. All three can be launched by a single Delta-II 7925H. After launch, the trio separate and use their ion drives to reach their operational orbits in 13 months. There, they jettison their propulsion modules and attitude and drag-free control will be left to μN thrusters.

Each spacecraft carries two 30 cm-diameter steerable high-gain antennas for communication with Earth. Using the 34 m antennas of the Deep Space Network and 5 W transmitter power, data can be transmitted in the X-band at a rate of 7 kbit/s. Data are transmitted for 8 h every 2 days and stored onboard in a solid-state mass memory of 1 Gb during times of no communication. Only one spacecraft is used to transmit data to Earth; the other two transmit their data to the 'master spacecraft' via the laser link between the trio. Nevertheless, all three spacecraft are identical which not only reduces cost but also increases redundancy because each could become the master spacecraft. The nominal mission lifetime is 2 years once the spacecraft reached their operational orbits.

Payload

Each spacecraft contains two optical assemblies (Fig. 5.4.3). The two assemblies on one spacecraft point towards an identical assembly on the other two. In this way, the spacecraft form two independent Michelson interferometers, providing redundancy. A 1 W IR laser beam (1064 nm wavelength) is transmitted to the corresponding remote spacecraft via a 30 cm-aperture f/1 Cassegrain telescope. The same telescope is used to focus the very weak beam (a few pW) coming from the distant spacecraft and to direct the light to a sensitive photodetector (a quadrant photodiode), where it is superimposed with a fraction of the original local light. At the heart of each assembly is a vacuum enclosure containing a free-flying polished platinum-gold 40 mm cube – the proof mass – that serves as the optical reference (mirror) for the light beams. A passing gravitational wave will change the length of the optical path between the proof masses of one arm of the interferometer relative to the other arm. The distance fluctuations are measured to a precision of 40 pm (averaged over 1 s) which, when combined with the large separation between the spacecraft, allows LISA to detect gravitational wave strains down to a level of order $\Delta\lambda/\lambda = 10^{-23}$ in 1 year of observation with a signal-to-noise ratio of 5.

The spacecraft serves mainly to shield the proof masses from the adverse effects of solar radiation pressure so that they follow a purely gravitational orbit. Although the position of the spacecraft does not enter directly into the measurement, it is nevertheless necessary to keep all spacecraft moderately accurately centred on their respective proof masses to reduce spurious local noise forces. This is achieved by a drag-free control system consisting of an accelerometer (or inertial sensor) and a system of µN thrusters.

Capacitive sensing in three dimensions measures the displacements of the proof masses relative to the spacecraft. These position signals are used in a feedback loop to command Field Emission Electric Propulsion (FEEP) thrusters to follow the proof masses precisely. As a reference point for the drag-free system, one or the other mass (or any point between) can be chosen. The FEEP thrusters are also used to control the attitude of the spacecraft relative to the incoming optical wave fronts using signals derived from the quadrant photodiodes.

Although the spacecraft shields its proof masses from non-gravitational forces, cosmic rays and solar flare particles can cause a significant charging of the proof masses. A discharging system, consisting of a fibre-coupled UV light source, will be operated at regular intervals.

As the 3-spacecraft constellation orbits the Sun in the course of a year, the observed gravitational waves are Doppler-shifted by the orbital motion and amplitude-modulated by the non-isotropic antenna pattern of the detector. This allows determination of the direction of the source and assessment of some of its characteristics, e.g. its orientation if the signal is periodic and has a sufficiently large signal-to-noise ratio. Depending on the strength of the source, a precision for determining the position of up to an arcminute can be achieved.

Status

LISA and its technology-demonstrating precursor LISA Pathfinder form an ESA/NASA collaborative project, selected as an ESA Cornerstone and included in NASA's 'Beyond Einstein' initiative, with a launch in 2012/2013. During the restructuring exercise of ESA's science programme in October 2003, LISA and LISA Pathfinder were confirmed. The share of responsibilities and hardware between the agencies is currently negotiated on the basis of ESA taking responsibility for the payload and NASA for the spacecraft, integration and launch vehicle. About half of the payload hardware will be provided by NASA, the other half by European institutes.

5.5 JWST

Introduction

NASA, ESA and the Canadian Space Agency (CSA) have since 1996 collaborated on the definition of a successor to the Hubble Space Telescope (HST). Known initially as the Next Generation Space Telescope (NGST), in 2002 the project was renamed the James Webb Space Telescope (JWST) in honour of NASA's second Administrator, who led the agency during the Apollo programme.

The JWST observatory consists of a passively cooled, 6.55 m-aperture telescope, optimised for diffraction-limited performance in the near-IR (1-5 µm) region, but with extensions to either side into the visible (0.6-1 µm) and mid-IR (5-28 µm) regions. The large aperture and shift to the IR embodied by JWST is first and foremost driven scientifically by the desire to follow the contents of the faint extragalactic Universe back in time and redshift to the epoch of 'First Light' and the ignition of the very first stars. Nonetheless, like its predecessor, JWST will be a general-purpose observatory and carry a suite of astronomical instruments capable of addressing a very broad spectrum of outstanding problems in galactic and extragalactic astronomy. In contrast to HST, however, JWST will be placed into a Sun-Earth L2 halo orbit and will not be serviceable after launch.

Science

The science case for the JWST mission has been documented in quantitative detail by a joint Science Working Group (SWG). The blueprints for an observatory architecture capable of meeting the derived scientific requirements were drawn up in 1999-2000. The scientific goals of the JWST mission can be sorted into four broad themes:

— First Light (after the Big Bang);
— Assembly of galaxies;
— Birth of stars and proto-planetary systems;
— Planetary systems and the origins of life.

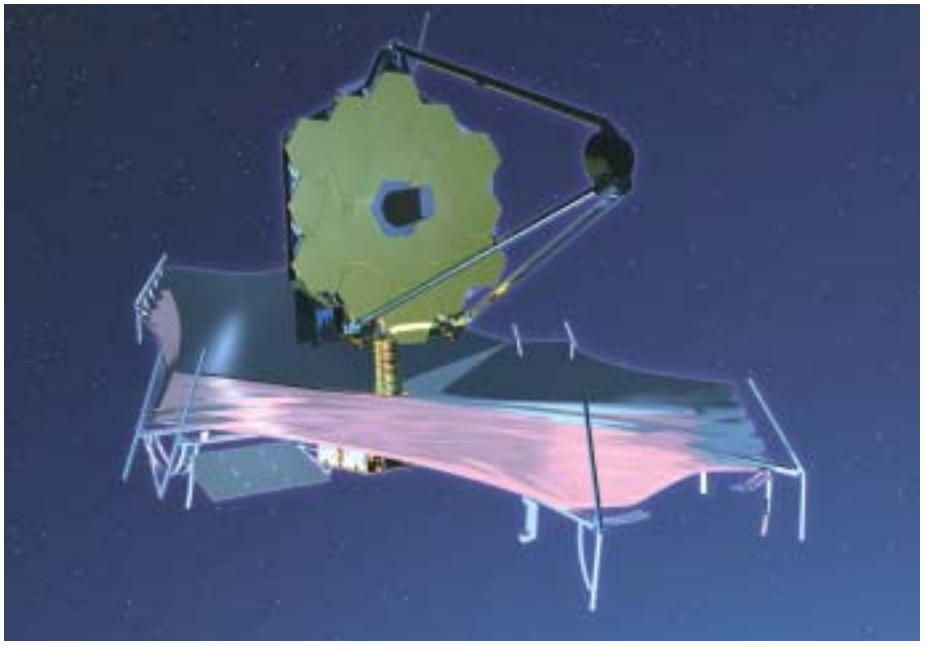

Figure 5.5.1. JWST observatory in orbit, showing the deployed 6.55 m-diameter telescope and the large sunshade (Northrop Grumman/Ball).

For further information, see http://sci.esa.int/jwst

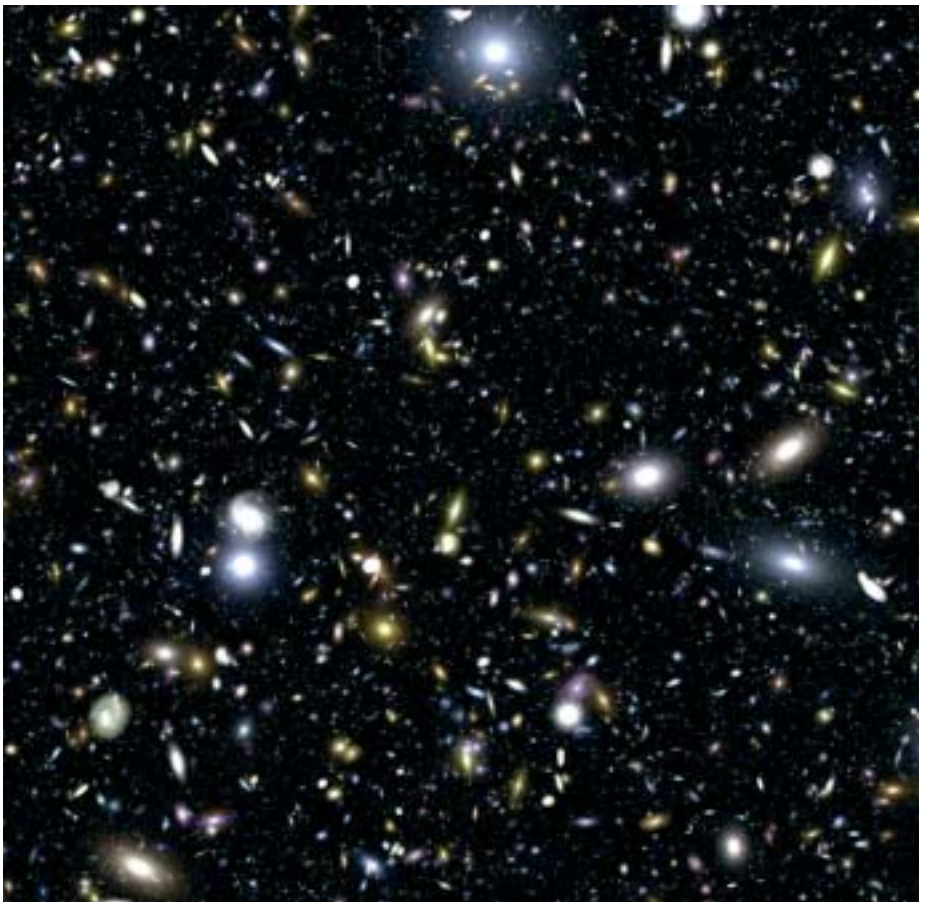

Figure 5.5.2. Simulated deep JWST image. (STScI)

Although the first two themes are extragalactic and concerned with exploring the formation of stars and galaxies in the remote Universe at the earliest times, they are intimately linked to the latter two, mainly galactic, themes, which aim at understanding the detailed process of star- and planet-formation in our own Galaxy.

ESA's participation in JWST was initially approved by the Science Programme Committee in November 2000 at the level of a Flexi-mission. This level secures ESA a ~15% partnership as well as a continuation of its present participation in HST to the end of that observatory's operational life.

In 2002, NASA selected Northrop Grumman Space Technology as the prime contractor for the observatory. The JWST project is presently poised to enter its final design phase. Launch is currently scheduled for 2011.

JWST will carry three main instruments:

— NIRCam: a wide-field (2.2 x 4.4 arcmin) near-IR camera covering wavelengths 0.6-5µm;
— NIRSpec: a wide-field (3.5 x 3.5 arcmin) multi-object near-IR spectrometer covering wavelengths 0.6-5 µm at spectral resolutions of R~100, R~1000 and R~3000;
— MIRI: a combined mid-IR camera (1.4 x 1.9 arcmin) and spectrograph (R~3000) covering wavelengths 5-27 µm.

In addition, the Fine Guidance System (FGS) will include a near-IR tunable filter imaging capability (2.3 x 2.3 arcmin; R~100) covering wavelengths 0.6-5 µm.

The JWST telescope proper and its associated instruments will be cooled in bulk to ~37K, a temperature determined by the operating temperature of the HgCdTe detector arrays employed by NIRCam, NIRSpec and FGS. Cooling is to be attained passively by placing the observatory at L2 and keeping the telescope and its instrumentation in perpetual shadow under a large deployable sunshade. The telescope is made up of 18 hexagonal segments, and is specified to yield diffraction-limited performance at wavelengths above 2 µm in the near-IR. In order to fit into the fairing of the Ariane-5 launcher, the 6.55 m primary mirror needs to be folded and deployed along with the secondary mirror in orbit. Fine pointing will be achieved by deflecting the beam by means of a fast steering mirror controlled by the FGS (to be provided by Canada) located in the telescope focal plane.

The 0.6 µm visible wavelength limit allows the use of gold as the reflecting coating in the telescope and instruments. For reasons of cost, diffraction-limited performance will not be obtained at wavelengths in the region of overlap with HST below 2 µm. Nonetheless, depending on the character of the residual aberrations, the image quality is expected to match that of HST (which is less than half the size) in terms of resolving power.

The performance at longer wavelengths in the mid-IR is a slightly more complex story. The primary source of stray light in the mid-IR is thermal radiation emitted by the backside of the sunshield and scattered off the largely unbaffled telescope. Provided the temperature of the sunshield can be kept below ~110K and the dust contamination of the JWST optics can be kept sufficiently low, the intensity of this stray light contribution can be kept below that of the zodiacal light at wavelengths shorter than ~10 µm. The JWST specifications are designed to assure such sky-limited performance throughout the core 1-5 µm region and out to at least 10 µm.

The telescope will be fully diffraction-limited throughout the mid-IR. However, the candidate Si:As detector arrays needed to reach wavelengths beyond 5 µm require an operating temperature of ~7K, which is significantly below the ~30-50K ambient environment of the telescope and instrument module. Active cooling by means of a solid hydrogen cryostat is therefore called for as part of the mid-IR instrument.

Although observations beyond 10 µm will not be sky-limited and subject to thermal self-emission from the observatory, the sheer size and location of the telescope assures that its performance will be vastly superior to anything that can be done from the ground at these wavelengths. The extreme long wavelength cut-off of is expected to fall just shortward of ~28 µm, a limit dictated by the sensitivity cut-off of the baseline Si:As detectors.

The components of Europe's contributions to JWST were approved by the SPC in February 2003. The level of participation closely follows the HST model, and consists of three main elements: scientific instrumentation, non-instrument flight hardware and contributions to operations.

ESA will provide NIRSpec and, through special contributions from its member states, 50% to MIRI (be developed jointly with NASA). These instruments will enter their final design and implementation phases in 2004.

As its non-instrument contribution, ESA will provide the Ariane-5 ECA launcher that will place the observatory in an orbit around the anti-Sun Earth-Sun Lagrangian point, L2.

Responsibility for scientific operation of JWST lies with the Space Telescope Science Institute (STScI) in Baltimore, working under contract to NASA. A yet-to-be negotiated number of ESA staff will be posted at STScI in support of the European

payload components. The observing programme will be determined by the astronomical community on the basis of periodic competitive peer reviews organised by the STScI. The overriding motivation for ESA's partnership in the mission is to secure member-state scientists with full access to compete for time on JWST on an equal footing with their US and Canadian counterparts.

5.6 Eddington

Introduction

Eddington has two primary science goals: to produce the data on stellar oscillations necessary to understand stellar structure and evolution, and to detect and characterise habitable planets around other stars. These goals will be achieved through extremely sensitive, continuous photometric monitoring of a very large number of stars, at an accuracy level that requires space-based observations.

Science goals

Stellar structure and evolution

Eddington will produce the data necessary for a detailed understanding of the internal structure of stars and the physical processes that govern their evolution, providing the empirical basis for developing the theory of stellar evolution to the stage where it can be used with confidence to address some of the major issues in contemporary astrophysics, such as: how old is the Universe, what is the age of an individual galaxy, or an individual stellar aggregate, and how do galaxies evolve?. This will be achieved using stellar seismology (asteroseismology), the study of the resonant oscillation frequencies of stars of different masses, ages and chemical composition. Oscillations probe the interiors of stars, yielding data on the internal structures that cannot be obtained by classical observations. The primary data product of Eddington will be long, accurate photometric time series of a large number of stars, spanning a wide range in age, mass and chemical composition. Asteroseismic analyses will yield quantitative measurements of (for example) stellar ages and the sizes of convective cores to few-percent accuracy, far superior than usual in astronomy, and will yield a detailed understanding of the physical processes that govern stellar evolution and a quantitative determination of the internal structure of stars in different stages of evolution, such as stars that ultimately become type-II supernovae and major contributors to the chemical evolution of galaxies.

Habitable planets

Eddington will detect terrestrial planets around other stars, in particular planets within the ‘habitable zone’ and thus in principle able to sustain life. Habitable planets are defined as those with a rocky surface (implying a size similar to the Earth) and with temperatures compatible with the presence of liquid water ($0 < T < 100°C$). The photometric dips caused by the transit of a planet in front of its parent star will allow its detection using long, accurate stellar photometric time series. In addition to finding a significant number of habitable planets, Eddington will discover large numbers of giant planets in a variety of orbits, and of smaller planets outside the habitable zone, providing unique physical information on their properties and yielding a large database for investigations into the origin of planetary systems.

Additional science goals

In parallel, the Eddington data will allow several other scientific programmes to be carried out in stellar physics and fields such as detection and light curves of supernovae, low surface brightness galactic halos, and photometric variability of quasars.

Payload

The Eddington payload can be described as a wide-field, high-accuracy optical photometer, mounted on a 3-axis stabilised platform, and it is characterised by its simplicity and robustness. A parallel detailed systems definition study is being finalised, which has resulted in a multiple parallel telescope payload: three identical, co-aligned 70 cm-diameter telescopes with a 6-CCD mosaic camera at the focal plane. The CCDs are 2k x 6k chips operated in frame transfer mode (with a 2k x 3k

For further information, see http://sci.esa.int/eddington

imaging area). Each telescope will have a different colour filter (broad-band, blue and red), allowing for colour information to be derived for the brighter targets.

Observing programme

Eddington will determine the interior structure of stars spanning the H-R diagram, with different ages and chemical composition. Its payload has been specified to reach magnitudes as faint as V = 11 for low-mass stars, and as faint as V = 13 for higher-mass stars, allowing for the rarer and fainter stellar types in crucial stages of evolution to be studied. Two years of observations dedicated mainly to asteroseismic science are foreseen, with each observing run lasting between one and a few months. Asteroseismic data will be collected on some 50 000 stars. While the observing programme will be the subject of an open Announcement of Opportunity (with some usual allowance for guaranteed-time observers), a baseline observing programme will include several of the nearby open clusters – where homogeneous samples of stars of the same age and chemical composition, but spanning a range of masses, are available – as well as several individual stellar fields. For the planet-finding phase, a single, long (≥ 3 years) observation of a single rich stellar field is planned, to ensure the detection of multiple (n ≥ 3) transits for planets with the same orbital period as Earth. This will also provide lower time resolution asteroseismic data especially valuable for the seismological investigation of long-period oscillating stars. Also, several periodic transits of short-period planets and individual transits of longer-period planets will be found in the 1-2 month asteroseismic observations, allowing study of a significantly larger number of stars. During the 5-year mission, some 500 000 stars will be searched for planetary transits, with accuracy sufficient to yield a significant crop of habitable planets, as well as large number of higher mass and hotter planets.

The Eddington mission will bring to maturity one of the cornerstones of modern astrophysics: the theory of stellar structure and evolution. It will place it on solid experimental foundations, by collecting data that will, for the first time, allow direct and quantitative testing of its underlying assumptions and hypothesis. At the same time, Eddington will discover other planetary systems, with terrestrial planets in the habitable zone, in principle able to sustain life. It will detect a large number of planets spanning a wide range of characteristics, thereby allowing a statistical study of the properties of planetary systems as a function of stellar parameters. Eddington will thus supply the data needed for a complete theory of planetary system formation. In both fields – stellar structure and evolution and exoplanet studies – the European scientific community has a leading role and a tradition of strong expertise. The Eddington mission represents a unique opportunity to bring this lead to full fruition.

Conclusions

Unfortunately, the financial difficulties of the ESA science programme forced its restructuring in the course of 2003, which resulted in the cancellation of Eddington.

6. Missions under Study

6.1 Solar Orbiter

Introduction

The Sun's atmosphere and the heliosphere are uniquely accessible domains of space, where fundamental physical processes common to solar, astrophysical and laboratory plasmas can be studied in detail and under conditions impossible to reproduce on Earth or to study from astronomical distances.

The results from missions such as Helios, Ulysses, Yohkoh, SOHO, TRACE and RHESSI have significantly advanced our understanding of the solar corona, the associated solar wind and the 3-D heliosphere. Further progress is to be expected with the launches of STEREO, Solar-B and the first of NASA's Living With a Star (LWS) missions, the Solar Dynamics Observatory (SDO). Each mission has a specific focus, being part of an overall strategy of coordinated solar and heliospheric research. An important element of this strategy, however, has yet to be implemented. We have reached the point where further *in situ* measurements, now much closer to the Sun, together with high-resolution imaging and spectroscopy from a near-Sun and out-of-ecliptic perspective, promise to bring about major breakthroughs in solar and heliospheric physics. Solar Orbiter will, through a novel orbital design and an advanced suite of instruments, provide the required observations. The unique mission profile of Solar Orbiter will, for the first time, make it possible to:

— explore the uncharted innermost regions of the Solar System;
— study the Sun from close by (45 solar radii, or 0.21 AU);
— swing by the Sun, tuned to its rotation, and examine the solar surface and the space above from a quasi-heliosynchronous vantage point;
— to provide images of the Sun's polar regions from heliographic latitudes up to 38°.

Fig. 6.1.1. Artist's impression of the Solar Orbiter spacecraft near perihelion.

Science goals

Within the framework of the global strategy outlined above, the top-level scientific goals of the Solar Orbiter mission are to:

— determine the properties, dynamics and interactions of plasma, fields and particles in the near-Sun heliosphere;
— investigate the links between the solar surface, corona and inner heliosphere;
— explore, at all latitudes, the energetics, dynamics and fine-scale structure of the Sun's magnetised atmosphere;
— probe the solar dynamo by observing the Sun's high-latitude field, flows and seismic waves.

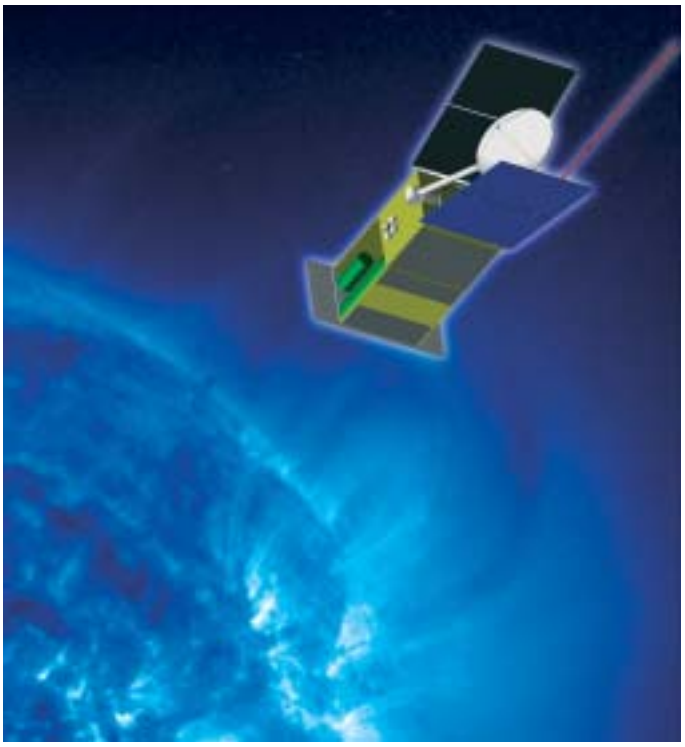

The near-Sun interplanetary measurements together with simultaneous remote-sensing observations of the Sun will permit us to disentangle spatial and temporal variations during the co-rotational phases. They will allow us to understand the characteristics of the solar wind and energetic particles in close linkage with the plasma conditions in their source regions on the Sun. By approaching as close as 45 solar radii, Solar Orbiter will view the solar atmosphere with unprecedented spatial resolution (goal: 35 km pixel size, equivalent to 0.05 arcsec from Earth). Over extended periods, Solar Orbiter will deliver images and data of the polar regions and the side of the Sun not visible from Earth. This latter aspect is a key factor in Solar Orbiter's role as a Solar Sentinel within the framework of the International Living With a Star (ILWS) initiative.

For further information, see http://sci.esa.int/solarorbiter

Status

Solar Orbiter was selected as an ESA Flexi-mission in 2000, and reconfirmed in 2002 to be implemented as a common development with the BepiColombo mission to Mercury. In order to arrive at a detailed definition of the model payload, and to identify necessary payload technology developments, two Solar Orbiter Payload Working Groups (one for *in situ* instruments, and one for remote-sensing instruments) were established in 2002. In 2003, a Solar Orbiter Science Definition Team (SDT) was given the task of reviewing the scientific goals of the mission as presently understood, refining these goals where needed, and prioritising them in order to achieve a well-balanced, and highly focused scientific mission. The SDT was also given the task of defining the sets of measurements needed to achieve the mission's scientific goals, taking into account, where appropriate, the output of the Payload Working Group activity. The principal output of the SDT was the Solar Orbiter Science Requirements Document (Sci-RD), issued in December 2003. Taking into account these science requirements, the SDT defined a baseline model payload that would meet the solar and heliospheric science objectives. This model payload includes the following instrument packages:

— *heliospheric in-situ instruments:* plasma package (solar wind analyser); fields package (radio and plasma wave analyser, magnetometer, coronal sounding); particles package (energetic particle detectors, interplanetary dust detector, neutral particle detector, solar gamma-ray and neutron detector);
— *solar remote sensing instruments:* visible-light imager and magnetograph; EUV full-Sun and high-resolution imager; EUV spectrometer; X-ray spectrometer/telescope; coronagraph.

Following the SDT activities in 2003, Solar Orbiter is now undergoing re-assessment in ESA and industry. Specific activities include:

— Payload Integration Study performed in industry (January-June 2004);
— ESTEC Concurrent Design Facility (CDF) Study, which is an update to the CDF study performed in 1999 (four sessions, March 2004);
— two parallel System-level Assessment Studies performed in industry (April-December 2004).

Solar Orbiter is currently foreseen to be launched no earlier than October 2013.

6.2 Darwin

Introduction

Darwin is an ESA mission aimed at the search for, and the study of, terrestrial exoplanets orbiting nearby (< 25 pc) stars within their Habitable Zone (HZ). The mission objectives make this the most ambitious enterprise in space exploration by any space agency, especially in the technology requirements. The purpose of Darwin is two-fold. Regardless of the eventual success of occultation missions such as COROT and Kepler, Darwin will first have to perform a search for terrestrial planets orbiting nearby stars. This is because, for the occultation method to work, COROT and Kepler will observe distant stars, thereby excluding any of the Darwin target stars. Furthermore, it is physically impossible to detect Earth-size planets in the habitable zone from the ground using radial velocity techniques, because they require a precision of 0.1 m/s, much below the 0.5 m/s fundamental limit set by the acoustic noise induced by p-mode oscillations in Sun-type stars. Darwin will therefore have to find its own Earth-like planets through a survey of a pre-determined list of targets. The second, and most ambitious, objective of the mission is to study all the terrestrial planets that it finds (in our Solar System, different types of rocky worlds in the HZ are Venus, Earth and Mars, plus Mercury outside the HZ), in order to determine their physical parameters – such as orbit, temperature, evolutionary status – and to search for and analyse their atmospheres. Darwin is also designed to identify worlds on which life as we know it could exist, to search for the signature of biological activities and to perform a rough evaluation of its evolutionary status. A successful Darwin mission will therefore have a profound impact on mankind's understanding of itself, the world we live on and our place in the cosmos.

The challenge

The main difficulty in detecting an Earth-size planet orbiting close enough to its star to be in the HZ is the great contrast between star and planet. A G2V Sun-type star outshines its planet by a factor > 10^9 in the visible and ~10^6 in the mid-IR near 10 µm. This is aggravated by the proximity of the planet to its parent star; typically 1 AU corresponds to 0.1 arcsec from a distance of 10 pc. Further, the flux of the planet is intrinsically faint and therefore demands a large collecting area.

The past 8 years have seen the field of exoplanets explode, with the discovery of more than a hundred planets within about 50 pc. All of these are, however, something more akin to Jupiter, and thus several hundred times more massive than Earth. Furthermore, these worlds often have orbits of very high eccentricities when compared to the eight major planets of our system. Lastly, owing to the selection effect, many of these exoplanets orbit very closely (a few 0.01 AU) to their parent stars, leading to the term 'Hot Jupiters'. Nevertheless, some basic facts emerge from the current set of observations: all exoplanets found so far revolve around stars of high metallicity (solar or higher); almost 15% of Sun-type stars surveyed for a sufficient time possess one or more planets; the mass function of exoplanets rises exponentially towards lower masses.

The number of detected systems is the success parameter of the mission. One may argue that detecting *one* other Earth would in itself be a major achievement. However, one of Darwin's goals is to make inferences about the origin of the Solar System, its evolutionary history and future development. This requires detection of a number of planetary systems, at least one per evolutionary stage and ideally many more. The number is currently under intense scrutiny, but a tentative baseline would be to detect and study at least 15 such systems. Assuming a random age distribution, this yields a sampling interval of 300 million years, roughly equivalent to the duration of major geological eras in Earth's history. It is not known what the prevalence, η_E, of small (0.5-2 R_E) rocky bodies orbiting other Sun-like stars is. To date, about 3000 stars have

For further information, see http://sci.esa.int/darwin

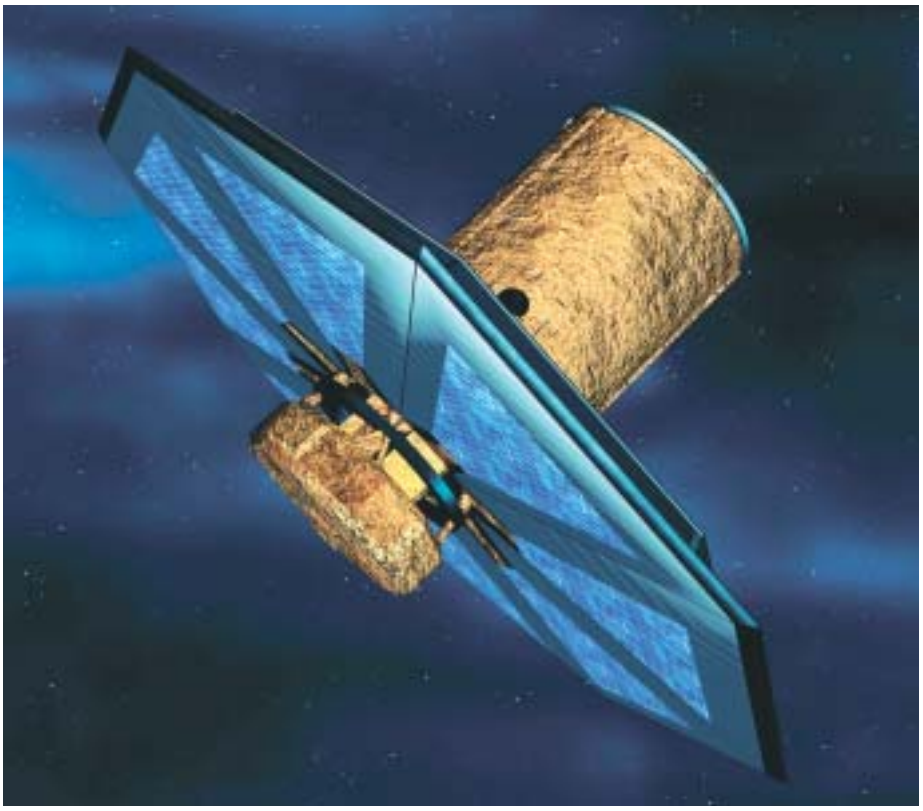

Figure 6.2.1. Artist's impression of one of the individual telescopes in the free-flying Darwin array. The warm electronics and the spacecraft bus are below the passive cooling shield. The solar arrays are also mounted on the sunward side.

been monitored with radial velocity techniques, resulting in the detection of about 120 planets, with masses of between 0.12 M_{Jup} and ~10 M_{Jup} (40-3180 M_E). An Earth-like or rocky planet is expected to have a mass below 10 M_E. Admittedly, the current searches are biased towards large planets and short orbital periods. The latter bias is, however, being remedied as time passes. Nevertheless, despite the fact that several stars have now been under continuous surveillance for more than 10 years, not a single planetary system analogue to ours has been found so far. The prevalence of Earth-like planets thus remains very uncertain but the current best guess puts it at $1 < \eta_E < 10\%$. We therefore need to survey at least 150 stars to be able to detect between 1.5 and 15 planets.

A major goal of the mission is not only to detect terrestrial exoplanets, but also to investigate if the conditions on the planets would allow life as we know it to exist – and possibly to detect its presence. The simultaneous detection of water and molecular oxygen at a temperature of about 300K would be a clear indication of life. This is because oxygen is one of the most reactive substances. If all life on the Earth were removed suddenly, all of the free oxygen in the atmosphere would disappear in the geologically short time of 4 million years. The atmosphere is out of equilibrium, as evidenced by comparison with models or with the other terrestrial planets in the Solar System (Mars and Venus). This disequilibrium is caused by the living things on Earth. Previous to this era, our biosphere was dominated by oxygen-generating species; the atmosphere of the early Earth was out of equilibrium in methane. Other molecules, such as ozone and carbon dioxide, are also good tracers of biological activities.

Technology

There are basically two types of design that would allow the detection of a faint planet close to a star that is at least a million times brighter. The first is visual coronography using a single telescope that must be at least 10 m in diameter. The second solution employs the new technology of nulling interferometry. This was selected as the baseline design for Darwin and an ambitious technology development and verification programme has been initiated.

Nulling interferometry can be described by considering two apertures, separated by a baseline D, pointing at the same star. If the optical path lengths from both apertures are the same, the amplitudes of the light outputs will interfere when they are combined. This is interferometry in the classical sense, producing dark and bright bands known as fringes. If instead the light from one of the telescopes is made to arrive at the site of beam combination with an added phase shift, π, the light along the optical axis will instead interfere destructively (the dark fringes appear 'on top' of the star). At the same time, waves arriving from a small angle θ away will interfere constructively; the separation θ depends on the distance between the two telescopes. So if a star is orbited by a planet at an angle θ away, the light from the star is extinguished and the planetary light is highlighted. The contrast between the star and planet is restricted to light leaks from the 'central null' owing to imperfections in the optics and the jitter of mechanical components. By using more telescopes it is possible to create a more complex transmission pattern. The actual pattern depends on the number of apertures, and the geometrical configuration. The Darwin baseline configuration consists of six telescopes in a hexagonal pattern, with all telescopes equidistant from a seventh spacecraft acting as the central beam combiner. Then the pattern is roughly doughnut-shaped. It is possible to tune the array to each individual star that is observed, such that the transmission ring sits on top of the habitable zone. The signal also needs to be modulated, in order to separate out the desired signal from other sources, such as exozodiacal light, and to discriminate between different combinations of planets in the observed system. This can be performed either by rotating the array of telescopes, switching between different combinations of apertures, or by a combination of both. The latter option is chosen as the baseline for Darwin. The minimum diameter of the array is $D = 40$ m and the maximum is 250 m. A separate eighth spacecraft carries the systems required for metrology, array control and communication. The eight spacecraft orbit around the Sun-Earth L2 Lagrangian point, where there is a favourable thermal environment and low level of background light. To reduce costs, studies are investigating arrays with fewer apertures. Currently, a system consisting of three spacecraft, including a beam combiner collocated with one of the telescopes and excluding the command and control satellite, is showing great promise.

To achieve its goal of investigating the physical parameters (density, pressure, temperature profile, …) and chemical composition of the planetary atmosphere, with a particular emphasis on biomarkers such as water, oxygen, ozone, carbon dioxide and methane, Darwin must operate in the wavelength range 6.5-18 µm and have a spectral resolution of at least 20.

Future

Because of its cost, Darwin will most likely be an international endeavour. Collaboration has begun with NASA's equivalent Terrestrial Planet Finder (TPF). A Letter of Agreement has been signed between ESA and NASA for 2003-2006. The NASA TPF Science Working Group and the ESA Terrestrial Exoplanets Science Advisory Team are mandated to define and agree on a common set of detailed scientific objectives by 2006. These objectives will in turn serve as a basis to define the exact design of the mission in 2007. Darwin itself is projected for a launch not earlier than 2015.

6.3 XEUS

Introduction

The X-ray Evolving Universe Spectroscopy (XEUS) mission is the potential follow-on to XMM-Newton and aims to provide an X-ray capability comparable in sensitivity to the future generation of ground- and space-based observatories such as ALMA and JWST. The goals are to study the evolution of the hot baryons in the Universe and in particular: detect massive black holes in the earliest AGN and estimate their mass, spin and redshift through Fe line and continuum variability studies; study the formation of the first gravitationally-bound, dark matter-dominated, groups of galaxies and trace their evolution into today's massive clusters; study the evolution of metal synthesis to the present epoch using, in particular, observations of hot intra-cluster gas; and characterise the mass, temperature and density of the intergalactic medium, much of which is in a hot filamentary structure, using absorption line spectroscopy of intense background sources.

XEUS is being jointly studied by ESA and ISAS/JAXA. The original intention was to obtain a mirror area of 30 m^2, sufficient to sensitively probe the environment of the massive black holes in AGN at redshifts > 5. Such a large mirror area implies a long focal length of around 50 m, which makes a single spacecraft impractical. Thus, XEUS will need to consist of separate mirror (MSC) and detector spacecraft (DSC) flying in formation and separated by the focal length. If the conventional nickel X-ray optics technology of XMM-Newton were to be used, such a large mirror area could best be achieved by rendezvous and docking of the MSC to the International Space Station (ISS), where robotic assembly will be employed to add the massive mirror segments delivered to the ISS by the Space Shuttle. Significant work has been carried out in industry to confirm the feasibility of this assembly concept; this approach continues to be studied. Its major disadvantages are the complexity and cost of multiple launches, and the rating and qualification of the MSC to visit the ISS.

Spacecraft and science

The XEUS Science Advisory Group has therefore endorsed the study of a revised XEUS programme consisting of two missions. The initial mission is called Perxeus and would be launched around 2015 to be followed, some 10 years later, by Chronos. Both missions aim to achieve the maximum effective telescope area through autonomous deployment, avoiding the complexity of the MSC visiting the ISS. By far the greatest challenge to such a concept is the development of suitable lightweight optics. To address this, a number of optics technology developments are being followed, including lightweight mirror shell technologies and micro-channel plate focusing optics. Rapid progress is being made and angular resolutions in the class 10-20 arcsec FWHM have been achieved in prototype versions. Continued development will ensure that a mirror area of 10 m^2 with a spatial resolution of 2 arcsec HEW (goal) and 5 arcsec HEW (specification) for Perxeus can be met with a single Soyuz-Fregat 2B launch to the L2 Earth-Sun Lagrangian point, and autonomous deployment. In this concept, the JAXA-provided DSC will be launched separately and rendezvous with the MSC once at L2. In the original concept, the lifetime of the DSC was limited by propellant usage because it had to track the MSC 50 m away and so was always in a non-Keplerian orbit. At L2, this is no longer a major issue, resulting in the possibility of a much longer lifetime as well as higher operational efficiency. The Chronos mission concept is similar to that of Perxeus, but uses the more capable Ariane-5 launcher to place the MSC at L2. The interval between the two missions is needed to develop the mirror technology further to provide the 0.5 arcsec HEW (goal) and 1 arcsec HEW (specification) optics needed to match the proposed 60 m^2 mirror area.

The proposed Perxeus focal plane configuration has an Advanced Pixel Sensor at

For further information, see http://sci.esa.int/xeus/

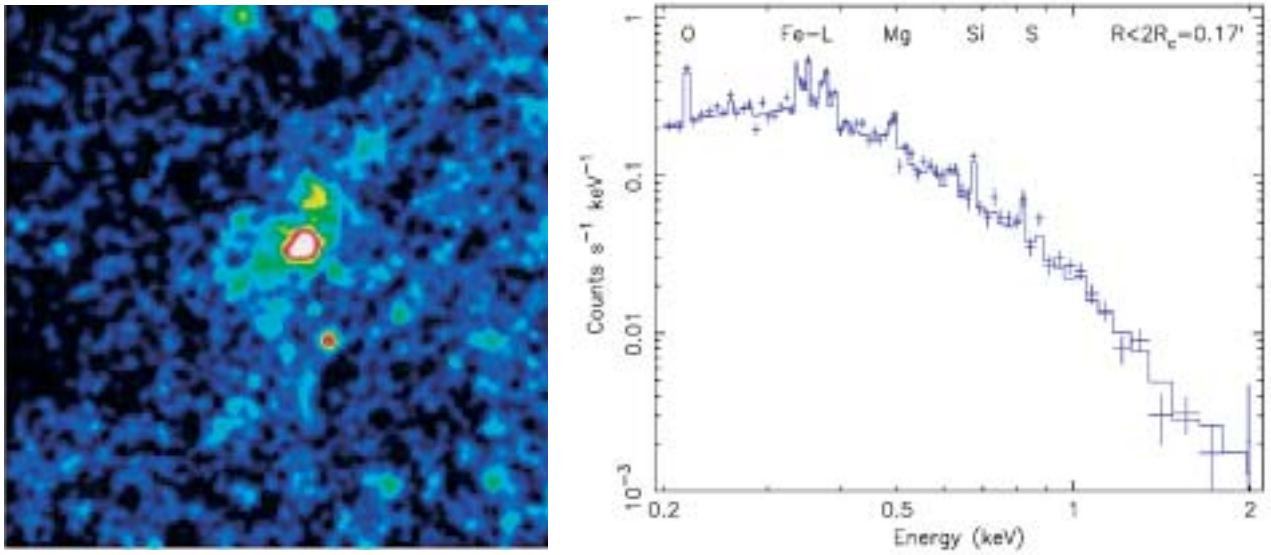

Figure 6.3.1. Simulated Perxeus image of a Hickson group of galaxies with a luminosity of 10^{32} erg s^{-1} at $z = 2$ (left). Right: the simulated spectrum of the same group.

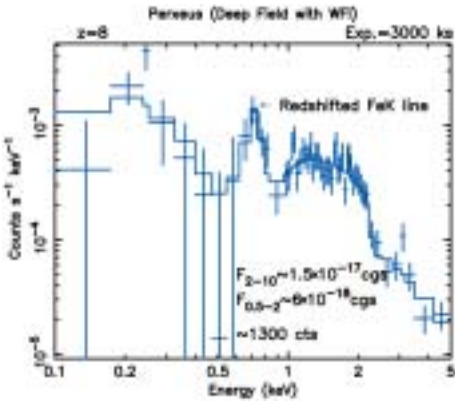

Figure 6.3.2. Perxeus simulation of a $2x10^{42}$ erg s^{-1} (0.1-2.0 keV) object with a composite absorbed AGN and starburst spectrum. The simulation is for an object at $z = 8$ observed for 3000 ks.

the centre of a larger, more conventional, CCD array with a hard X-ray detector mounted under the CCDs. Additionally, four small high-countrate diodes would be positioned around the outer edge of the conventional CCDs. All these instruments could be operated in parallel to provide a FOV of 15 arcmin diameter. Alternatively, one of two small-FOV (0.5 arcmin diameter) cryogenic detectors could be placed in the focal plane for high spectral resolution studies.

To illustrate the potential of Perxeus to study the formation of large-scale structures, Fig. 6.3.1 shows a simulation of a distant ($z = 2$) galaxy group. In standard cosmological models, these groups are the first emerging massive objects, with masses of ~10^{13} solar masses. The epoch of their first formation depends critically on the adopted cosmology and is likely to be $z \sim 2$-5. Therefore, the study of groups will provide a powerful probe of the early Universe. These systems and their dark matter haloes are the smallest units by which to study the hot thermal intergalactic gas trapped in the deep, dark matter-dominated, gravitational wells. In the simulation, emission lines of O, Fe, Mg and Si are clearly evident. The temperature can be determined to better than ±3%, and the Fe and O abundances to better than 10% and 20%, respectively.

Spectroscopy is at the heart of XEUS; a key capability is to distinguish between different spectral components in distant active galaxies. As an example, an object with a composite spectrum consisting of a highly absorbed AGN and a starburst component was simulated. The starburst emission was assumed to be a thermal gas with a temperature of 3 keV and an abundance of 0.3 M_{Sun}. The absorbed AGN is assumed to show up with a strong (equivalent width of 1 keV) Fe line due to transmission through a 10^{24} atom cm^{-2} column of absorbing material. Such a model is comparable to the emission seen from galaxies such as NGC 6240, NFC 4945 and Mkn 3. Fig. 6.3.2 shows the simulated Perxeus spectrum when the object is placed at $z = 8$ and observed in a very deep exposure (3000 ks) to obtain a spectrum with ~1300 counts. The redshifted Fe line is clearly detected and the AGN and starburst components are well separated. Such X-ray spectra would be the most direct way of finding evidence for the existence of dust-enshrouded AGN at such large redshifts – if they exist.

6.4 Hyper

Introduction

Atomic quantum sensors are a major breakthrough in the technology of time and frequency standards, as well as ultra-precise sensing and monitoring of accelerations and rotations. They apply a new kind of optics based on matter waves. Today, atomic clocks are the standard for time and frequency measurement at the highest precisions. Inertial and rotational sensors using atom interferometers have a similar potential for replacing state-of-the-art sensors in other fields. Hyper ('hyper-precision cold atom interferometry in space') is designed to realise two different types of sensors based on atom interferometers, each optimised for a specific scientific objective: a Mach-Zehnder interferometer to measure rotations and accelerations, and a Ramsey-Bordé interferometer to measure frequencies.

In a Mach-Zehnder interferometer slowly drifting atoms are coherently split, redirected and recombined such that the atomic trajectories enclose a surface as large as possible. Beam splitting is achieved by atom-light interaction. During each interaction sequence, the atoms cross two counter-propagating laser beams. An atom absorbs a photon out of one laser beam and is stimulated by the other laser beam to re-emit the photon. In this way, twice the recoil of a photon is transferred coherently to the atomic wave (rather than atoms), such that the atomic wave is either equally split, deflected or recombined. The Mach-Zehnder interferometer senses both rotations and accelerations in only one particular direction. Two interferometers with counter-propagating atoms are required in order to discriminate between both kinds of motion. This combination of two interferometers is called an Atomic Sagnac Unit (ASU).

In the Ramsey-Bordé interferometer, atoms at rest are split by a temporal sequence of four laser pulses retro-reflected on one mirror such that two atom interferometers are formed. The frequency sensitivity is due to the asymmetry of the beam splitting. The part of the matter wave that is split off is excited and experiences the recoil shift, while the other part of the matter wave remains unaffected. In the two interferometers, the frequency shifts have opposite signs because the roles of the ground and excited states are reversed.

Scientific objectives

The primary scientific objectives of the Hyper mission are:

— to test General Relativity by mapping for the first time the spatial (latitudinal) structure (magnitude and sign) of the gravitomagnetic (frame-dragging or Lense-Thirring) effect of the Earth with about 10% precision;
— to determine independently from Quantum Electrodynamics (QED) theories the fine structure constant α by measuring the ratio of Planck's constant to the atomic mass one to two orders of magnitude more precise than present knowledge.

As a secondary objective, Hyper will investigate matter-wave decoherence to set an upper bound for quantum gravity models.

Atom interferometry also allows a test of the Equivalence Principle (EP) with quantum particles by comparing the free fall of two distinct atomic species (rubidium and caesium). This measurement complements the Microscope mission, which will investigate the free fall of macroscopic objects. Hyper's atom interferometer should reach an accuracy of about one part in 10^{16}. The mass and power constraints imposed by the satellite make it difficult to pursue both the measurement of the Lense-Thirring effect and test of the EP. Testing the EP is therefore considered as an alternative objective.

Hyper carries four cold-atom interferometers that can operate in the Mach-Zehnder

For further information, see http://sci.esa.int/hyper

or Ramsey-Bordé modes. For the measurement of the gravitomagnetic effect of the Earth, the four atom interferometers are used in the Mach-Zehnder mode. For the measurement of the fine structure constant, they are used in the Ramsey-Bordé mode. In space, the drift velocity of the atoms can be reduced to 20 cm/s, which gives 3 s of drift time in a 60 cm enclosure. The temperature of the atoms is 1µK, corresponding to a thermal velocity of ~1 cm/s.

Payload and spacecraft

The Payload Module, with a mass of 240 kg and 200 W power consumption, consists essentially of:

Optical Bench, carrying the optical elements for coherent atom manipulation; high-precision star tracker (200 mm-diameter Cassegrain telescope, pointing accuracy 6 x 10^{-9} rad at 1 Hz readout frequency); two drag-free proof masses.

Atom Preparation Bench, carrying the four atom interferometers based on caesium or rubidium, accommodated in two magnetically shielded vacuum chambers; optics for atom preparation and detection.

Laser Bench, carrying the laser for atom interferometry, preparation (e.g. trapping, cooling) and detection of the atoms; high-precision microwave synthesiser for the hyperfine transitions of caesium or rubidium.

The Payload Module, a cylinder of 0.9 m diameter and 1.3 m height, is accommodated in the centre of the box-shaped Service Module. Together, they are the spacecraft, which has a launch mass of 767 kg. Hyper will be launched by a Rockot from Plesetsk Cosmodrome into a 700 km circular Sun-synchronous orbit. Drag-free performance to a level of 10^{-9} m s^{-2} at 0.3-3 Hz is achieved by a drag-free control system, comprising two drag-free proof masses and their capacitive sensors and 16 proportional Field Emission Electric Propulsion (FEEP) thrusters mounted externally, each with a thrust authority of 150 µN. Nominal mission lifetime is 2 years.

Status

Hyper was proposed in January 2000, in response to ESA's Call for Mission Proposals for the second and third Flexi-missions (F2/F3). It was selected for a study at assessment level, which was carried out March-July 2000 by the Concurrent Design Facility (CDF) Team at ESTEC. In its evaluation of the Hyper study, the Fundamental Physics Advisory Group (FPAG) in September 2000 concluded that 'Hyper is a mission in a completely new field of space science and has, therefore, not quite reached the technical maturity of other extensively studied projects. Also, the field of cold atoms and matter-wave interferometry is developing rapidly and thus the FPAG recommended not to select Hyper for a flight mission at this time (as one of the F2/F3 missions) but to continue studies of the Hyper mission and to initiate technology development in areas relevant for Hyper'. This recommendation is being implemented by ESA. An industrial study at Phase-A level was carried out from June 2002 to March 2003, a proposal for payload technology development (four topics) was submitted to ESA in 2003 for inclusion in the TRP in the 2004-2006 timeframe and, furthermore, a mission in the field of cold-atom interferometry is a candidate for a Technology Reference Mission (TRM). However, given the budget limitations of ESA's science programme and the long list of missions awaiting approval, it is clear that a mission in the field of cold-atom interferometry can be realised only after 2015.

6.5 EUSO-ISS

Introduction

The Earth is continuously bombarded by high-energy cosmic rays. While cosmic rays with energies up to 10^{15} eV almost certainly originate from Galactic objects, such as the expanding shocks of exploded stars, understanding the origin of the highest energy cosmic rays with energies above 5 x 10^{19} eV is one of the great challenges in astrophysics. Although these extreme energy cosmic rays (EECRs), believed to be probably mostly protons, are very rare (only around 1/km^2 per century!) they are the most energetic particles known in the Universe, with energies 10^8 greater than produced in the most powerful particle accelerators on Earth. Only a few dozen such events have been detected using different ground-based air shower detectors in the past 30 years. There has been no convincing identification of any of these events with a likely astronomical source.

Scientific goals

At such extreme energies, cosmic ray protons interact with the cosmic microwave background that permeates space, and the distance that an EECR can travel is limited to our galactic neighbourhood (< 50 Mpc). Intriguingly, known astronomical objects that could conceivably produce EECRs, such as massive black holes, colliding galaxies and gamma-ray bursts are much further away than this. This has led to the idea that the decay of topological defects or other massive relics of the Big Bang may instead produce EECRs – unless generally accepted laws of physics, such as the invariance of Lorentz transformations, do not apply in this energy domain. If this is indeed the case, then it implies the existence of 'new physics'. These paradoxes are at the heart of the ambitious EUSO (Extreme Universe Space Observatory) mission to study EECRs from space by using the Earth's atmosphere as a giant cosmic ray detector. EUSO will observe the flash of fluorescence UV light when an EECR interacts with the atmosphere and the Cerenkov light reflects from clouds or the Earth's surface. Direct imaging of the light track and its intensity variations will allow the sky position of the event, as well as the overall energy, to be reconstructed. EUSO will take advantage of the continuous nadir pointing provided by the lowest locations of the Columbus module on the International Space Station (ISS) to observe the Earth's atmosphere with a 60° field of view. EUSO will detect several thousand EECR events, allowing a sensitive search for the objects producing them.

Protons are not the only type of extreme-energy particle that will be observed by EUSO. Many models for the production of EECRs indicate that large numbers of neutrinos should also be produced. Since neutrinos propagate, on average, much deeper into the atmosphere than protons before interacting, EUSO will be able to distinguish between the two types of particles by selecting an interaction depth. This would open up the new field of high-energy neutrino astronomy. Since most sources of EECRs are expected to be transparent to their own neutrinos, these particles would allow observations deep inside sources to view the particle acceleration mechanism directly.

Status

EUSO is close to completing an ESA Phase-A study, jointly funded by the Directorates of Human Spaceflight and Science. The EUSO Principle Investigator, Prof. L. Scarsi from IASF-CNR, Palermo (I), is leading a large consortium of scientists from Europe, the US and Japan. EUSO will consist of a UV telescope with a large collecting area and FOV using a lightweight double Fresnel lens optics system (provided by the EUSO group at NASA Marshall Space Flight Center), a highly segmented focal surface detector array, an atmospheric sounding device and a sophisticated onboard image processing (Fig. 6.5.1). The image processing will

For further information, see http://www.euso-mission.org/

Figure 6.5.1. The baseline EUSO in-orbit accommodation on the ISS. ESA's Columbus module is the cylindrical structure on the right to which are attached four payload platforms. EUSO is attached to the lower-right starboard panel. The two Fresnel lenses are separated from the focal plane detectors by the tubular structure. The steerable lidar is mounted on the lower side of EUSO, towards Columbus.

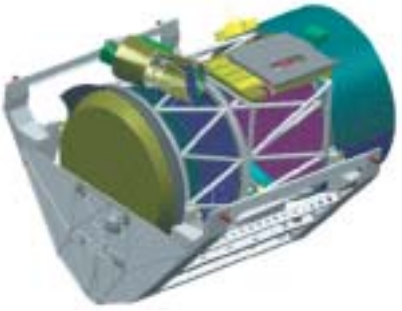

Figure 6.5.2. A launch and transportation option being considered for EUSO for around 2009 is a dedicated cradle inserted into the cargo bay of the Space Shuttle.

provide a sensitive discrimination between EECRs and other forms of UV radiation such as lightening, meteoroids, aurorae and man-made illumination. Atmospheric sounding using a single wavelength lidar is necessary to measure the effects of cloud cover, aerosols and the like on the fluorescent and Cerenkov EECR signals. The estimated payload mass of 1.8 t provides a major challenge for its accommodation and transportation to the ISS. As well as the baseline location on ESA's Columbus External Payload Facility on the ISS, other options for accommodating EUSO, such as on the main truss, are being considered.

6.6 Lobster-ISS

Introduction

The X-ray sky is highly variable and unpredictable. A new X-ray source may suddenly appear, out-shine its contemporaries and then disappear a few days later. Sometimes a well known source will behave in a new and unexpected way. A highly sensitive X-ray mission such as ESA's XMM-Newton observes only a small region of sky at any one time and could easily miss such unpredictable events. An all-sky X-ray monitor (ASM), such as Lobster-ISS, can alert astronomers to important events occurring anywhere in the sky, allowing other facilities to be rapidly repointed to take advantage of new opportunities. The importance of this capability was recognised as early as the 1960's, and the sensitivity of ASMs has steadily improved since then. Currently, astronomers benefit from the ASM on NASA's Rossi X-ray Timing Explorer (RXTE). This will be followed in 2005 by the Japanese MAXI ASM on the International Space Station (ISS). MAXI will be around 10 times more sensitive than RXTE's ASM. ESA is proposing to fly Lobster-ISS, an even more sensitive (by another factor of 10) ASM on the ISS in around 2010. As well as acting as an alert facility, this dramatic increase in sensitivity will open up many new areas of science that cannot be addressed by the previous generation of ASMs.

Scientific goals

The Lobster-ISS Principle Investigator is Prof. G. Fraser from the University of Leicester (UK), with co-investigators from the Los Alamos National Laboratory (USA), NASA Goddard Space Flight Center, Institute of Astronomy Cambridge (UK), Univ. Southampton (UK), Univ. Melbourne (Australia), Univ. Helsinki (FIN), IASF Bologna (I), Univ. Ferrara (I) and SRON, Utrecht (NL). Lobster-ISS will use a novel form of micro-channel plate X-ray optics developed under the ESA Technology Research Programme to provide this unprecedented sensitivity. It will be the first true imaging X-ray ASM monitor and will be able to locate X-ray sources to within 1 arcmin to allow the rapid identification of new transient sources. Lobster-ISS will produce a catalogue of 200 000 X-ray sources every 2 months which will be rapidly made available via the Internet. The high sensitivity will allow many topics to be studied, including the long-term variability of AGN and stars, X-ray bursts and super-bursts, super-soft sources, black holes in X-ray binaries, and the highly topical X-ray afterglows of gamma-ray bursts and X-ray flashes. The advantage of this type of optics for an X-ray ASM is its extremely large simultaneous field of view. This is achieved by accurately bending the thousands of tiny glass pores that make up each micro-channel plate by exactly the right amount, in order to focus incident X-rays like in a telescope. This explains where the name comes from, since this is similar to how the eye of a crustacean works.

The scientific instrumentation consists of six individual telescope modules, pointing in different directions, and a gamma-ray burst monitor. The optimum location for Lobster-ISS is on the zenith platform of the External Payload Facility (EPF) of ESA's Columbus module. Unlike a conventional satellite, the ISS keeps its main axis parallel to the local horizon. This is a great advantage for an ASM because it means that the 162 x 22.5° FOV will automatically scan most of the sky during each ISS revolution. The ESA Phase-A study is nearing completion and is demonstrating that Lobster-ISS is well suited to being an external payload on the EPF.

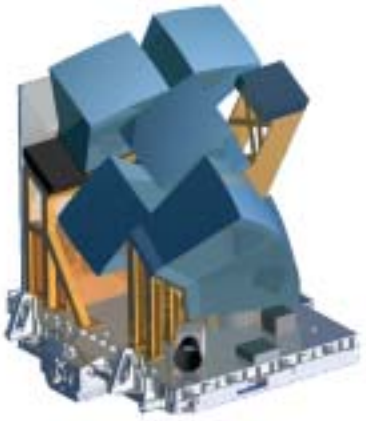

Figure 6.6.1. The 1 m³ Lobster-ISS consists of six individual telescope modules pointing in different directions, gamma-ray burst detector, star tracker, particle monitor and associated structure, radiator and electronics. It is mounted on a standard adapter plate that attaches directly to the Columbus External Payload Facility.

For further information, see http://www.src.le.ac.uk/lobster/

6.7 ROSITA

Introduction

The ROSITA (ROentgen Survey with an Imaging Telescope Array) mission is being studied jointly by ESA's Directorates of Science and Human Spaceflight. The goal is to perform an all-sky medium-energy X-ray survey by placing an array of sensitive X-ray telescopes on the Exposed Payload Facility of ESA's Columbus module on the International Space Station (ISS). ROSITA continues the pioneering work performed by European scientists on X-ray surveys using the German/US/UK Rosat observatory, which produced the first all-sky imaging survey. Technology limitations of the time meant that Rosat was sensitive only below 3 keV, where the effects of source and interstellar obscuration are strongest in the X-ray band.

The ROSITA Principal Investigator is Dr. Prof. G. Hasinger, who leads a team of scientists from the Max-Planck-Institut für extraterrestrische Physik (MPE), Garching (D), the Astrophysikalisches Institut Potsdam (D), and the Institut für Astronomie und Astrophysik der Universität Tübingen (D). The proposed survey will have 100 times the sensitivity and 100 times the angular resolution of the previous medium-energy (2-10 keV) survey, which was performed in the 1970s by the non-imaging HEAO-A2. In addition, the ROSITA survey will be more sensitive and have a substantially better energy and angular resolution than the Rosat all-sky survey.

Scientific goals

A survey in the hard X-ray band was defined as one of the future priorities in the last 'Decadal Survey' of the US National Academy of Sciences. This was also the goal of the Abrixas satellite, which unfortunately failed in 1999 owing to a design error in its power system. During the planned 3-year lifetime, ROSITA will detect about 50 000 sources above 2 keV. These will be mainly AGN, half of which will be completely unknown because they are too absorbed to be seen in the earlier Rosat survey. For the others, new data in the hard band will be collected. The sources will be located with an accuracy of better than 20 arcsec and their temporal behaviour will be measured

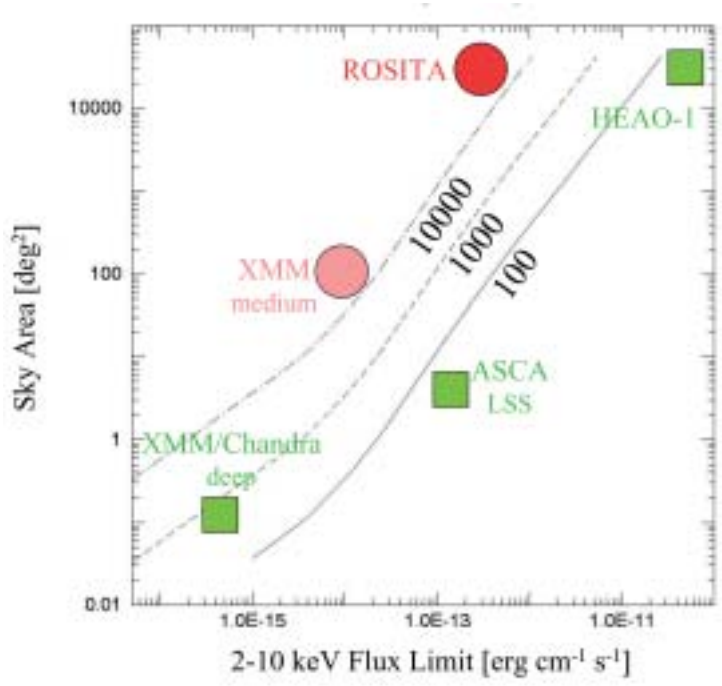

Figure 6.7.1. Existing (green) and planned (red) surveys in the hard X-rays. The lines give the number of expected sources in the total survey.

on a variety of time scales. ROSITA is expected to find several 10 000 clusters of galaxies and to obtain data about the nature of the cosmic X-ray background. X-ray and optical observations of such a large sample of clusters of galaxies will allow the nature of dark matter to be sensitively probed. This is because the X-ray cluster emission is dominated by hot gas trapped in the deep, dark matter-dominated, gravitational field. ROSITA will also contribute to galactic science because it will detect the hard emission from stellar coronae, stellar flares and embedded protostars, and will determine long-term light curves and perform spectro-photometry of many galactic X-ray binaries

The telescope employs copies of the seven 27-fold nested Wolter-1 mirrors flown on Abrixas and a novel detector system being developed by MPE based on the successful XMM-Newton pn-CCD technology, a potential prototype for the future ESA mission XEUS. Major improvements for the new camera include a higher time resolution and significantly reduced ghost images. Following an internal ESA study that confirmed the overall feasibility of accommodating the payload on the ISS, ROSITA has been approved for a Phase-A study, which is expected to start during 2004.

Acronyms

AAT	Anglo-Australian Telescope
ACE	Atmospheric Composition Explorer
ACR	Anomalous Cosmic Rays
ACS	Advanced Camera for Surveys (HST)
ADS	Astrophysics Data System (NASA)
AFM	Atomic Force Microscope
AGB	Asymptotic Giant Branch
AGN	Active Galactic Nuclei
AGU	American Geophysical Union
AIV	Assembly, Integration & Verification
ALICE	Rosetta Orbiter UV imaging spectrometer
ALMA	Atacama Large Millimetre Array
AMIE	Asteroid Moon micro-Imager Experiment (SMART-1)
AO	Announcement of Opportunity
APXS	Alpha-Proton-X-ray Spectrometer (Rosetta)
ASI	Italian Space Agency
ASIC	Application Specific Integrated Circuit
ASM	All-Sky Monitor
ASPOC	Active Spacecraft Potential Control (Cluster)
ASU	Atomic Sagnac Unit
AU	Astronomical Unit
AVM	Avionics Model
c	speed of light
CAA	Cluster Active Archive
CADC	Canadian Astronomical Data Centre
CBRF	Cosmic Background Radiation Field
CCD	Charge Coupled Device
CDF	common data format
CDF	Chandra Deep Field; Concurrent Design Facility (ESTEC)
CDMS	Cluster Data Management System
CDR	critical design review
CDS	Coronal Diagnostics Spectrometer (SOHO)
CDS	Command & Data Subsystem
CDS	Centre de Données astronomiques de Strasbourg
CdTe	cadmium telluride
CELIAS	Charge, Element and Isotope Analysis System (SOHO)
CEPHAG	Centre d'Etude des Phenomenes Aleatoires et Geophysiques (France)
CERN	Centre Européen de Recherches Nucléaires (France)
CESR	Centre d'Etude Spatial des Rayonnements (France)
CFHT	Canadian-French-Hawaiian Telescope
CGRO	Compton Gamma Ray Observatory (NASA)
CIR	Corotating Interaction Region
CIS	Cluster Ion Spectrometry
CIVA	Comet Infrared and Visible Analyser (Rosetta)
CMB	Cosmic Microwave Background
CMD	colour magnitude diagram
CME	Coronal Mass Ejection
CMOS	Complementary Metal Oxide Semiconductor
CNES	Centre National d'Etudes Spatiales
CNR	Consiglio Nazionale della Ricercha (Italy)
CNRS	Centre National de la Recherche Scientifique (France)
CNSA	China National Space Administration
Co-I	Co-Investigator
COBE	Cosmic Background Explorer (NASA)
COMPTEL	Compton Telescope (CGRO)
CONSERT	Comet Nucleus Sounding Experiment by Radiowave Transmission (Rosetta)
COPUOS	Committee for the Peaceful Use of Outer Space (United Nations)
COROT	COnvection, ROtation and planetary Transits
COS	Cosmic Origins Spectrograph (HST)
COSAC	Comet Sampling and Composition Experiment (Rosetta)
COSIMA	Cometary Secondary Ion Mass Analyser (Rosetta)
COSPAR	Committee on Space Research
COSPIN	Cosmic Ray & Solar Charged Particles Investigation (Ulysses)
COSTEP	Comprehensive Measurements of the Supra-Thermal and Energetic Particles Populations (SOHO)
CP	Charge Parity
CPM	Chemical propulsion Module (BepiColombo)
CQM	Cryogenic Qualification Model
CR	Carrington Rotation
CSA	Canadian Space Agency
CSDS	Cluster Science Data System
CsI	caesium iodide
CSSAR	Centre for Space Science and Applied Research (China)
CTIO	Cerro Tololo Inter-American Observatory
CTP	Core Technology Programme
D-CIXS	Demonstration of a Compact Imaging X-ray Spectrometer (SMART-1)
DESPA	Observatoire de Paris, Département Spatial
DISR	Descent Imager/Spectral Radiometer (Huygens)
DLR	Deutsches Zentrum für Luft- und Raumfahrt
DPC	Data Processing Centre
DROID	distributed readout architecture
DRS	Disturbance Reduction System (LISA)
DSDS	Double Star Data System
DSN	Deep Space Network
DSP	Double Star Programme
DSP	Digital Signal Processor
DSRI	Danish Space Research Institute

EAS	European Astronomical Society
ECF	European Coordinating Facility
EECR	extreme energy cosmic ray
EFW	Electric Field and Wave experiment (Cluster)
EGS	European Geophysical Society
EIT	Extreme UV Imaging Telescope (SOHO)
EQM	Electrical Qualification Model
EM	Electrical Model, Engineering Model
EOF	Experiment Operations Facility (SOHO)
EP	Equivalence Principle
EPAC	energetic particle instrument (Ulysses)
EPDP	Electric Propulsion Diagnostic Package (SMART-1)
EPF	External Payload Facility (Columbus)
EPIC	European Photon Imaging Camera (XMM)
EPOS	European Payload Operation Services (Double Star)
EPS	European Physical Society
ERNE	Energetic and Relativistic Nuclei and Electron experiment (SOHO)
ERO	Early Release Observation
ESA	European Space Agency
ESLAB	European Space Laboratory (former name of RSSD)
ESO	European Southern Observatory
ESOC	European Space Operations Centre, Darmstadt (Germany)
ESRIN	ESA's Documentation and Information Centre (Italy)
ESRO	European Space Research Organisation
ESTEC	European Space Research and Technology Centre, Noordwijk (The Netherlands)
EUSO	Extreme Universe Space Observatory
EUV	Extreme Ultra-Violet
Exosat	European X-ray Observatory Satellite (ESA)
FEEP	Field Emission Electric Propulsion
FES	Fine Error Sensor
FGS	Fine Guidance Sensor
FIRST	Far Infrared and Submillimetre Space Telescope (now Herschel)
FM	Flight Model
FMI	Finnish Meteorological Institute
FOC	Faint Object Camera (HST)
FOS	Faint Object Spectrograph (HST)
FOV	Field of View
FP	Fabry-Pérot
FPA	Focal Plane Assembly
FPAG	Fundamental Physics Advisory Group
FTE	flux transfer event
FTS	Fourier Transform Spectrometer
FUV	far-ultraviolet
FWHM	Full Width at Half Maximum
GaAs	gallium arsenide
GC	Galactic Centre
GEMS	Galaxy Evolution from Morphologies and SEDS
GI	Guest Investigator
GIADA	Grain Impact Analyser and Dust Accumulator (Rosetta)
GMT	Greenwich Mean Time
GOODS	Great Observatories Origins Deep Survey
GONG	Global Oscillation Network Group
GR	General Relativity
GRB	Gamma Ray Burst
GSE	Ground Support Equipment
GSFC	Goddard Space Flight Center (NASA)
GSPC	Gas Scintillation Proportional Counter
GSTP	General Support & Technology Programme (ESA)
GTO	Geostationary Transfer Orbit
HASI	Huygens Atmospheric Structure Instrument
HCS	Heliospheric Current Sheet
HDF	Hubble Deep Field
HEB	Hot Electron Bolometer
HEMT	High Electron Mobility Transistor
HEW	Half Energy Width
HFI	High Frequency Instrument (Planck)
HGA	High-Gain Antenna
HIFI	Heterodyne Instrument for the Far-IR (Herschel)
HPGSPC	High Pressure Gas Scintillation Proportional Counter (BeppoSAX)
HPOC	Huygens Probe Operations Centre
HR	Hertzsprung-Russell
HRTS	High Resolution Telescope and Spectrograph
HSC	Herschel Science Centre
HST	Hubble Space Telescope
HUDF	Hubble Ultra Deep Field
HZ	Habitable Zone
IAC	Instituto de Astrofisica de Canarias
IACG	Inter-Agency Consultative Group for Space Science
IAS	Institut d'Astrophysique Spatiale, Orsay (France)
IAS	Istituto di Astrofisica Spaziale (Rome)
IASTP	Inter-Agency Solar-Terrestrial Physics
IAU	International Astronomical Union
IBIS	Integral imager
ICC	Instrument Control Centre (Herschel)
IDA	ISO Data Archive
IDC	ISO Data Centre
IDS	Interdisciplinary Scientist
IDT	Instrument Dedicated Team
IFSI	Istituto Fisica Spazio Interplanetario (Italy)
IFTS	Imaging Fourier Transform Spectrometer
IGPP	Institute of Geophysics & Planetary Physics

ILEWG	International Lunar Exploration Working Group
ILWS	International Living With a Star
IMEWG	International Mars Exploration Working Group
IMF	Initial Mass Function
IMF	Interplanetary Magnetic Field
INT	Isaac Newton Telescope
INTA	Instituto Nacional de Técnica Aerospacial (Spain)
IOA	Institute of Astronomy (Cambridge, UK)
IPAC	Infrared Processing Analysis Centre
IR	Infrared
IRAS	Infrared Astronomy Satellite
IRF-U	Institute for Space Physics-Uppsala (Sweden)
ISAAC	Infrared Spectrometer and Array Camera
ISAS	Institute of Space and Astronautical Science (Japan)
ISDC	Integral Science Data Centre
ISGRI	Integral Soft Gamma Ray Imager
ISL	Instrument Sonde de Langmuir
ISM	Interstellar Medium
ISO	Infrared Space Observatory (ESA)
ISOC	Integral Science Operations Centre
ISS	International Space Station
ISSI	International Space Science Institute, Bern (Switzerland)
ISTP	International Solar-Terrestrial Physics
ITT	Invitation to Tender
IUE	International Ultraviolet Explorer
IUPAP	International Union of Pure and Applied Physics
IUS	Inertial Upper Stage
JAXA	Japan Aerospace Exploration Agency
JCMT	James Clark Maxwell Telescope
JEM-X	Integral X-ray monitor
JPL	Jet Propulsion Laboratory (NASA)
JSOC	Joint Science Operation Centre (Cluster)
JWST	James Webb Space Telescope; previously Next Generation Space Telescope
KATE	X/Ka-band Telemetry & Telecommand Experiment (SMART-1)
KBO	Kuiper Belt Object
KPNO	Kitt Peak National Observatory (USA)
KSC	Kennedy Space Center (NASA)
LAEFF	Laboratory for Space Astrophysics and Fundamental Physics
LAP	Langmuir Probe (Rosetta)
LAPP	Laboratoire d'Annecy-Le-Vieux de Physique des Particules (CNRS, France)
LASCO	Large Angle Spectroscopic Coronagraph (SOHO)
LASP	Laboratory for Astronomy and Solar Physics (NASA)
LET	Low Energy Telescope (Ulysses)
LFCTR	Laboratorio di Fisica Cosmica e Techologie Relative del CNR (Italy)
LFI	Low Frequency Instrument (Planck)
LIM	local interstellar medium
LISA	Laser Interferometer Space Antenna
LMC	Large Magellanic Cloud
LOI	Luminosity Oscillation Imager (SOHO)
LOWL	Ground-based instrument for observing solar low *p*-modes, High Altitude Observatory, USA
LPCE	Laboratoire de Physique et Chemie, de l'Environnement (France)
LPSP	Laboratoire de Physique Stellaire et Planétaire (France)
LTP	LISA Technology Package
LWS	Long Wavelength Spectrometer (ISO); Living With a Star
MBH	massive black hole
MCP	Microchannel Plate
MDI	Michelson Doppler Imager (SOHO)
MEWG	Mercury Exploration Working Group
Microscope	MICROSatellite à traînée Compensée pour l'Observaton du Principe d'Equivalence (CNES)
MIDAS	Micro-Imaging Dust Analysing System (Rosetta)
MIP	Mutual Impedance Probe (Rosetta)
MIRO	Microwave Instrument for the Rosetta Orbiter (Rosetta)
MMO	Mercury Magnetospheric Orbiter (BepiColombo)
MOC	Mission Operations Centre
MOS-CCD	Metal Oxide Semiconductor - Charge Coupled Device
MoU	Memorandum of Understanding
MPAE	Max-Planck-Institut für Aeronomie
MPE	Max-Planck-Institut für Extraterrestrische Physik
MPI	Max-Planck Institut (Germany)
MPIA	MPI für Astronomie
MPIK	Max-Planck-Institut für Kernphysik
MPO	Mercury Planetary Orbiter (BepiColombo)
MSE	Mercury Surface Element (BepiColombo)
MSP	Master Science Plan
MSSL	Mullard Space Science Laboratory (UK)
MTR	mid-term review
MUPUS	Multi-Purpose Sensors for Surface and Subsurface Science (Rosetta)
MUSICOS	Multi-Site Continuous Spectroscopy
NAC	Narrow Angle Camera (OSIRIS)
NASA	National Aeronautics & Space Administration (USA)
NFI	Narrow Field Instrument (BeppoSAX)

NGST	Next Generation Space Telescope; now James Webb Space Telescope
NHSC	NASA Herschel Science Centre
NICMOS	Near-Infrared Camera and Multi-Object Spectrometer (HST)
NIS	normal incidence spectrometer
NLR	Narrow Line Region
NOT	Nordic Optical Telescope
NRAO	National Radio Astronomy Observatory (USA)
NSSDC	National Space Science Data Center (at GSFC, USA)
NTT	New Technology Telescope
NVSS	NRAO/VLA Sky Survey
OHP	Observatoire de Haute-Provence
OLP	off-line processing
OM	Optical Monitor (XMM-Newton)
OMC	Optical Monitor Camera (Integral)
OSSE	Oriented Scintillation Spectrometer Experiment (CGRO, NASA)
OSIRIS	Optical and Spectroscopic Remote Imaging System (Rosetta)
PACS	Photodetector Array Camera and Spectrometer (Herschel)
PAH	Polycyclic Aromatic Hydrocarbon
PAM	Payload Assist Module
pc	parsec
PCA	Proportional Counter Array
PCD	Photon Counting Detector
PDP	Project Data Base
PDR	preliminary design review
PDS	Planetary Data System
PEN	penetrator
PI	Principal Investigator
PIA	(ISO)PHOT Interactive Analysis
PLM	Payload Module
PN	Planetary Nebula
POS	Payload Operations Service
PP	Permittivity Probe (SESAME on Rosetta)
PPDB	Primary Parameter Data Base (Cluster)
ppm	parts per million
PPN	Parameterised Post-Newtonian
PROM	Programmable Read-Only Memory
PS	Project Scientist
PSE	Probe Support Equipment (Huygens)
PSF	Point Spread Function
PST	Project Science Team
PWA	Permitivity, Waves and Altimetry (part of HASI on Huygens)
QM	Qualification Model
QPO	Quasi Periodic Oscillations
QSO	Quasi Stellar Object
R&D	Research and Development
RAL	Rutherford Appleton Laboratory (UK)
RD	Requirements Document
RF	Radio Frequency
RGS	Reflection Grating Spectrometer (XMM-Newton)
RHESSI	Reuven Ramaty High Energy Solar Spectroscopic Imager
RMOC	Rosetta Mission Operations Centre
ROLIS	Rosetta Lander Imaging System
ROMAP	RoLand Magnetometer & Plasma Monitor (Rosetta)
ROSINA	Rosetta Orbiter Spectrometer for Ion and Neutral Analysis (Rosetta)
ROSITA	Roentgen Survey with an Imaging Telescope Array
RPC	Rosetta Plasma Consortium
RSI	Radio Science Investigation
RTG	Radioisotope Thermoelectric Generator
RSOC	Rosetta Science Operations Centre
RXTE	Rossi X-ray Timing Explorer (NASA)
SAO	Smithsonian Astrophysical Observatory (US)
SAp/Saclay	Service d'Astrophysique (Commissariat à l'Energie Atomique; Saclay, France)
SAS	Scientific Analysis System (XMM-Newton)
SAX	Satellite per Astronomia in raggi X (Italy/The Netherlands)
SCD	Swept Charge Device
SCUBA	Submillimetre Common User Bolometer Array
SDO	Solar Dynamics Observatory (NASA)
SDT	Science Definition Team
SED	Spectral Energy Distribution
SEPM	Solar Electric Propulsion Module (BepiColombo)
SEPP	Solar Electric Primary Propulsion
SESAME	Surface Electric, Seismic and Acoustic Monitoring Experiment (Rosetta)
SiC	silicon carbide
SIRTF	Space IR Telescope Facility (NASA)
SIS	Superconductor-Insulator-Superconductor
SLP	Segmented Langmuir Probe
SMART	Small Mission for Advanced Research in Technology (ESA)
SMC	Small Magellanic Cloud
SMOG	Survey of Molecular Oxygen in the Galaxy (SMART-1)
SN	Supernova
SNR	Supernova Remnant
SOC	Science Operations Centre
SOHO	Solar and Heliospheric Observatory

SOPC	Science Operations & Planning Computer
SOS	Silicon-on-Sapphire
SOT	Science Operations Team
SPC	Science Programme Committee (ESA)
SPDB	Secondary Parameter Data Base (Cluster)
SPEDE	Spacecraft Potential, Electron & Dust Experiment (SMART-1)
SPI	Integral spectrometer
SPIRE	Spectral and Photometric Imaging Receiver (Herschel)
SRON	Space Research Organisation Netherlands
SRR	system requirements review
SSAC	Space Science Advisory Committee (ESA)
SSP	Surface Science Package (Huygens and Rosetta)
SSWG	Solar System Working Group
ST	Science Team; Space Technology (NASA)
ST-ECF	Space Telescope European Coordinating Facility
STEP	Satellite Test of the Equivalence Principle
STEREO	Solar-Terrestrial Relations Observatory
STIS	Space Telescope Imaging Spectrograph
STJ	Superconducting Tunnel Junction
STScI	Space Telescope Science Institute
STSP	Solar Terrestrial Science Programme
SUMER	Solar UV Measurements of Emitted Radiation (SOHO)
SVM	Service Module
SWAN	Solar Wind Anisotropies (SOHO)
SWG	Science Working Group
SWS	Short Wavelength Spectrometer (ISO)
SWT	Science Working Team
ToO	Target of Opportunity
TPF	Terrestrial Planet Finder (NASA)
TRACE	Transition Region & Coronal Explorer (NASA)
TRP	Technology Research Programme (ESA)
TWTA	Travelling Wave Tube Amplifier
UCB	University of California Berkeley
UCLA	University of California Los Angeles
ULIRG	Utra-Luminous IR Galaxy
UV	Ultraviolet
UVCS	Ultraviolet Coronal Spectrometer (SOHO)
VILSPA	Villafranca Satellite Tracking Station
VIRGO	Variability of Irradiance and Gravity Oscillations (SOHO)
VIRTIS	Visible Infra Red Thermal Imaging Spectrometer (Rosetta)
VLA	Very Large Array
VLBI	Very Long Baseline Interferometry
VLT	Very Large Telescope
WAC	Wide Angle Camera (OSIRIS on Rosetta)
WEC	Wave Experiment Consortium (Cluster)
WFC	Wide-Field Camera
WFE	wavefront error
WFPC	Wide-Field Planetary Camera (HST)
WHT	William Herschel Telescope
WWW	World Wide Web
XEUS	X-ray Evolving Universe Spectroscopy mission (ESA)
XMM	X-ray Multi-Mirror Mission (ESA)
XSA	XMM-Newton Science Archive
XSM	X-ray Solar Monitor (SMART-1)